

# **Structure and Functionality of Green Polyesters from Lipids**

A Thesis Submitted to the Committee on Graduate Studies  
in Partial Fulfillment of the Requirements for the Degree of Master of  
Science  
in the Faculty of Arts and Science

TRENT UNIVERSITY

Peterborough, Ontario, Canada

© Copyright by Ghazaleh Pourfallah

Materials Science M.Sc. Graduate Program

January 2013



Library and Archives  
Canada

Published Heritage  
Branch

395 Wellington Street  
Ottawa ON K1A 0N4  
Canada

Bibliothèque et  
Archives Canada

Direction du  
Patrimoine de l'édition

395, rue Wellington  
Ottawa ON K1A 0N4  
Canada

*Your file Votre référence*

*ISBN: 978-0-494-93867-6*

*Our file Notre référence*

*ISBN: 978-0-494-93867-6*

#### NOTICE:

The author has granted a non-exclusive license allowing Library and Archives Canada to reproduce, publish, archive, preserve, conserve, communicate to the public by telecommunication or on the Internet, loan, distribute and sell theses worldwide, for commercial or non-commercial purposes, in microform, paper, electronic and/or any other formats.

The author retains copyright ownership and moral rights in this thesis. Neither the thesis nor substantial extracts from it may be printed or otherwise reproduced without the author's permission.

#### AVIS:

L'auteur a accordé une licence non exclusive permettant à la Bibliothèque et Archives Canada de reproduire, publier, archiver, sauvegarder, conserver, transmettre au public par télécommunication ou par l'Internet, prêter, distribuer et vendre des thèses partout dans le monde, à des fins commerciales ou autres, sur support microforme, papier, électronique et/ou autres formats.

L'auteur conserve la propriété du droit d'auteur et des droits moraux qui protègent cette thèse. Ni la thèse ni des extraits substantiels de celle-ci ne doivent être imprimés ou autrement reproduits sans son autorisation.

---

In compliance with the Canadian Privacy Act some supporting forms may have been removed from this thesis.

While these forms may be included in the document page count, their removal does not represent any loss of content from the thesis.

Conformément à la loi canadienne sur la protection de la vie privée, quelques formulaires secondaires ont été enlevés de cette thèse.

Bien que ces formulaires aient inclus dans la pagination, il n'y aura aucun contenu manquant.

Canada

## ABSTRACT

### Structure and Functionality of Green Polyesters from Lipids

Ghazaleh Pourfallah

Poly( $\omega$ -hydroxyfatty acid/esters)s ( P( $\omega$ -OHFA)s and P( $\omega$ -Me-OHFA)s) are a class of linear aliphatic polyesters consisting of ester and methylene ( $\text{CH}_2$ ) groups in the chain backbone with terminal hydroxyl and carboxylic acid/ester groups. The hydrolyzable ester linkages in P( $\omega$ -OHFA)s and P( $\omega$ -Me-OHFA)s provides biodegradability. The hydrophobic methylene chain length controls the crystalline behaviour and the related thermal as well as mechanical properties of P( $\omega$ -OHFA)s and P( $\omega$ -Me-OHFA)s.

In the present study P( $\omega$ -OHFA)s and P( $\omega$ -Me-OHFA)s were prepared by polycondensation of  $\omega$ -hydroxyfatty acids ( $\omega$ -OHFA)s and  $\omega$ -hydroxyfatty esters ( $\omega$ - Me-OHFA)s, respectively. Monomers with three different number of ( $\text{CH}_2$ ) groups, namely, (9-hydroxynonanoic acid ( $\omega$ -OHC9) and methyl 9-hydroxynonanoate ( $\omega$ -Me-OHC9)), (13-hydroxytridecanoic acid ( $\omega$ -OHC13) and methyl-13-hydroxytridecanoate ( $\omega$ -Me-OHC13)), and (18-hydroxyoctadecanoic acid ( $\omega$ -OHC18) and methyl 18-hydroxyoctadecanoate ( $\omega$ -Me-OHC18)) attached to the carboxylic carbon were studied. These monomers were synthesized initially from unsaturated fatty acids derived from vegetable oil, using a series of chemical reactions at the position of fatty

acid double bonds. Cross metathesis reactions as well as the ozonolysis followed by subsequent reduction of the ozonide were the major chemical reaction routes used. The monomers obtained were characterized using Nuclear Magnetic Resonance (NMR) and Mass Spectroscopy (MS) techniques.

The polycondensation of ( $\omega$ -OHFA)s and (Me- $\omega$ -OHFA)s were optimized for the catalyst concentration, reaction time and temperature to obtain P( $\omega$ -OHFA)s and P( $\omega$ -Me-OHFA)s with desirable polyester molar masses and distributions. It has been found that the polymerization proceeded faster for ( $\omega$ -Me-OHFA)s, compared to (Me- $\omega$ -OHFA)s. Physical properties of P( $\omega$ -Me-OHFA)s were further investigated for the effect of both polyester molecular weights and monomer chain lengths on various properties. The crystalline structure and related thermal transitions for P( $\omega$ -Me-OHFA)s were studied using Differential Scanning Calorimetry (DSC) and wide angle X-ray diffraction (WAXD). Thermogravimetric Analysis (TGA) was used to analyze the thermal stability of P( $\omega$ -Me-OHFA)s. The viscoelastic and mechanical properties of P( $\omega$ -Me-OHFA)s were investigated using Dynamic Mechanical Analysis (DMA) and Tensile measurements. The results demonstrated that increasing the length of monomeric units in P( $\omega$ -Me-OHFA)s can significantly improve the thermal and mechanical properties.

**Keywords:** Lipid, vegetable oil, polyesters,  $\omega$ -hydroxyfatty acids, Poly( $\omega$ -hydroxyfatty acid), polycondensation, polyethylene-like, thermal behaviour, mechanical properties, crystallinity.

## **ACKNOWLEDGEMENTS**

I would like to express the deepest of gratitude to my supervisor Professor Suresh Narine whose patience, vision, encouragement and advice guided me through my MSc. program and the completion of this thesis.

I would also like to thank my committee members Dr. Andrew Vreugdenhil and Dr. Brad Easton for their guidance on my research. I am especially thankful to them for all that I have learned during the courses taken under their training, and for helping me to better improve my presentation and writing skills.

My special thanks to Dr. Laziz Bouzidi, Dr. Jesmy Jose and Dr. Shaojun Li for their guidance in physical properties analyses, research techniques, and thesis writing. I am heartily grateful to Laziz for his valuable advice not only in terms of the science but also for introducing the ways to improve my personality, skills and talents.

I would also like to thank Ali Mahdevvari, Carolyn Payne and John Breukelaar for their technical support. I give my best regards to my colleagues within the Trent Biomaterials Research Group, my friends, and all others who have assisted me in any way during my study in Canada.

I am warmly thankful to my parents for their unwavering support during my studying abroad. My cheerful thank you goes out to my husband for his constant encouragement and reliance when I felt alone, weak and tired.

Finally, I would like to thank the Ontario Soybean Growers /Grain Farmers of Ontario, Elevance Renewable Sciences, NSERC, GPA-EDC, Industry Canada, and Trent University for their generous support and funding during the course of my research.

# TABLE OF CONTENTS

Structure and Functionality of Green Polyesters from Lipids .....	i
ABSTRACT .....	ii
ACKNOWLEDGEMENTS .....	iv
TABLE OF CONTENTS .....	v
LIST OF FIGURES .....	viii
LIST OF TABLES .....	xiv
LIST OF ABBREVIATIONS .....	xvi
1 Introduction .....	1
1.1 Scope .....	1
1.2 Research objectives .....	4
1.3 Hypotheses .....	4
2 Literature review .....	6
2.1 General introduction to polymers .....	6
2.2 General introduction to aliphatic polyesters .....	6
2.2.1 Physical properties of linear aliphatic polyesters .....	8
2.2.2 Linear aliphatic polyesters as analogues for polyethylene-like polymers..	12
2.2.3 Biodegradability of aliphatic polyesters .....	13
2.2.4 Applications of aliphatic polyesters .....	14
2.3 General introduction to poly( $\omega$ -hydroxyfatty acid) .....	14
2.3.1 ( $\omega$ -OHFA)s derived from petroleum resources .....	16
2.3.2 ( $\omega$ -OHFA)s derived from renewable resources (vegetable oil) .....	17
2.4 Introduction to methods and mechanisms for synthesis of ( $\omega$ -OHFA)s .....	18
2.4.1 Ozonolysis .....	19
2.4.2 Reduction of the ozonide .....	21
2.4.3 Esterification reaction .....	22
2.4.4 Cross metathesis reaction .....	23
2.4.5 Introduction to melt polycondensation .....	24
2.4.6 Introduction to polycondensation catalysts .....	27
3 Synthesis and characterization of monomers .....	30

3.1	Introduction.....	30
3.2	Materials.....	30
3.3	Synthesis procedure of monomers .....	31
3.3.1	Methyl 9-hydroxynonanoate ( $\omega$ -Me-OHC9) .....	31
3.3.2	9-Hydroxynonanoic acid ( $\omega$ -OHC9).....	32
3.3.3	13-Hydroxytridecanoic acid ( $\omega$ -OHC13).....	32
3.3.4	Methyl 13-hydroxytridecanoate ( $\omega$ -Me-OHC13) .....	32
3.3.5	Methyl 18-Hydroxyoctadecanoate ( $\omega$ -Me-OHC18) .....	33
3.3.6	18-Hydroxyoctadecanoic acid ( $\omega$ -OHC18).....	34
3.4	Characterization techniques .....	34
3.4.1	Nuclear Magnetic Resonance.....	34
3.4.2	Mass spectrometry.....	35
3.4.3	High performance liquid chromatography .....	35
3.5	Result and discussions .....	37
3.5.1	Methyl 9-hydroxynonanoate ( $\omega$ -Me-OHC9) .....	37
3.5.2	9-Hydroxynonanoic acid ( $\omega$ -OHC9).....	40
3.5.3	13-Hydroxytridecanoic acid ( $\omega$ -OHC13).....	42
3.5.4	Methyl-13-Hydroxytridecanoate ( $\omega$ -Me-OHC13) .....	42
3.5.5	Methyl 18-Hydroxyoctadecanoate ( $\omega$ -Me-OHC18) .....	47
3.5.6	18-Hydroxyoctadecanoic acid ( $\omega$ -OHC18).....	48
3.6	Summary .....	51
4	Melt condensation polymerization of polyesters .....	52
4.1	Introduction.....	52
4.2	Theoretical Background.....	54
4.2.1	Thermodynamic aspects.....	54
4.2.2	Kinetics study .....	55
4.3	Experimental .....	56
4.3.1	Materials.....	56
4.3.2	Melt polycondensation of P( $\omega$ -OHFA)s and P( $\omega$ -Me-OHFA)s.....	57
4.3.3	Characterization techniques .....	58
4.4	Results and discussions.....	58

4.4.1	Characterization of P( $\omega$ -OHFA)s and P(Me- $\omega$ -OHFA)s .....	58
4.4.2	Optimization results .....	59
4.5	Summary .....	88
5	Physical properties of aliphatic polyesters: Influence of monomer chain length on structure and physical functionality .....	89
5.1	Introduction .....	89
5.2	Experimental .....	90
5.3	Characterization techniques for physical properties .....	91
5.3.1	Thermogravimetric analysis .....	91
5.3.2	Wide-angle X-ray diffraction .....	91
5.3.3	Differential scanning calorimetry (DSC) .....	93
5.3.4	Dynamic Mechanical Analysis .....	94
5.3.5	Tensile Analysis .....	95
5.4	Result and discussion .....	96
5.4.1	Thermal stability of the polyesters .....	96
5.4.2	Crystalline structure of P( $\omega$ -Me-OHFA)s .....	105
5.4.3	Crystallization and melting behaviour studied by DSC .....	112
5.4.4	Mechanical properties of P( $\omega$ -Me-OHFA)s by DMA <b>Error! Bookmark not defined.</b>	
5.4.5	Glass transition temperature .....	<b>Error! Bookmark not defined.</b>
5.4.6	Mechanical properties of P( $\omega$ -Me-OHFA)s by tensile analysis .....	129
5.5	Comparison of physical properties of aliphatic polyesters .....	136
5.6	Summary .....	139
6	Conclusions .....	140



## LIST OF FIGURES

<b>Figure 2–1.</b> General structure of aliphatic polyesters. ....	8
<b>Figure 2–2.</b> Structure of PGA .....	10
<b>Figure 2–3.</b> Structure of PLA.....	11
<b>Figure 2–4.</b> Structure of PCL.....	12
<b>Figure 2–5.</b> Chemical structure of P( $\omega$ -OHFA)s .....	15
<b>Figure 2–6.</b> Structure of triglycerides ( $R_1$ , $R_2$ & $R_3$ are long hydrocarbon chain).....	17
<b>Figure 2–7.</b> Structures of the most important fatty acids.....	18
<b>Figure 2–8.</b> Three step reactions of ozonolysis of oleic acid. Step 1: formation of primary ozonide, step 2: fragmentation of primary ozonide to form aldehyde or ketone, step 3: recombination of carbonyl oxide to form secondary ozonide. ....	20
<b>Figure 2–9.</b> Reduction of ozonide product in the presence of catalyst. ....	21
<b>Figure 2–10.</b> Fischer esterification mechanism .....	23
<b>Figure 2–11.</b> Cross metathesis reactions.....	24
<b>Figure 2–12.</b> Polycondensation of hydroxy acid-derivative .....	25
<b>Figure 2–13.</b> Reaction scheme for the Ravindranath mechanism for a simple polycondensation reaction.....	28
<b>Figure 3–1.</b> A typical HPLC calibration curve (this curve is for ( $\omega$ -Me-OHC18))......	36
<b>Figure 3–2.</b> $\omega$ -Me-OHC9 synthesized from methyl oleate via ozonolysis and hydrogenation. ...	39
<b>Figure 3–3.</b> Synthesis of $\omega$ -OHC9 from $\omega$ -Me-OHC9 by saponification.....	41
<b>Figure 3–4.</b> Synthesis of $\omega$ -OHC13 from erucic acid via ozonolysis and hydrogenation. ....	43
<b>Figure 3–5.</b> Synthesis of methyl erucate from erucic acid by Fischer Esterification .....	45

**Figure 3–6.** Synthesis of  $\omega$ -Me-OHC13 from ozonolysis and hydrogenation of methyl erucate 46

**Figure 3–7.** Synthesis of  $\omega$ -Me-OHC18 from methyl oleate and oleyl alcohol using cross metathesis followed by hydrogenation. .... 49

**Figure 3–8.** Synthesis of  $\omega$ -OHC18 from  $\omega$ -Me-OHC18 by saponification..... 50

**Figure 4–1.** Reaction scheme for melt polycondensation of P(Me- $\omega$ -OHFA)s and P( $\omega$ -OHFA)s. .... 53

**Figure 4–2.** Mechanism of catalytic polycondensation of  $\omega$ -OHFAs and  $\omega$ -Me-OHFAs..... 61

**Figure 4–3.** Variation of  $\bar{M}_n$  and PDI as a function of catalyst concentration (a) P( $\omega$ -OHC9) and P( $\omega$ -Me-OHC9), (b) P( $\omega$ -OHC13) and P( $\omega$ -Me-OHC13), (c) P( $\omega$ -OHC18) and P( $\omega$ -Me-OHC18). Symbols are: ( $\Delta, \blacktriangle$ )  $\bar{M}_n$  of P( $\omega$ -Me-OHFA) and P( $\omega$ -OHFA), respectively, ( $\circ, \bullet$ ): PDI of P( $\omega$ -Me-OHFA) and P( $\omega$ -OHFA), respectively. .... 63

**Figure 4–4.** (a) to (f).  $\bar{M}_n$  and PDI as a function of reaction time during the second phase of the polymerization at different catalyst concentrations (50-500 ppm). Symbols are: ( $\Delta, \blacktriangle$ )  $\bar{M}_n$  of P( $\omega$ -Me-OHC9) and P( $\omega$ -OHC9), respectively. ( $\circ, \bullet$ ): PDI of P( $\omega$ -Me-OHC9) and P( $\omega$ -OHC9), respectively. .... 67

**Figure 4–5.** (a) to (f)  $\bar{M}_n$  and PDI as a function of reaction time during the second phase of the polymerization at different catalyst concentrations (50-500 ppm). Symbols are: ( $\Delta, \blacktriangle$ )  $\bar{M}_n$  of P( $\omega$ -Me-OHC13) and P( $\omega$ -OHC13), respectively. ( $\circ, \bullet$ ): PDI of P( $\omega$ -Me-OHC13) and P( $\omega$ -OHC13), respectively. .... 68

**Figure 4–6.** (a) to (f)  $\bar{M}_n$  and PDI as a function of reaction time during the second phase of the polymerization at different catalyst concentrations (50-500 ppm). Symbols are: ( $\Delta, \blacktriangle$ )  $\bar{M}_n$  of

P( $\omega$ -Me-OHC18) and P( $\omega$ -OHC18), respectively. (○, ●): PDI of P( $\omega$ -Me-OHC18) and P( $\omega$ -OHC18), respectively. .... 69

**Figure 4–7.** Linear performance of experimental  $\bar{X}_n$  as a function of reaction time for (a) P( $\omega$ -OHC9) and (b) P( $\omega$ -Me-OHC9), respectively. (★) percentage residual values, ( $R^2 > 0.9945$ ).... 73

**Figure 4–8.** Comparison of kinetic study between P( $\omega$ -OHC9), (●), and P( $\omega$ -Me-OHC9), (▲) ..... 76

**Figure 4–9.** Linear performance of experimental  $\bar{X}_n$  as a function of reaction time for (a) P( $\omega$ -OHC13) and (b) P( $\omega$ -Me-OHC13), respectively. (★) percentage residual values, ( $R^2 > 0.9827$ ).78

**Figure 4–10.** Comparison of kinetic study between (●) P( $\omega$ -OHC13) and (▲) P( $\omega$ -Me-OHC13). ..... 79

**Figure 4–11.** Linear relationship between  $\bar{X}_n$  and reaction time for (a) P( $\omega$  -OHC18) and (b) P( $\omega$ -Me-OHC18), ( $R^2 > 0.9831$ )..... 82

**Figure 4–12.** Comparison of kinetic study between (●) P( $\omega$ -OHC18) and (▲) P( $\omega$ -Me-OHC18). ..... 83

**Figure 4–13.**  $\bar{M}_n$  and PDI as function of temperature of (a) P( $\omega$ -OHC9) and P( $\omega$ -Me-OHC9), (b) P( $\omega$ -OHC13) and P( $\omega$ -Me-OHC13), (c) P( $\omega$ -OHC18) and P( $\omega$ -Me-OHC18). Symbols are: (Δ, ▲)  $\bar{M}_n$  of P( $\omega$ -Me-OHC13) and P( $\omega$ -OHC13), respectively. (○, ●): PDI of P( $\omega$ -Me-OHC13) and P( $\omega$ -OHC13), respectively. .... 87

**Figure 5–1.** TGA and DTG traces of (a<sub>1</sub>) ( $\omega$ -Me-OHC9), (b<sub>1</sub>) ( $\omega$ -Me-OHC13) and (c<sub>1</sub>) ( $\omega$ -Me-OHC18). TGA and DTG traces of (a<sub>2</sub>) P( $\omega$ -Me-OHC9), and (b<sub>2</sub>) P( $\omega$ -Me-OHC13), and (c<sub>2</sub>) P( $\omega$ -Me-OHC18)..... 98

**Figure 5–2.** Onset temperature of degradation ( $T_d(on)$ ) as a function  $\bar{M}_n$  for P( $\omega$ -Me-OHC9), (●), P( $\omega$ -Me-OHC13), (▲), and P( $\omega$ -Me-OHC18), (■). Dashed lines are linear fits ( $R^2 > 0.9945$ ).

..... 101

**Figure 5–3.** (a) Characteristic thermal degradation temperatures of monomers (Onset temperature of degradation ( $T_d(on)$ ) and leading DTG peak temperature ( $T_{d(max)}$ ) of monomers ( $\Delta$  and  $\circ$ , respectively), and polymers with the maximum  $\bar{M}_n$  (▲ and ●) as a function of monomeric unit length ( $n$ , carbon atoms). (b)  $T_{d(max)}$  as a function of monomeric unit length ( $n$ , carbon atoms) of P( $\omega$ -Me-OHFA)s (●) and of polyesters from the literature measured at the same conditions (★).

..... 104

**Figure 5–4.** WAXD patterns of (a) P( $\omega$ -Me-OHC9), (b) P( $\omega$ -Me-OHC13) and (c) P( $\omega$ -Me-OHC18).

..... 106

**Figure 5–5.** d-spacing of the P( $\omega$ -Me-OHFA)s in the range of  $2\theta = 3-90^\circ$  as a function of the number of carbon atoms in the monomeric unit.

..... 107

**Figure 5–6.** Degree of crystallinity  $X_c$  (%) as a function of  $\bar{M}_n$  for P( $\omega$ -Me-OHC9), (●), P( $\omega$ -Me-OHC13), (▲), and P( $\omega$ -Me-OHC18), (■).

..... 111

**Figure 5–7.** Degree of crystallinity as a function of length of monomers of the P( $\omega$ -Me-OHFA) samples with the lowest (▼) and highest (●)  $\bar{M}_n$ .

..... 113

**Figure 5–8.** DSC thermograms of (a) P( $\omega$ -Me-OHC9), (b) P( $\omega$ -Me-OHC13) and (c) P( $\omega$ -Me-OHC18) obtained with heating and cooling rate of  $3^\circ\text{C}/\text{min}$ .

..... 116

**Figure 5–9.** Enthalpies of (a) melting and (b) crystallization of the P( $\omega$ -Me-OHFA)s as a function of  $\bar{M}_n$ . P( $\omega$ -Me-OHC9): (●), P( $\omega$ -Me-OHC13): (▲) and P( $\omega$ -Me-OHC18): (■).

..... 118

**Figure 5–10.** Onset; (▲), offset; (■) and peak temperature (●) of (a) melting and (b) crystallization of P( $\omega$ -Me-OHFA)s. (c) Melting; (●) and crystallization (▲) temperature of P( $\omega$ -Me-OHFA)s; (★) represent peak temperature of melting,  $T_m$ , of aliphatic polyesters mined from the literature.(d) Enthalpies of melting (●) and crystallization (▲) as a function of the number of carbons in the monomeric unit. .... 120

**Figure 5–11.** Storage modulus, loss modulus and tan  $\delta$  versus  $T$  curves of (a) P( $\omega$ -Me-OHC9), (b) P( $\omega$ -Me-OHC13) and (c) P( $\omega$ -Me-OHC18) obtained from DMA..... 122

**Figure 5–12.** Storage modulus of P( $\omega$ -Me-OHC9), (●), P( $\omega$ -Me-OHC13), (▲), and P( $\omega$ -Me-OHC18), (■), as a function of  $\bar{M}_n$  ..... 124

**Figure 5–13.** Storage modulus as a function of monomeric unit length at 37 °C of P( $\omega$ -Me-OHFA)s with lowest  $\bar{M}_n$  (▼) and highest  $\bar{M}_n$  (●)..... 125

**Figure 5–14.** (a) Glass transition temperature ( $T_g$ ) as a function of  $\bar{M}_n$  for P( $\omega$ -Me-OHC9), (●), P( $\omega$ -Me-OHC13), (▲), and P( $\omega$ -Me-OHC18), (■), (b) Glass transition temperature versus monomeric unit length for the P( $\omega$ -Me-OHFA) with the lowest  $\bar{M}_n$  (●) and highest  $\bar{M}_n$  (▼). 128

**Figure 5–15.** (a) Typical stress-strain curve of polymers. The four regions are (i) linear and non-linear (ii) neck region (iii) plastic flow and (iv) strain hardening. (b). Stress-strain curves obtained for (a) P( $\omega$ -Me-OHC9), (b) P( $\omega$ -Me-OHC13) and (c) P( $\omega$ -Me-OHC18)..... 130

**Figure 5–16.** (a), (b) and (c) Tensile properties as a function of  $\bar{M}_n$  for P( $\omega$ -Me-OHC9), (●), P( $\omega$ -Me-OHC13), (▲), and P( $\omega$ -Me-OHC18), (■). (d) Young’s modulus versus degree of crystallinity ..... 133

**Figure 5–17.** Young’s modulus as a function of monomeric unit length of the P( $\omega$ -Me-OHFA)s with the lowest (▼) and highest (●)  $\bar{M}_n$ ..... 135

<b>Figure A- 1.</b> NMR Spectrum of ( $\omega$ -OHC9) .....	145
<b>Figure A- 2.</b> NMR Spectrum of ( $\omega$ -Me-OHC9) .....	146
<b>Figure A- 3.</b> NMR Spectrum of ( $\omega$ -OHC13) .....	147
<b>Figure A- 4.</b> NMR spectrum of ( $\omega$ -Me-OHC13) .....	148
<b>Figure A- 5.</b> NMR spectrum of ( $\omega$ -Me-OHC18) .....	149
<b>Figure A- 6.</b> NMR Spectrum of ( $\omega$ -OHC18) .....	150
<b>Figure A- 7.</b> NMR Spectrum of P( $\omega$ -OHC9) and P( $\omega$ -Me-OHC9) .....	151
<b>Figure A- 8.</b> NMR Spectrum of P( $\omega$ -OHC13) and P( $\omega$ -Me-OHC13) .....	152
<b>Figure A- 9.</b> NMR Spectrum of P( $\omega$ -OHC18) and P( $\omega$ -Me-OHC18) .....	153
<b>Figure B- 1.</b> Mass Spectrum of ( $\omega$ -Me-OHC9) .....	154
<b>Figure B- 2.</b> Mass spectrum of ( $\omega$ -OHC9) .....	155
<b>Figure B- 3.</b> Mass Spectrum of ( $\omega$ -OHC13) .....	156
<b>Figure B- 4.</b> Mass Spectrum of ( $\omega$ -Me-OHC13) .....	157
<b>Figure B- 5.</b> Mass spectrum of ( $\omega$ -Me-OHC18) .....	158
<b>Figure B- 6.</b> Mass Spectrum of ( $\omega$ -OHC18) .....	159
<b>Figure C- 1.</b> HPLC Calibration Curve of ( $\omega$ -OHC9) .....	160
<b>Figure C- 2.</b> HPLC Calibration Curve of ( $\omega$ -Me-OHC9) .....	161
<b>Figure C- 3.</b> HPLC Calibration Curve of ( $\omega$ -OHC13) .....	162
<b>Figure C- 4.</b> HPLC Calibration Curve of ( $\omega$ -Me-OHC13) .....	163
<b>Figure C- 5.</b> HPLC Calibration Curve of ( $\omega$ -OHC18) .....	164
<b>Figure C- 6.</b> HPLC Calibration Curve of ( $\omega$ -Me-OHC18) .....	165

## LIST OF TABLES

<b>Table 2-1.</b> List of common aliphatic and cyclic monomers used to prepare linear aliphatic polyesters .....	7
<b>Table 2-2.</b> List of important linear aliphatic polyesters and their physical properties, $T_m$ , $T_g$ and $T_d$ are melting, glass transition and maximum degradation temperatures, respectively.....	9
<b>Table 4-1.</b> $\bar{M}_w$ , $\bar{M}_n$ and PDI obtained at the optimum catalyst concentrations for P( $\omega$ -OHFA) and P( $\omega$ -Me-OHFA) .....	65
<b>Table 4-2.</b> Experimental (exp) and mathematical (calc) results obtained from the kinetic analysis of (a) P( $\omega$ -OHC9). (b) P( $\omega$ -Me-OHC9). $M_0=156$ g/mol. ....	71
<b>Table 4-3.</b> Experimental (exp) and mathematical (calc) results obtained from the kinetic analysis of (a) P( $\omega$ -OHC13) and (b) P( $\omega$ -Me-OHC13). $M_0 = 212$ g/mol.....	77
<b>Table 4-4.</b> Experimental (exp) and mathematical (calc) data of (a) P( $\omega$ -OHC18) and (b) P( $\omega$ -Me-OHC18). $M_0= 282$ g/mol. ....	81
<b>Table 4-5.</b> Reaction rate and equilibrium constant of polycondensation of acid and ester terminated polymers.....	85
<b>Table 4-6.</b> $\bar{M}_n$ and PDI values of P( $\omega$ -OHFA)s and P( $\omega$ -Me-OHFA)s versus temperature .....	86
<b>Table 5-1.</b> Average number of molecular weight $\bar{M}_n$ , Onset temperature of degradation, $T_d(on)$ , and DTG peak maximum temperature, $T_{d(max)}$ , of the P( $\omega$ -Me-OHFA)s.....	99
<b>Table 5-2.</b> Degree of crystallinity $X_c$ (%) of P( $\omega$ -Me-OHFA)s as a function of $\bar{M}_n$ .....	110
<b>Table 5-3.</b> Thermal characteristic parameters of P( $\omega$ -Me-OHFA)s obtained by DSC. Average number of molecular weight, $\bar{M}_n$ , onset, $T_{on}$ , offset, $T_{off}$ and peak temperature of melting, $T_m$ , and	

crystallization,  $T_c$ , and enthalpy of melting,  $\Delta H_m$ , and crystallization,  $\Delta H_c$ . Subscripts 1 and 2 denote first and second heating cycles, respectively. The uncertainties attached to the characteristic temperatures and enthalpies are better than 0.5°C and 8 J/g, respectively..... 115

**Table 5-4.** Glass transition temperature ( $T_g$ ) of P( $\omega$ -Me-OHFA)s with different  $\bar{M}_n$ . ..... 127

**Table 5-5.** Tensile properties of P( $\omega$ -Me-OHFA) samples as a function of  $\bar{M}_n$  ..... 132

**Table 5-6.** Comparison of thermal, crystalline and mechanical properties of synthetic aliphatic polyesters with HDPE..... 138



## LIST OF ABBREVIATIONS

$\omega$ -OHFA	$\omega$ -hydroxyfatty acid
$\omega$ -Me-OHFA	$\omega$ -hydroxyfatty acid methyl ester
$\omega$ -OHC9	$\omega$ -9-hydroxynonanoic acid
$\omega$ - Me-OHC9	$\omega$ -9-hydroxynonanoate
$\omega$ -OHC13	$\omega$ -13-hydroxytridecanoic acid
$\omega$ -Me-OHC13	$\omega$ -13-hydroxytridecanoate
$\omega$ -OHC18	$\omega$ -18-hydroxyoctadecanoic acid
$\omega$ -Me-OHC18	$\omega$ -18-hydroxyoctadecanoate
ASTM	American Society for Testing and Materials
Calc	Calculated
CDCl <sub>3</sub>	Deuterated chloroform
CI	Criegee Intermediate
DMA	Dynamic Mechanical Analysis
DMT	Dimethyl terephthalate
DSC	Differential Scanning Calorimetry
ET	Ethylene glycol
Exp	Experimental
FWHM	Full width at half maximum
GPC	Gel Permeation Chromatography

HDPE	High density polyethylene
HPLC	High Performance Liquid Chromatography
IUPAC	International Union of Pure and Applied Chemistry
$K_c$	Equilibrium constant
$k_r$	Reaction rate constant
LDPE	Low density polyethylene
LLDPE	Linear low density polyethylene
$M_n$	Number Average Molecular Weight
MPa	Mega Pascal
MS	Mass Spectrometry
$M_w$	Weight Average Molecular Weight
NMR	Nuclear Magnetic Resonance
PE	Polyethylene
PCL	Poly-( $\epsilon$ -caprolactone)
PDI	Polydispersity Index
PET	Polyethylene terephthalate
PGA	Polyglycolide
PLA	Polylactide
PS	Polystyrene
ppm	Parts Per Million

Psi	Pounds per Square Inch
$T_c$	Crystallization Temperature
$T_d$	Decomposition Temperature
$T_{on}$	Onset temperature
$T_{off}$	Offset temperature
$T_{d(max)}$	Maximum temperature of degradation
$Ti(OiPr)_4$	Titanium (IV) isopropoxide
TGA	Thermogravimetric Analysis
$T_g$	Glass Transition Temperature
TLC	Thin Layer Chromatography
$T_m$	Melting Temperature
WAXD	Wide angle X-ray Diffraction
XRD	X-ray Diffraction
$\bar{X}_n$	Number average degree of polymerization

# 1 Introduction

## 1.1 Scope

Vegetable oils are readily available, nontoxic and relatively low cost feedstock that presents viable opportunities for the preparation of renewable and bio-based polymers. Fatty acids derived from triglyceride molecules of vegetable oils are considered an emerging class of chemicals for the synthesis of bio-based polymers. These fatty acids can contain long chain linear segments as well as Carbon-Carbon double bonds in their structure. One of the important derivatives of unsaturated fatty acids is  $\omega$ -hydroxyfatty acids.  $\omega$ -hydroxyfatty acids are straight chain aliphatic organic acids that can be obtained from unsaturated fatty acids by various chemical reactions. They are attractive candidates for polycondensation or polyesterification by virtue of containing two reactive functional groups; hydroxyl and carboxylic acid (Jain, Sokolsky et al. 2008).

Poly( $\omega$ -hydroxyfatty acids/esters) abbreviated as P( $\omega$ -OHFA)s and P( $\omega$ -Me-OHFA)s are obtained by polycondensation of  $\omega$ -hydroxyl fatty acids or esters. The structure of P( $\omega$ -OHFA)s consists of hydrophobic methylene chains linked by ester groups in the backbone. The hydrophobic methylene groups provide well-defined physical properties such as crystallinity, thermal stability and strength (Petrović, Milić et al. 2010). Concurrently, the hydrolyzable ester groups offer biocompatibility and biodegradability (Nair and Laurencin 2007). By varying the number of methylene ( $\text{CH}_2$ ) and ester groups in the repeating units in P( $\omega$ -OHFA)s, it should be possible to design and control the physical properties of P( $\omega$ -OHFA)s for suitable applications.

In the recent past, growing concerns over environmental impacts and sustainability have promoted the synthesis of biodegradable polyesters from renewable resources. These polyesters

are being increasingly preferred over their petroleum-based counterparts (Gross and Kalra 2002). Well known examples of polyesters obtained from renewable sources are polyhydroxyalkanoates (PHA), poly(glycolic acid) (PGA) and poly(lactic acid) (PLA) (Mecking 2004). However, these polymers have some functional limitations because of their short chain repeating units. For example, PLA suffers from poor thermal stability, which restricts its thermoplastic processing (Cai, Yao et al. 2002). P( $\omega$ -OHFA)s have been found to provide improved physical properties to overcome such limitations (Cai, Liu et al. 2010; Lu, Ness et al. 2010). P( $\omega$ -OHFA)s, with long monomeric methylene chain have been established to introduce properties comparable to commodity plastics like polyethylene (de Geus, van der Meulen et al. 2010). Polyethylene (PE) is the most popular thermoplastic in the world. It has been used in many diverse applications from packaging to medical applications. However, polyethylene is non-biodegradable and derived from petrochemical feedstock (van der Meulen, Gubbels et al. 2011). Efforts to produce bio-based, renewable polymers which display similar properties to PE has been of interest for a long time (Barbiroli, Lorenzetti et al. 2003). Their susceptibility to hydrolytic cleavage as well as their low environmental impact suggests that P( $\omega$ -OHFA)s are potentially good replacements for petroleum based plastics (Lu, Ness et al. 2010).

Linear aliphatic polyesters are mostly developed from (a) polycondensation of diacid/diester and a diol, (b) polycondensation of hydroxyfatty acid/ester (c) ring opening polymerization of lactones monomers. Polycondensation of diacids-diols has been extensively studied (Edlund and Albertsson 2003; Mahapatro, Kumar et al. 2004). Polycondensation, known as step growth polymerization, involves a series of steps to obtain a high molecular weight polymer (Stille 1981). Polyesters, polyamides and polyurethanes are polymers that are mostly produced by polycondensation.

Recently, interest in  $\omega$ -hydroxyl fatty acids derived from vegetable oils as monomers for polycondensation reactions have been resuscitated (Petrović, Milić et al. 2010; Liu, Liu et al. 2011). However, these monomers are not commercially available, although it is possible to obtain them through a series of specific chemical reactions. Oxidation (ozonolysis), reduction, epoxidation, etc. are reactions that have been widely used on lipid feedstock to produce  $\omega$ -hydroxyl fatty acids. In this thesis, self and cross metathesis reactions are also investigated as potential routes to producing  $\omega$ -hydroxyl fatty acids from lipids.

This study was ultimately targeted at the development of novel linear aliphatic polyesters derived from vegetable oils that would be thermally stable, potentially biodegradable, and with improved physical properties comparable to that of PE.  $\omega$ -hydroxyl fatty acids and their methyl esters were synthesized by ozonolysis, reduction and cross metathesis reactions. These monomers were  $\omega$ -9-hydroxynonanoic acid ( $\omega$ -OHC9),  $\omega$ -9-hydroxynonanoate ( $\omega$ -Me-OHC9),  $\omega$ -13-hydroxytridecanoic acid ( $\omega$ -OHC13),  $\omega$ -13-hydroxytridecanoate ( $\omega$ -Me-OHC13),  $\omega$ -18-hydroxyoctadecanoic acid ( $\omega$ -OHC18) and  $\omega$ -18-hydroxyoctadecanoate ( $\omega$ -Me-OHC18).

Melt condensation polymerization was performed both on the acids and their methyl esters, to obtain desirable poly( $\omega$ -hydroxyl fatty acids/esters). To the best of our knowledge there has been no report on optimization of polycondensation reactions based on  $\omega$ -hydroxyl fatty acids and their methyl esters. A systematic comparison of the stepwise polymerization of  $\omega$ -hydroxyl fatty acids and their methyl esters was conducted by varying the polymerization conditions. Physical and thermal properties of the P( $\omega$ -OHFA)s were also related to the structure of the individual monomers.

The obtained polyesters were poly( $\omega$ -hydroxynonanoic acid) P( $\omega$ -OHC9), poly( $\omega$ -hydroxynonanoate) P(Me- $\omega$ -OHC9), poly( $\omega$ -hydroxytridecanoic acid) P( $\omega$ -OHC13), poly( $\omega$ -hydroxytridecanoate) P(Me- $\omega$ -OHC13), poly( $\omega$ -hydroxyoctadecanoic acid) P( $\omega$ -OHC18), and poly( $\omega$ -hydroxyoctadecanoate) P(Me- $\omega$ -OHC18).

## 1.2 Research objectives

- 1 Use of naturally occurring vegetable oils as starting materials for the synthesis of a series of monomers: ( $\omega$ -OHC9), ( $\omega$ -Me-OHC9), ( $\omega$ -OHC13), ( $\omega$ -Me-OHC13), ( $\omega$ -OHC18) and (Me-OHC18) fatty acid/ester monomers.
- 2 Optimization of polycondensation reactions by varying the reaction conditions such as time, temperature and catalyst concentration to produce poly( $\omega$ -hydroxyfatty acid and esters) such as P( $\omega$ -OHC9), P(Me- $\omega$ -OHC9), P( $\omega$ -OHC13), P(Me- $\omega$ -OHC13), P( $\omega$ -OHC18) and P(Me- $\omega$ -OHC18) with desirable molecular weights and polydispersity indexes.
- 3 Investigation of the relationships of monomeric structure to polymeric structure, and to physical properties so as to propose optimized designed of polyesters from omega hydroxyl fatty acids/esters.

## 1.3 Hypotheses

1. ( $\omega$ -OHC18) and ( $\omega$ -Me-OHC18) can be synthesized through a cross metathesis reaction of oleic acid and oleyl alcohol.
2. The polycondensation reaction is a function of reaction time, temperature and catalyst concentration. Optimization of these parameters can optimize, molecular weights and polydispersity of polyethylene-like poly( $\omega$ -hydroxyl fatty acids/esters).

3. Long chain of methylene groups in  $\omega$ -hydroxyl fatty acids are factors to improve thermal stability of the polymer by increasing the Van der Waals attractive forces. Increasing the number of  $-(CH_2)-$  groups in the repeating structure units of the polymer can increase the thermal stability of the poly( $\omega$ -hydroxyl fatty acids/esters).
4. Hydrophobic methylene chains are responsible in crystalline properties of the polyester. The melting temperature and the degree of crystallinity of the poly( $\omega$ -hydroxyl fatty acids/esters) can be affected by varying the number of  $-(CH_2)-$  groups in the repeating structure units of the polymer.
5. Glass transition temperature is affected by crystalline structure of polyester. The increase in the number of  $-(CH_2)-$  groups in the repeating structure units of the poly( $\omega$ -hydroxyl fatty acids/esters) can affect the glass transition temperature ( $T_g$ ) of the polymers.
6. Mechanical properties such as tensile strength are affected by molecular weight of the polymer. An increase in molecular weight of poly( $\omega$ -hydroxyl fatty acids/esters) can increase the ultimate strength as well as maximum strain of the polymers.



## **2 Literature review**

### **2.1 General introduction to polymers**

Polymers are macromolecules composed of repeating structural units of low molar mass molecules linked to each other, primarily by covalent bonds. The low molar mass molecules are called monomers and the process of linking monomers by chemical reactions is termed polymerization. The term “polymer” is generally used to refer to a large class of natural and synthetic materials with a variety of properties and applications.

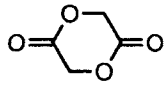
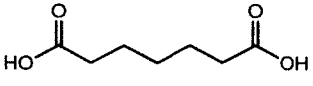
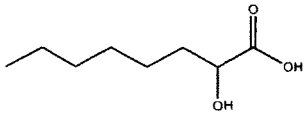
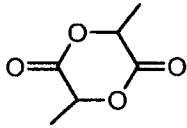
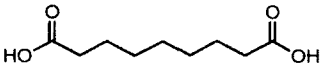
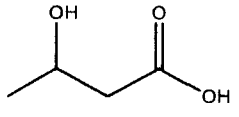
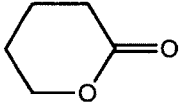

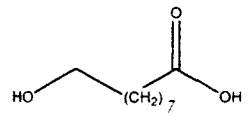
The size and functionality of the repeating units influence the structure and physical properties of polymers. Polyethylene (PE), for example, consists of a simple set of repeating methylene units  $-(CH_2)-$  and is one of the most widely used commodity polymers. Polyamide is also a well-known polymer having amide linkages  $-(NHCO)-$  in the repeating units. Another group of polymers is polyurethane that has urethane linkages  $-(NHCOO)-$  in the polymeric backbone. Polyesters are yet another important group of polymers having hydrolysable ester groups in their repeating units and are well known for their biodegradable properties.

### **2.2 General introduction to aliphatic polyesters**

Aliphatic polyesters are polymers containing methylene segments with ester linkages in the repeating aliphatic units. Based on the structure of their monomers, linear aliphatic thermoplastic polyesters are classified into (i) Polylactones, derived from cyclic lactone monomers, such as lactide, glycolide,  $\epsilon$ -caprolactone (Abraham and Narine 2009; Oledzka and Narine 2011;

Oledzka, Kaliszewska et al. 2012)etc. (ii) Poly(alkylene dicarboxylate)s, derived from diol (HO-R<sub>1</sub>-OH) and dicarboxylic acid monomers (HOOC-R<sub>2</sub>-COOH), and (iii) Poly(hydroxy acid)s (P(OHA)s), derived from hydroxy acid monomers (HO-(CH<sub>2</sub>)<sub>n</sub>-COOH). Table 2-1 summarizes some of the most common lactones, dicarboxylic acids, and hydroxyacid monomers available and their sources.

**Table 2-1.**List of common aliphatic and cyclic monomers used to prepare linear aliphatic polyesters

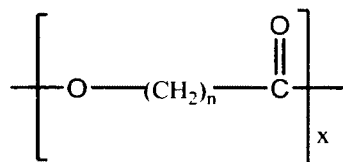
Lactones	Dicarboxylates/diols	Hydroxy acids
Sources: carbohydrates, microbial, petroleum	Sources: natural substances, petroleum	Sources: animal or vegetable based lipids, petroleum
 Glycolide	 Heptanedioic acid	 2-Hydroxyoctanoic acid
 Lactide	 1,9-Nonanedioic acid	 3-Hydroxybutanoic acid
 ε-caprolactone	 1,9-Dihydroxynonane	 9-Hydroxynonanoic acid

Poly(hydroxy acid)s (P(OHA)s) are further classified into α-, β- and ω- poly(hydroxyfatty acid) depending on the position of the hydroxyl (OH) group from the carboxyl carbon of the hydroxy acid monomer. Poly(ω-hydroxyfatty acid) (P(ω-OHFA)) is P(OHA) derived from ω-

hydroxyfatty acid monomers having the hydroxyl group at the  $\omega$ - position with respect to the carboxylic carbon atom.

### 2.2.1 Physical properties of linear aliphatic polyesters

Aliphatic polyesters possess desirable physical properties such as flexibility, crystallinity, strength and biodegradability. The various physical properties are determined by factors such as the structure of monomer units, molar mass, flexibility of the chain, presence of polar groups etc, in these polyesters. In fact, the hydrophobic methylene segments in linear aliphatic polyesters are responsible for the crystalline phase behaviour, strength and stability (Trzaskowski, Quinzler et al. 2011). Figure 2-1 shows the general structure of linear aliphatic polyesters.



**Figure 2–1.** General structure of aliphatic polyesters.

Physical properties of aliphatic polyesters can be modified by altering the length of the monomeric unit. Table 2-2 lists some of the important aliphatic polyesters and their various physical properties.  $T_m$ ,  $T_g$  and  $T_d$  are melting, glass transition and maximum degradation temperatures, respectively

**Table 2-2.** List of important linear aliphatic polyesters and their physical properties,  $T_m$ ,  $T_g$  and  $T_d$  are melting, glass transition and maximum degradation temperatures, respectively.

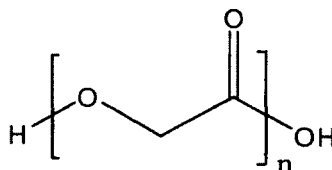
No. of methylene groups	polyesters	$T_d$ (°C)	$T_m$ (°C)	$T_g$ (°C)	Young's Modulus (MPa)	Crystal structure
n=1	poly(glycolic acid) (PGA)	250 <sup>a</sup>	220 <sup>a</sup>	40 <sup>a</sup>	6900 <sup>b</sup>	Orthorhombic <sup>c</sup>
n=1+methyl group	poly(hydroxypropionic acid)(PLA)	270 <sup>d</sup>	160 <sup>d</sup>	35 <sup>d</sup>	1300 <sup>e</sup>	Hexagonal <sup>f</sup>
n=5	poly(1,4-hydroxybutyrate) (PCL)	350 <sup>g</sup>	60 <sup>g</sup>	-60 <sup>g</sup>	400 <sup>h</sup>	Orthorhombic <sup>i</sup>
n=8	Poly( $\omega$ -hydroxynonanoate) P( $\omega$ -OHC9)	410 <sup>j</sup>	70 <sup>j</sup>	-31 <sup>j</sup>	200 <sup>j</sup>	--
n=8	Poly( $\omega$ -hydroxynonanoate) P( $\omega$ -OHC9)	380 <sup>k</sup>	70 <sup>k</sup>	-30 <sup>k</sup>	--	--
n=13	Poly( $\omega$ -hydroxytetradecanoate) P( $\omega$ -OHC14)	458 <sup>l</sup>	92 <sup>l</sup>	-29 <sup>l</sup>	486 <sup>l</sup>	Orthorhombic <sup>l</sup>
n=14	Poly(pentadecalactone) (PPDL)	--	92 <sup>m</sup>	-27 <sup>m</sup>	690 <sup>m</sup>	Orthorhombic <sup>m</sup>
n=19	Poly([1,20-eicosadiyl-1,20-eicosanedioate)	--	108 <sup>n</sup>	--	--	--
	HDPE	470 <sup>o</sup>	125 <sup>p</sup>	-120 <sup>q</sup>	800-1100 <sup>r</sup>	Orthorhombic <sup>s</sup>

<sup>a</sup>(Nair and Laurencin 2007);<sup>b</sup>(Philip, Keshavarz et al. 2007);<sup>c</sup>(Singh and Tiwari 2010); <sup>d</sup>(Van de Velde and Kiekens 2002); <sup>e</sup>(Madhavan Nampoothiri, Nair et al. 2010); <sup>f</sup>(Narladkar 2008); <sup>g</sup>(Labet and Thielemans 2009); <sup>h</sup>(Nair and Laurencin 2007); <sup>i</sup>(Bittiger, Marchessault et al. 1970); <sup>j</sup>(Petrović, Milić et al. 2010);<sup>k</sup>(Liu, Kong et al. 2008);<sup>l</sup>(Liu, Liu et al. 2011); <sup>m</sup>(Cai, Liu et al. 2010); <sup>n</sup>(Trzaskowski, Quinzler et al. 2011); <sup>o</sup>(Mengeloglu and Karakus 2008);<sup>p</sup>(Cho, Jeon et al. 1993); <sup>q</sup>(Gaur and Wunderlich 1980); <sup>r</sup>(Matsuo and Sawatari 1986); <sup>s</sup>(Bunn 1939).

Among the polyesters with varying number of methylene groups, polyglycolide (PGA), polylactide (PLA) and polycaprolactone (PCL) are the most studied, and are therefore discussed in detail below.

#### 2.2.1.1 Polyglycolide (PGA)

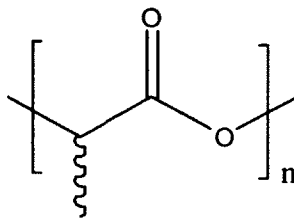
PGA is the simplest linear aliphatic polyester (Figure 2-2), obtained by the ring opening polymerization (ROP) of glycolide. The polymer chains exist in an orthorhombic packing, with a relatively high melting point at  $\sim 220^{\circ}\text{C}$ . PGA is the strongest material among these kinds of polyesters, with a tensile strength of around 70 MPa. It is however very brittle, showing only few percents of extensibility. The glass transition temperature ( $T_g$ ) of PGA is at around  $40^{\circ}\text{C}$  (Nair and Laurencin 2007). The application of PGA is limited to selected fields such as medical, due to their non-solubility in most of the organic solvents. PGA also suffers from poor thermal stability (see Table 2-2).



**Figure 2–2.** Structure of PGA

#### 2.2.1.2 PLA

PLA is well-known aliphatic polyester having a methyl side chain attached to the polymeric backbone (Figure 2-3). This makes PLA more hydrophobic compared to PGA. High molecular weight PLA is obtained by ROP of lactide under mild conditions. PLA is mostly synthesized from renewable carbohydrate feedstocks such as sugar beet and corn.

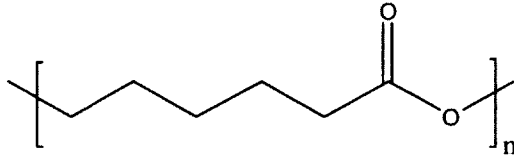


**Figure 2–3.** Structure of PLA

It has a hexagonal packing of chains in its unit cell (Henton, Gruber et al. 2005). PLA exhibits fairly high melting (around 160 °C) and glass transition (between 45-55 °C) temperatures (Van de Velde and Kiekens 2002). The mechanical properties of PLA are quiet similar to PGA, i.e., strong but brittle (Madhavan Nampoothiri, Nair et al. 2010). PLA also suffers from poor thermal stability ( $T_d= 270$  °C; Table 2-2).

### 2.2.1.3 PCL

PCL is obtained from ROP of  $\epsilon$ -caprolactone, which is a relatively inexpensive cyclic monomer obtained from petroleum resources. The structure of PCL is shown in Figure 2-4. PCL crystallizes into an orthorhombic crystal packing, similar to polyethylene (Bittiger, Marchessault et al. 1970). Thermal stability of PCL ( $T_d = 350$  °C) is higher than that of PLA and PGA (Labet and Thielemans 2009). PCL has lower melting and glass transition temperatures,  $\sim 60$  °C and  $-60$  °C respectively, compared to PGA and PLA. Mechanical properties of PCL are also lower than that of PLA and PGA. PCL is often used as a compatilizer or as blends with other polymers (Mochizuki and Hiramami 1998; Nair and Laurencin 2007).



**Figure 2–4.** Structure of PCL

It is seen that with increasing number of methylene groups from  $n=1$  to 5, i.e. from PGA to PLA and PCL, the melting temperature of the short chain polyesters decreases. The glass transition temperatures for the short chain polyesters also vary in a similar manner. However, the melting temperatures increased for medium and long chain polyesters from  $n=8$  to 19, as can be seen from Table 2-2. For the medium and long chain polyesters the glass transition temperatures increased beyond  $n=5$  (PCL), but were comparable for  $n=8$  to 14 (Table 2-2). The thermal stabilities of aliphatic polyesters increased with the number of methylene groups in their monomer units (Table 2-2) (Trzaskowski, Quinzler et al. 2011).

### **2.2.2 Linear aliphatic polyesters as analogues for polyethylene-like polymers**

Polyethylene (PE) is one of the most widely used commodity polymers. Its structural versatility enables an existence in different packing densities such as high density polyethylene (HDPE), low density polyethylene (LDPE), linear low density polyethylene (LLDPE) etc. HDPE exhibits high crystallinity, thermal stability (450-500 °C), flexibility ( $T_g = -120$  °C), and modulus (80-1100 MPa). HDPE however is not biodegradable.

Long chain linear aliphatic polyesters exhibit crystalline structure, thermal stability, phase transition behaviour and mechanical properties closer and/or comparable to that of HDPE (Table

2-2). This similarity is related to the longer methylene chain segments in these polyesters. In fact, long methylene segments provide significant crystallinity, improved melting, thermal stability and mechanical properties (Trzaskowski, Quinzler et al. 2011). Thus, as can be seen from Table 2-2, by further increasing the methylene chain lengths of the monomeric units, it is expected that the thermal and mechanical properties of aliphatic polyesters would approach to that of HDPE.

The enhancement in physical properties is one of the most important aspects that long chain P( $\omega$ -OHFA) provides over traditional aliphatic polyesters. Furthermore, the presence of hydrolysable ester linkages in these PE-like long chain aliphatic polyesters would render biodegradability. Therefore, these polymers could act potentially as PE's biodegradable alternative.

### **2.2.3 Biodegradability of aliphatic polyesters**

Aliphatic polyesters have gained significant attention owing to their susceptibility to biodegradation. According to the American Standards for Testing Materials (ASTM), biodegradation is defined as a process by which microorganisms, such as bacteria or algae, break down plastics to small and harmless substances such as water or carbon dioxide (ASTM D-6400-99). The ester linkages in aliphatic polyesters are hydrolysable, consequently these plastics could degrade in the environment, either naturally or chemically (Chandra and Rustgi 1998). Biodegradability is however dependent on several factors, such as polyester structure, molecular weight, crystallinity, etc. Aliphatic polyesters degrade through a mechanism so-called surface mechanism. In this mechanism, water is being absorbed by the polymer and hydrolytic ester cleavage occurs at the surface of the polymer matrix. This generates chain fragments and produces low molecular weight products (Palmisano and Pettigrew 1992).



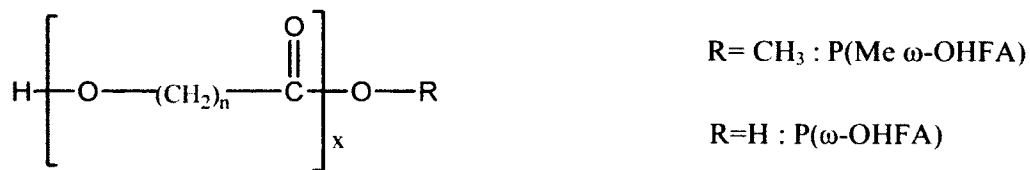
#### **2.2.4 Applications of aliphatic polyesters**

Linear aliphatic polyesters have been used in a wide range of diverse applications ranging from packaging to biomedical fields. The mechanical versatility, crystallinity, hydrophobicity and biocompatibility of aliphatic polyesters make them potential biomaterials for medical applications, such as tissue scaffolding and therapeutic drug delivery (Ulery, Nair et al. 2011). PLA, PGA (Athanasίου, Niederauer et al. 1996; Ulery, Nair et al. 2011) and poly( $\alpha$ -hydroxy acids)(Vert, Li et al. 1992) are some examples of biocompatible aliphatic polyesters particularly used in biomedical implants. Biocompatibility of these polyesters are related to the hydrolytic cleavage of ester groups to give decomposition products that are normal intermediates of cell metabolism(Vert, Li et al. 1992). PCL is the most commonly used aliphatic polyester for drug delivery applications(Albertsson and Varma 2002).

Aliphatic polyesters such as PLA obtained from corn starch have been increasingly used in the packaging industry because of their availability, sustainability, biodegradability and low price compared to polyethylene based materials (Auras, Harte et al. 2004).

#### **2.3 General introduction to poly( $\omega$ -hydroxyfatty acid)**

P( $\omega$ -OHFA)s are obtained by polycondensation of  $\omega$ -hydroxyfatty acid monomers generally derived from vegetable oils. These polyesters are a class of linear aliphatic polyesters consisting of ester and methylene ( $\text{CH}_2$ ) groups in the chain backbone with terminal hydroxyl and carboxylic acid/ester groups. Figure 2-5 shows the chemical structure of P( $\omega$ -OHFA)s.



**Figure 2-5.** Chemical structure of P( $\omega$ -OHFA)s

Ester terminated P( $\omega$ -OHFA)s, named as P( $\omega$ -Me-OHFA)s are obtained by replacing the carboxylic acid terminal group with an ester linkage in the backbone (Fig. 2-5). The ester group in P( $\omega$ -OHFA)s offers biodegradability by providing the hydrolytic chain cleavage at the ester linkages. The hydrophobic methylene  $-(\text{CH}_2)-$  segments offer desirable properties such as crystallinity, strength and stability for P( $\omega$ -OHFA)s.

Liu *et al.* (Liu, Kong et al. 2008) synthesized poly(9-hydroxynonanoic acid) from ROP of 9-hydroxynonanoic acid's dilactone. The poly(9-hydroxynonanoic acid) obtained exhibited a melting temperature at 70 °C were thermally stable up to 380 °C. The same group further investigated the physical properties of poly(9-hydroxynonanoic acid) in comparison with PCL. They noticed that the melting temperature for poly(9-hydroxynonanoic acid) is higher compared to PCL. The enzymatic biodegradation of the vegetable oil-based poly(9-hydroxynonanoic acid) was also investigated as an alternative for PCL in drug delivery applications (Abraham and Narine 2009).

Petrović *et al.* (Petrović, Milić et al. 2010) also compared the physical properties of Poly(methyl 9-hydroxynonanoate) ( $M_w = 62200$  g/mol) with PCL. Poly (methyl 9-hydroxynonanoate) obtained by polycondensation reaction exhibited higher melting and glass transition temperatures, as well as a greater thermal stability (refer to Table 2-2). Some of its mechanical properties were found to be in the range of HDPE. They also expected poly(methyl 9-

hydroxynonanoate) to exhibit improved biodegradability, and, therefore suggested replacing PCL with poly(methyl 9-hydroxynonanoate) for suitable applications.

Liu *et al.* (Liu, Liu et al. 2011) synthesized a further long chain poly( $\omega$ -hydroxytetradecanoic acid) P( $\omega$ -OHC14) from methyl  $\omega$ -hydroxytetradecanoate (Table 2-2). Thermal stability ( $T_d=450^\circ\text{C}$ ) and melting temperatures ( $T_m=96^\circ\text{C}$ ) of P( $\omega$ -OHC14) were found to be further closer to that of HDPE (Table 2-2). The P( $\omega$ -OHC14) Young's modulus varied with molecular weight also in a manner similar to that of HDPE. The same group also reported similar findings for poly( $\omega$ -pentadecalactone), a long chain aliphatic polyester with 14 methylene groups in the aliphatic back bone (Cai, Liu et al. 2010). It is therefore expected that the thermal stability, melting temperature and mechanical properties of P( $\omega$ -OHFA)s will increase by increasing the methylene chain length. Furthermore, P( $\omega$ -OHFA)s with sufficiently longer methylene chains are expected to demonstrate physical properties similar to HDPE.

### **2.3.1 ( $\omega$ -OHFA)s derived from petroleum resources**

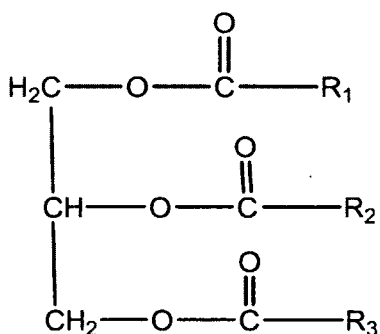
Industrial production of polyesters obtained from petroleum derived ( $\omega$ -OHFA)s having moderately stretched methylene chains are restricted due to the high cost and limited practical routes to their synthesis. The chemical routes for the synthesis of  $\omega$ -hydroxyfatty acids from petrochemical feedstock mostly includes hydrogenation by a hydro-cracking catalyst and (ROP) in the presence of an alkali metal catalyst (Otera 2004). These chemical routes however require multiple steps as well as harsh chemical reagents which limits their potential commercialization (Suzuki 1981; Yamanaka 1982). Vegetable oils, on the other hand, are an effective raw material to synthesize P( $\omega$ -OHFA)s, mainly because of high availability, low toxicity and low cost. Fatty

acids derived from vegetable oils are biologically safe (Ogawa, Kishino et al. 2005) and are a major source of  $\omega$ -hydroxyacid.

### 2.3.2 ( $\omega$ -OHFA)s derived from renewable resources (vegetable oil)

$\omega$ -hydroxyfatty acids are not naturally occurring substances; nevertheless, small amounts of them have been reported in the royal jelly of the honey bee and also in swine livers. These fatty acids however, has been prepared easily from renewable lipid sources such as vegetable oils (Lu, Ness et al. 2010).  $\alpha$ -hydroxyfatty acid (2-hydroxyfatty acid) and  $\beta$ -hydroxyfatty acid (3-hydroxyfatty acid) are obtained from mammalian and microbial lipids, respectively. They are important substances for the cosmetic industry, mostly used in moisturising and skin protection products.

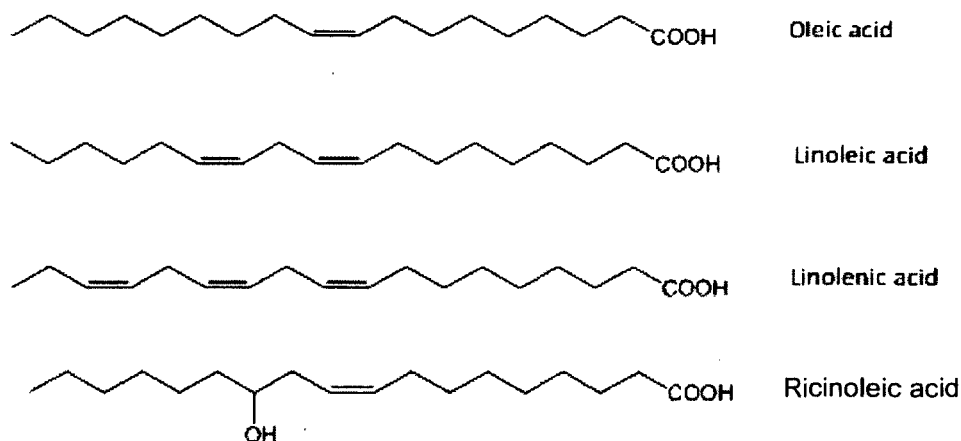
Chemically, vegetable oils consist of mainly triglycerides formed between glycerol and various fatty acids (Figure 2-6).



**Figure 2–6.** Structure of triglycerides ( $\text{R}_1$ ,  $\text{R}_2$  &  $\text{R}_3$  are long hydrocarbon chain).

Fatty acids are long straight-chain C16 and C18 carboxylic compounds with double bonds in most of them. The most important unsaturated fatty acids present in vegetable oils are oleic acid, linoleic acid, linolenic acid and ricinoleic acid (Figure 2-7). Canola oil, for example contains

around 55-75% of oleic acid along with other unsaturated fatty acids. The reactive functional groups as well as the C-C double bonds in these long chain fatty acids enable the modification of the original fatty acid structure to give monomers suitable for polymerization. These long chain fatty acids can be extracted from lipids using a series of chemical reactions (Rodrigues, Gonçalves et al. 2007).



**Figure 2–7.** Structures of the most important fatty acids

Hydroxyfatty acid monomers obtained by the chemical modification of plant oils are attractive monomers for making polyesters with moderately stretched methylene chains, including P( $\omega$ -OHFA)s (Liu, Kong et al. 2008; Abraham and Narine 2009).

#### **2.4 Introduction to methods and mechanisms for synthesis of ( $\omega$ -OHFA)s**

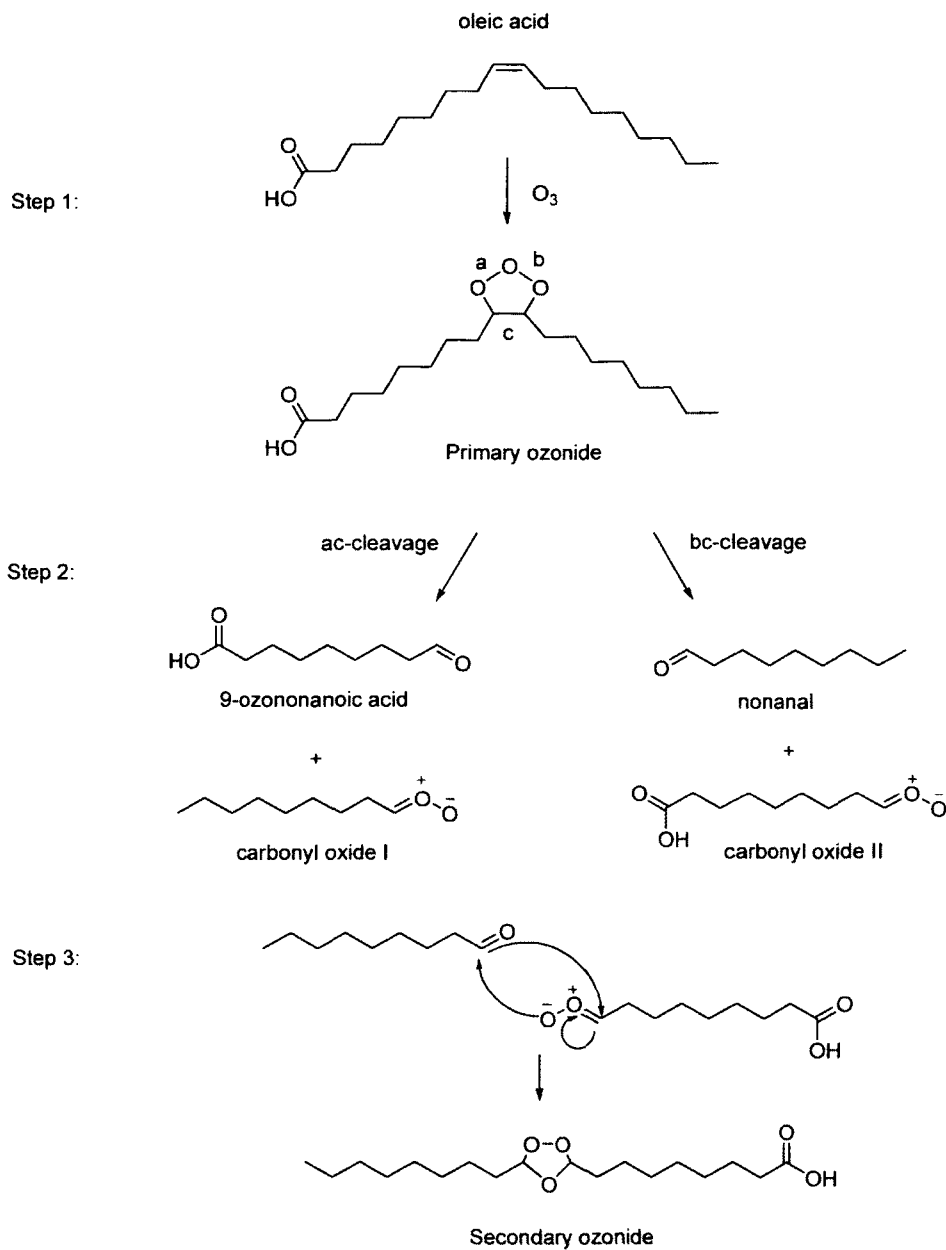
Triglycerides are chemically transformed into long chain  $\omega$ -hydroxyfatty acids by functionalization reactions at the double bonds of the unsaturated fatty acids. Ozonolysis, oxidation, reduction etc., are some of the most important functionalization reactions performed to obtain  $\omega$ -OHFAs. Carbon-carbon double bond in the fatty acid structure can be changed to

hydroxyl groups by ozonolysis followed by a subsequent reduction to give  $\omega$ -OHFAs. Cross metathesis of unsaturated fatty acids followed by reduction is another example for chemical routes adopted to make  $\omega$ -OHFA monomers. Details of these reactions are discussed in the following sections.

#### **2.4.1 Ozonolysis**

Ozone ( $O_3$ ) is a tri-atomic molecule and a colorless gas that has very strong oxidizing properties. It is a well-known environmentally acceptable oxidant because of the absence any harmful side-products generated during the process (Griffith 2001). Ozonolysis has been found to be a useful route for oxidative cleavage of double bonds in lipid compounds. Ozone reacts exclusively with the carbon-carbon double bond, without affecting any other functional groups in the lipid chain. The ozonolysis of lipid-based compounds has been extensively studied by our group (Kong, Yue et al. 2007; Narine, Kong et al. 2007; Narine, Kong et al. 2007; Narine, Yue et al. 2007; Hojabri, Kong et al. 2009; Zuo, Li et al. 2011).

Ozonolysis generally proceeds via a cyclo-addition reaction of ozone to the double bond to give a primary ozonide, followed by its decomposition to give aldehydes and carbonyl oxides. It is described by a simple three step mechanism (Vesna, Sax et al. 2009). Figure 2-8 gives the reaction scheme for the ozonolysis of oleic acid.

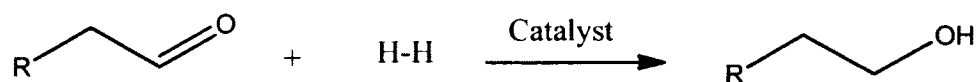


**Figure 2–8.** Three step reactions of ozonolysis of oleic acid. Step 1: formation of primary ozonide, step 2: fragmentation of primary ozonide to form aldehyde or ketone, step 3: recombination of carbonyl oxide to form secondary ozonide.

In step 1, ozone interacts with the double bond, and primary ozonide is formed. The primary ozonide undergoes fragmentation in step 2 to give aldehydes (or ketones) and carbonyl oxides, which are collectively, called Criegee intermediates (CI). The reactivity of CI is an important factor affecting the types of products and their distributions in this heterogeneous reaction. Two modes of fragmentation, determined by the position of the cleavage are possible in step 2 (Bailey and Ferrell 1978), (Harding and Goddard III 1978). Accordingly, the two different types of cleavages, named as “ac” and “bc” cleavages would lead to different types of carbonyl oxide-carbonyl pairs. In the ozonolysis of oleic acid (Figure 2-8), the ac-cleavage route gives 9-ozononanoic acid and a carbonyl oxide, and, the bc-cleavage route gives nonanal. In Step 3 the carbonyl oxide and aldehyde (or ketone) recombines to form the final ozonide, which is a secondary ozonide.

#### 2.4.2 Reduction of the ozonide

Ozonide can be further reduced to either aldehydes (ketones) or alcohols using suitable reducing agents. Some of well-known reducing agents are Lithium aluminum hydride ( $\text{LiAlH}_4$ ), Sodium borohydride ( $\text{NaBH}_4$ ), and hydrogenation in the presence of a metal catalyst. Figure 2-9 shows a general reaction scheme for the reduction of carbonyl compound obtained by ozonolysis in the presence of a reducing catalyst.



**Figure 2–9.** Reduction of ozonide product in the presence of catalyst.



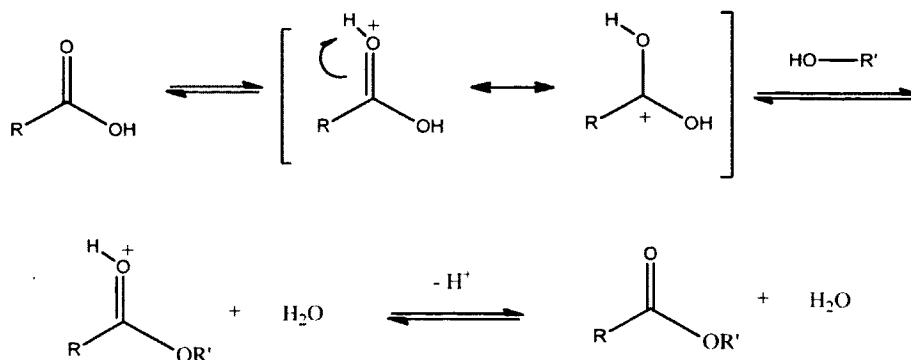
Sousa et al. (Sousa and Bluhm 1960) compared the yield for alcohols obtained by reducing oleic acid ozonide using  $\text{LiAlH}_4$  as well as  $\text{NaBH}_4$  and found that the yield increased when  $\text{LiAlH}_4$  (74%) was used as compared to  $\text{NaBH}_4$  (62%). Flippinet *al.* (Flippin, Gallagher et al. 1989) however observed that the efficiency of lithium aluminum hydride as reducing agent is limited in the presence of a variety of other functional groups. They also suggested that reduction using sodium borohydride is limited in the presence of highly polar solvents (Flippin, Gallagher et al. 1989).

Hydrogenation using a metal catalyst is another method for reducing ozonide to the corresponding alcohols. Hydrogenation is a chemical reaction between molecular hydrogen and the reactant molecule. With the exception of very rare cases, no reaction below 480 °C occurs between  $\text{H}_2$  and organic compounds in the absence of a metal catalyst (Ehwald, Shestov et al. 1994). Raney nickel has been known as a popular catalyst to produce polyol from vegetable oil (Narine, Kong et al. 2007; Narine, Yue et al. 2007; Liu, Kong et al. 2008). The molecular hydrogen reduces the oxygen atoms in the ozonide to give the corresponding alcohol in the presence of heat and Ni catalyst.

### **2.4.3 Esterification reaction**

Esterification involves the reaction between an alcohol and an acid to give an ester. Catalyst is often used to accelerate the reaction. The commonly used esterification reaction is Fischer Steglich esterification (Perveen, Yasmeen et al. 2010). Fischer esterification is an acid-catalyzed reaction of a carboxylic acid and a primary alcohol (Ganeshpure and Das 2007). Figure 2-10 show the reaction mechanism for Fischer esterification in the presence of acid catalyst. The first step involves protonation of the carbonyl oxygen, followed by the nucleophilic attack of the

alcohol. The alcohol added to the carbonyl atom and then water departs as a leaving group. The final de-protonation gives the ester product and regenerates the acid catalyst.

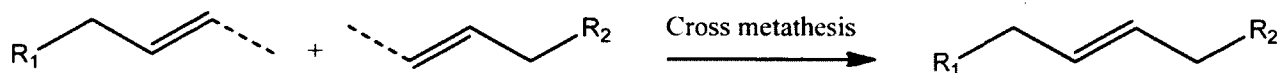


**Figure 2–10.** Fischer esterification mechanism

#### 2.4.4 Cross metathesis reaction

Metathesis is a chemical reaction involves the exchange of chemical species over a bond (or bonds). The bonding affiliations in the products, therefore are the same (or closely similar) to those in the reactants in terms of chemical structure. Molybdenum, titanium and tungsten metals have been used as a basic catalyst for metathesis reactions for a long time (Dolman, Hultsch et al. 2004; Mol 2004). These catalysts however had some drawbacks. They were sensitive to water and oxygen and their disposal were considered environmentally harmful. Olefin metathesis gained acceptance as a well-established process in petrochemical industry after the Nobel Prize winning study on the reaction mechanism and the discovery of efficient catalysts (Chauvin, Grubbs et al. 2006; Schrock 2006).

Figure 2-11 indicates a cross metathesis mechanism for a simple reaction. As can be seen, two alkene reactants exchange their species over the double bond and make an extended product having the same species involved in the reactants.



**Figure 2–11.** Cross metathesis reactions

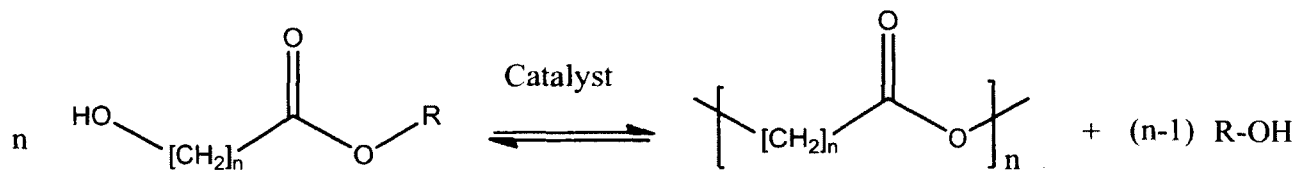
Olefin metathesis is a catalytic, solvent-free reaction performed under mild conditions. The development of first and second generation water-soluble ruthenium catalysts (Grubbs catalyst) enabled the synthesis of valuable and non-toxic unsaturated lipid derived compounds using metathesis (Kirkland, Lynn et al. 1998; Connon and Blechert 2002; Rybak, Fokou et al. 2008). The Grubbs catalyst is highly reactive and is extremely stable when exposed to water and/or air. The second generation Grubbs catalyst has been found to provide excellent results for the cross metathesis reactions between a series of unsaturated  $\alpha,\omega$  diester and methyl acrylate (Rybak and Meier 2007).

Hojabri *et al.* (Hojabri, Kong et al. 2010) prepared 1,18-Octadec-9-enedioic acid from oleic acid in high yield (64%) using self-metathesis reactions. The 1,18-octadec-9-endiol obtained by reducing the metathesis product was used further, as a monomer for making thermoplastic polyurethanes. The same group, using pure triolein as a model system, studied the role of reaction concentration on the Grubbs catalyzed metathesis of vegetable oil (Li, Hojabri et al. 2012).

#### **2.4.5 Introduction to melt polycondensation**

Polycondensation is a step-growth polymerization process, which involves a series of chemical reactions between bi-functional or multifunctional monomers to give polymeric condensates accompanied by the elimination of low molecular weight by-products (water, alcohol etc). Polycondensation leading to polyesters is also referred to as polyesterification and engages a

number of stepwise reactions between the hydroxyl and carboxyl functional groups of the reacting monomers. A general scheme for polyesterification of a hydroxyl acid monomer is shown in Figure 2-12.



**Figure 2-12.** Polycondensation of hydroxy acid derivative

Polyesterification is an equilibrium reaction and generally involves two phases; an esterification/transesterification phase followed by the polycondensation phase. The first phase, so-called pre-polymerization, proceeds through the formation of dimers, trimers, tetramers etc, by either esterification or transesterification reaction between the monomers. Esterification involves the reactions between an acid and hydroxyl functional groups, whereas in transesterification the reacting monomers are hydroxyl and ester functional groups. Most of the low molecular weight by-products would be eliminated in the first stage. The second phase is polycondensation. This phase is usually done at high temperatures (more than 200 °C) under vacuum (below 0.1 mm of Hg) so as to push the reaction forward by removing the condensation by-product. Suitable polycondensation catalysts, thermal stabilizers etc, are also used to obtain high molecular weight polyesters.

Polyesterification was first reported by Carothers in 1929. The pioneering studies by Carothers (Carothers 1929) and Flory (Flory 1946) paved the basis for systematic study on polycondensation reactions. The polyester chain length increases with conversion according to

Carothers equation (equation 2-1) (Flory 1953). Carothers equation explain the relationship between the degree of polymerization ( $\bar{X}_n$ ) and the extent of the reaction (p) :

$$\bar{X}_n = \frac{1}{1-p} \quad (2-1)$$

Where, p is the extent of the polymerization reaction and  $\bar{X}_n$  is the number average degree of polymerization, defined as the average length of monomeric units per polyester chain. The extent of polymerization depends on the stoichiometry of the reacting functional groups, reaction conditions etc. The highest molecular weight is obtained for a perfect 1:1 stoichiometry of the reacting functional groups.

Achieving high molecular weight polyester is one of the prime interests in polyesterification, in view of the improved physical properties exhibited by those polyesters. Generally, molecular weight of polymers is statistically expressed using the number average molecular weight  $\bar{M}_n$  and the weight average molecular weight  $\bar{M}_w$ . The number average molecular weight  $\bar{M}_n$  is defined as the total weight of a polymer sample divided by the total number of molecules in it. While,  $\bar{M}_w$  is the weight average molecular weight of the polymer and measure the size or weight of each polymer molecule.  $\bar{M}_n$  and  $\bar{M}_w$  are given by the following equations.

$$\bar{M}_n = \frac{\sum_i N_i M_i}{\sum_i N_i} \quad (2-2)$$

$$\bar{M}_w = \frac{\sum_i N_i M_i^2}{\sum_i N_i M_i} \quad (2-3)$$

where  $N_i$  is the number of polymer molecules having molecular weight  $M_i$ .

The relationship between  $\bar{M}_n$  and  $\bar{X}_n$  is given by equation 2-4.

$$\bar{M}_n = M_0 \times \bar{X}_n \quad (2-4)$$

Where,  $M_0$  is the average molecular weight of the repeating monomer units.

The distribution of the molecular masses in the polymer is often expressed as polydispersity index (PDI) and given by equation (2-5).

$$\text{PDI} = \bar{M}_w / \bar{M}_n \quad (2-5)$$

PDI value indicates the nature of distribution of molecular weights in a polymer sample, i.e., whether it has a broad or narrow distribution. A PDI value equal to 1 would suggest a mono disperse polymer. PDI values of synthetic polymers are mostly greater than 1. In the most step growth polymerizations  $\bar{M}_n \leq 30,000$  (g/mol) and PDI  $\sim 2.0$  is usually observed (Shibasaki, Araki et al. 2002).

The relationship between the polymer molecular weights and  $p$  is obtained from Carothers's equation as follows (equation 2-6 and 2-7).

$$\bar{M}_n = \frac{M_0}{1-p} \quad (2-6)$$

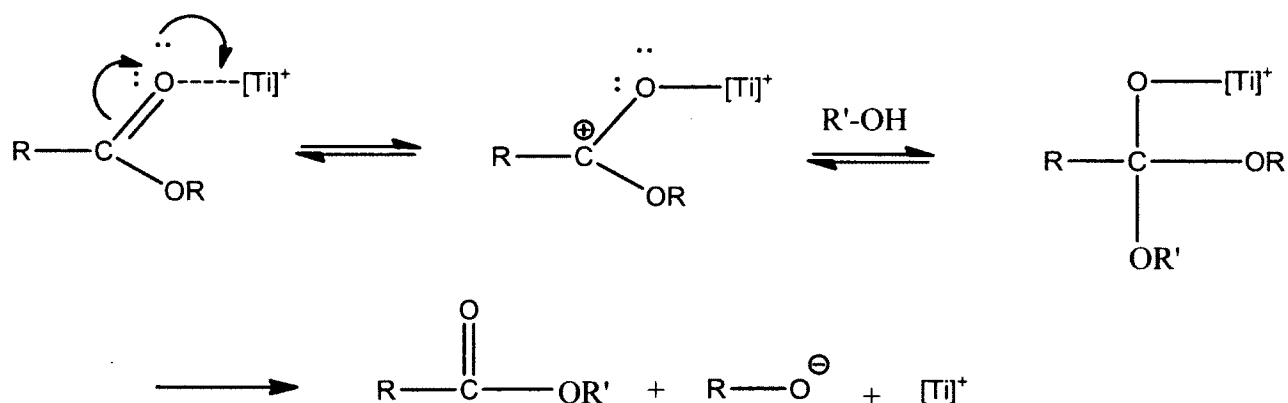
$$\bar{M}_w = \frac{M_0(1+p)}{1-p} \quad (2-7)$$

#### 2.4.6 Introduction to polycondensation catalysts

Catalysts are often used to obtain high molecular weight polyesters during polyesterification. Zinc acetate and manganese acetate are some examples for esterification/transesterification catalysts used for the first polymerization phase. Tomita *et al.* (Tomita and Ida 1973) compared the catalytic activity of zinc acetate and manganese acetate for transesterification between dimethyl terephthalate (DMT) and ethylene glycol (ET). A higher conversion was obtained with the manganese catalyst.

Titanium, antimony and tin-based compounds are the most reported catalysts used for the polycondensation (phase2). Shah *et al.* (Shah, Bhatta et al. 1984) investigated the effect of different metallic catalysts on the polycondensation of bis (hydroxyethyl) terephthalate to give polyethylene terephthalate (PET). The titanium-based catalyst was found the most effective. The order of the activities of various metallic catalyst varied as  $Ti > Sn > Sb > Mn > Pb$ . Similar findings were also noticed by Fradet *et al.* (Leverd, Fradet et al. 1987) for the polycondensation of octadecanoic acid and octadecanol. Recently, Liu *et al.* (Liu, Liu et al. 2011) used titanium isopropoxide ( $Ti(OiPr)_4$ ) for polycondensation of  $\omega$ -OHC14. The high catalytic activity, least environmental concerns and their acceptable prices for low-cost industrial processes favoured the widespread use of Ti derived catalysts for polyesterification.

The mechanism of the metallic catalyst in polycondensation is still poorly understood. Nonetheless, Ravindranath proposed a mechanism for catalytic polycondensation (MacDonald 2002). Figure (2-13) indicates a general mechanism of metal catalytic polycondensation.



**Figure 2–13.** Reaction schemes for the Ravindranath mechanism for a simple polycondensation reaction.

In the first step, the catalyst metal ion in the catalyst coordinates to the oxygen atom of the carbonyl group. The coordination of the ester carbonyl bond lowers the electron density of the carbonyl carbon atom and causes nucleophilic attack. The carbon atom of carbonyl group then is positively charged and the hydroxyl anion can attack the positively polarized carbonyl carbon to make an ester bond. The metal species goes through an intramolecular rearrangement. This process proceeds to obtain long polymeric chains and high molecular weight polymer.

Polyesterification catalyzed by non-metallic catalysts such as enzymes has also been of interest lately. Metal catalysts have some drawbacks such as decomposition of the metal ions at very high temperatures as well as the presence of metal might affect the biocompatibility of the polymer (Pang, Kotek et al. 2006). However, enzyme catalysts cannot provide a molecular weight as high as metal catalysts. Uyama *et al.* (Uyama, Yaguchi et al. 2000) studied the lipase-catalyzed polycondensation of divinyl sebacate diester and 1,4-butanediol and obtained the corresponding polyester having a molecular weight of 20,000 g/mol. The reaction was performed under mild conditions. However, the obtained molecular weight was too low for polymeric applications.



### 3 Synthesis and characterization of monomers

#### 3.1 Introduction

In this study a group of  $\omega$ -hydroxyl fatty acids ( $\omega$ -OHFA)s and methyl esters ( $\omega$ -Me-OHFA)s with different numbers of carbon atoms were synthesized from lipid based components. These are 9-hydroxynonanoic acid ( $C_9H_{18}O_3$ ) ( $\omega$ -OHC9), methyl 9-hydroxynonanoate ( $C_{10}H_{20}O_3$ ) ( $\omega$ -Me-OHC9), 13-hydroxytridecanoic acid ( $C_{13}H_{26}O_3$ ) ( $\omega$ -OHC13), methyl-13-hydroxytridecanoate ( $C_{14}H_{28}O_3$ ) ( $\omega$ -Me-OHC13), 18-hydroxyoctadecanoic acid ( $C_{18}H_{36}O_3$ ) ( $\omega$ -OHC18) and methyl 18-hydroxyoctadecanoate ( $C_{19}H_{38}O_3$ ) ( $\omega$ -Me-OHC18).  $\omega$ -OHC9 and  $\omega$ -Me-OHC9 were synthesized by ozonolysis followed by reduction of methyl oleate over Raney nickel. ( $\omega$ -OHC13) was similarly synthesized from purified erucic acid. To produce ( $\omega$ -Me-OHC13), erucic acid was first converted to methyl erucate through an acid catalyzed esterification reaction followed by ozonolysis and reduction. ( $\omega$ -OHC18) and ( $\omega$ -Me-OHC18) were synthesized by cross-metathesis of methyl oleate and oleyl alcohol.

#### 3.2 Materials

Erucic acid (90% purity), methyl oleate (70% purity), oleyl alcohol (85% purity), Raney nickel 2800 (slurry in water), sodium sulfate (anhydrous) ( $Na_2SO_4$ ), sodium hydroxide and filter agent Celite®545 were purchased from Sigma-Aldrich. The solvents used in this study were used without further purification. Ozone was generated from an Azcozon Model RMU-DG3 ozone generator (AZCO Industries Limited) which was connected to a PSA Model Topaz oxygen generator (AirSep® Corporation). Molecular sieve type 3A was purchased from Fisher. Silica gel

(230-400 mesh) was obtained from SiliCycleInc, QC, Canada. TLC plate (60Å) was also obtained from SiliCycle Inc.

### **3.3 Synthesis procedure of monomers**

#### **3.3.1 Methyl 9-hydroxynonanoate ( $\omega$ -Me-OHC9)**

##### ***Ozonolysis***

Methyl oleate (30 g, 0.1 mol) was dissolved in 200 mL of anhydrous ethyl alcohol. The solution was placed in a three neck flask equipped with a magnetic stirrer, inlet for ozone, and outlet for gas. The whole system was maintained at  $-5\text{ }^{\circ}\text{C}$  using an ice-salt bath. Ozone (concentration was  $62.0\text{ g/m}^3$ ) was bubbled into the reaction mixture with a flow rate of 5 L/min from an AZCOZON ozone generator (Azco Industries Limited). The reaction temperature was controlled to be lower than  $5\text{ }^{\circ}\text{C}$  and the reaction was monitored by thin layer chromatography (TLC) until the starting material was completely reacted. After 35 min, the ozone generator was shut off and the flask was purged with nitrogen for 10 min to remove any ozone residues in the reactor vessel. 200 mL of anhydrous ethyl alcohol was then added to the ozonide product.

##### ***Reduction***

Raney nickel catalyst (5.0 g, slurry in water) was added to the ozonide product in a hydrogenation vessel (600 mL, Parr Instrument Co.) equipped with a mechanical stirrer. First, the reaction vessel was purged with nitrogen gas and then charged with hydrogen to 100 psi and  $70\text{ }^{\circ}\text{C}$ . After 4 h, the hydrogen flow and heat were shut off and the reaction vessel was allowed to cool down to room temperature. The reaction vessel was finally purged with nitrogen gas to remove any residues of hydrogen. The resulting mixture was filtered through filter agent

Celite®545 in a Buchner funnel. The filtrate was then transferred to a flask, and solvent was removed by rotary evaporation.

### ***Chromatography***

Column chromatography was used to purify the resulting mixture by using a hexane/ethyl acetate eluting solvent (30:1, 20:1, 15:1, 10:1, and 5:1) to obtain 16 g of ( $\omega$ -Me-OHC9).

### **3.3.2 9-Hydroxynonanoic acid ( $\omega$ -OHC9)**

In order to synthesize ( $\omega$ -OHC9), the ( $\omega$ -Me-OHC9) that was previously obtained was saponified using 100 mL of sodium hydroxide solution (8%). The reaction was performed under reflux at 80°C for 3 hrs. The resulting mixture was then cooled down to room temperature and washed by ether (3×100). The aqueous layer cooled down to 0°C and then acidified by 8 mL concentrated HCl (36.5%). The acidified mixture was then extracted with ether (4×250). The ether layers were combined and washed by brine (3×100). The solution was then dried over magnesium sulfate and concentrated by rotary evaporation.

### **3.3.3 13-Hydroxytridecanoic acid ( $\omega$ -OHC13)**

The same procedure of ozonolysis-reduction-purification described in section 3.3.1 was done for a mixture of erucic acid (30 g, 0.1 mol.) and anhydrous ethyl alcohol (200 mL).

### **3.3.4 Methyl 13-hydroxytridecanoate ( $\omega$ -Me-OHC13)**

#### ***Synthesis of methyl erucate***

Erucic acid (50 g, 0.14 mol.) was dissolved in 350 mL dry methanol in a three neck 1 L round bottomed flask. The esterification reaction is reversible; therefore, the reaction must be performed with an excess amount of solvent. The mole ratio of acid to alcohol used was 1:60. 10

mL of hydrochloric acid (37%) was added as a catalyst. In order to absorb the water produced from the reaction; molecular sieve type 3A (10 g) was also added to the flask. The entire reaction was kept under reflux at 55°C and stirred for 4h. Thin layer chromatography (TLC) was used to monitor the progress of the reaction until the starting material was depleted. The reaction was then cooled down to room temperature by removing of the oil bath and quenched by adding 350 mL distilled water.

The resulting mixture was extracted by 2 × 200 mL of ethyl acetate. Afterward, the ethyl acetate phase was washed by brine, and dried over Na<sub>2</sub>SO<sub>4</sub>. The crude products were collected by removing the solvent under pressure. The desired product was purified by column chromatography hexane/ethyl acetate eluting solvent (30:1).

#### ***Ozonolysis-Reduction***

The pure methyl erucate obtained from the column, was transferred for ozonolysis-reduction reactions using the same procedure as described in section 3.3. Final purification was by column chromatography using a hexane/ethyl acetate eluting solvent (10:1)

### **3.3.5 Methyl 18-Hydroxyoctadecanoate ( $\omega$ -Me-OHC18)**

#### ***Cross metathesis reaction***

Methyl oleate (30.0 g, 0.1 mol) and oleyl alcohol (30.0 g, 0.1 mol) were transferred into a 500 mL three-necked round-bottomed flask equipped with a magnetic stirrer. The reaction mixture was stirred at 45 °C under nitrogen gas for 30 min. Grubbs catalyst, second generation (100 mg), was then added to reaction mixture. After 24 h, it was quenched with ethyl vinyl ether (10 mL), and excess ether was removed by rotary evaporation. The resulting mixture was then purified and the desired product was obtained from other by-products listed as alkene, diester, dialcohol

as well as the un-reacted starting material. Column chromatography was used for purification of the main product by hexane/ethyl acetate eluting solvent (10:1).

### ***Hydrogenation***

The purified product from the metathesis reaction was then reduced over Raney nickel 2800 (slurry in water). The mixture was added into the hydrogenation vessel by adding 5 g Raney nickel and 200 ml excess ethanol. First, the reaction vessel was purged with nitrogen gas and then charged with hydrogen at 100 psi and 85°C for 4 h. Temperature and pressure were slightly increased during the reaction up to 120°C and 125 psi. The reaction mixture was filtered using filter agent Celite®545 in a Buchner funnel. The product was then concentrated under pressure.

#### **3.3.6 18-Hydroxyoctadecanoic acid ( $\omega$ -OHC18)**

The obtained ( $\omega$ -Me-OHC18) was saponified by 100 mL of sodium hydroxide solution (8%) as described in 3.3.2.

### **3.4 Characterization techniques**

#### **3.4.1 Nuclear Magnetic Resonance**

NMR spectroscopy is a technique used to determine a compound's unique structure. One dimensional (1D)  $^1\text{H}$  NMR was used to qualitatively analyze the synthesized products in this study. Data was recorded at a Larmor frequency of 400 MHz, using a Varian Unity 400 NMR spectrometer (Varian, Inc., Walnut Creek, U.S.A.). Deuterated chloroform ( $\text{CDCl}_3$ ), which has a chemical shift of 7.26 ppm was used as a solvent.

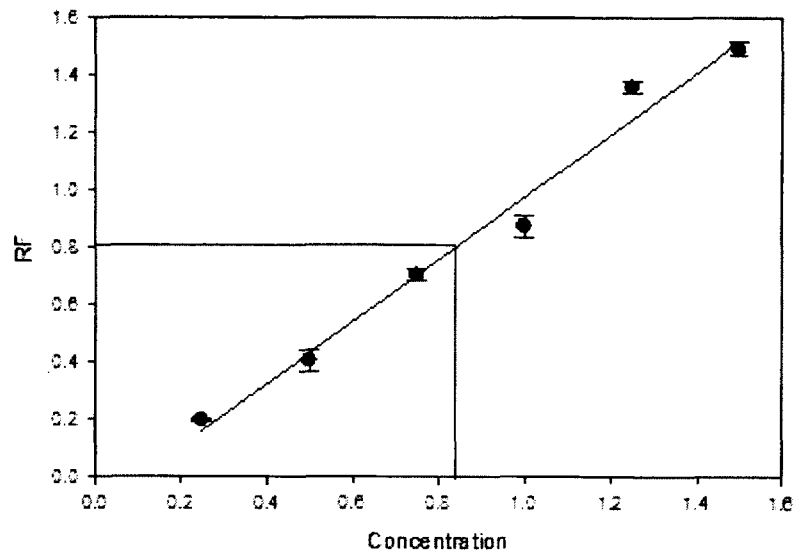
### **3.4.2 Mass spectrometry**

Further confirmation of the identity of each sample was obtained by mass spectrometry. Mass Spectra were acquired on a Quattro LC (Micromass) electro spray ionization (ESI) mass spectrometer with a syringe pump (Harvard). The photomultiplier detection system was used to detect the transmitted ions, and the signals were presented by the Mass Lynx 3.5 data system.

NMR and Mass Spectrometry (MS) are complementary techniques: while MS can tell the weight (and thus the molecular formula) of a molecule, NMR can differentiate between structural isomers and provide information about connectivity between atoms within a molecule. The  $^1\text{H}$  NMR and MS spectrum of each monomer is represented in appendix A and B respectively.

### **3.4.3 High performance liquid chromatography**

The purity of each sample of monomers was determined using High Performance Liquid Chromatography (HPLC) (WATERS 2424, ELS detector). HPLC is a separation technique that can identify a component or a mixture sample. For HPLC analysis, it is often necessary to generate a calibration curve by injecting standards of several known concentrations and computing response factors based on the linear regression of a plot of peak area versus concentration. In this study, HPLC calibration curves were generated for each monomer, using Tristearin (triglyceride) as an internal standard. This internal standard was chosen based on high purity (100%), different retention time with corresponding samples as well as having no interaction with the sample. Figure 3-1 shows a typical HPLC calibration curve. Each sample must be identified by its own calibration curve. As shown in Figure 3-1, by obtaining the response factor (RF) of each sample from HPLC, the corresponding concentration will be obtained from calibration curve. HPLC calibration curves for each synthesized monomer are represented in Appendix C.



**Figure 3-1.** A typical HPLC calibration curve (this curve is for ( $\omega$ -Me-OHC18)).

### 3.5 Result and discussions

#### 3.5.1 Methyl 9-hydroxynonanoate ( $\omega$ -Me-OHC9)

Methyl 9-hydroxynonanoate ( $\omega$ -Me-OHC9) was successfully synthesized from methyl oleate in a relatively high yield (84%) and high purity (97%). The yield was calculated by the theoretical yield divided by the actual yield. The purity of the product was determined by HPLC calibration curve. Since the product was made from different batches of experiments; each batch was compared with an internal standard to confirm the high purity of the sample (See appendix C).

Figure 3-2 shows the ozonolysis process of methyl oleate. The ozonolysis reaction is used to cleave the double bond in methyl oleate. As shown in Figure 3-2, the nucleophilic  $\pi$  electrons of C=C bond are attacked by the electrophilic electrons of the ozone oxygen atom. The other terminal oxygen atom in the ozone molecule which is partially negatively charged also attack to C=C, resulting in a second C-O bond. An unstable cyclic intermediate species is then produced which can re-arrange to the ozonide compound (Figure 3-2). Finally, the ozonide decomposes to two carbonyl terminated molecules. By reduction of the ozonide with Ni catalyst, the two carbonyl compounds were converted to alcohol-terminated molecules: Nonanol and  $\omega$ -Me-OHC9 as shown in Figure 3-2.

In the reduction step, each  $H_2$  molecule absorbs on the active sites on the surface of the metal catalyst e.g. Ni and converts to two positively charged hydrogen atoms. The carbonyl terminated compounds also attach to the metal surface and results in hydrogen transfer to the carbon atom. This mechanism was first proposed by Horiuti and Polanyi for the reduction of ethene with hydrogen on a nickel surface (Horiuti and Polanyi 1934) and has become a common mechanism



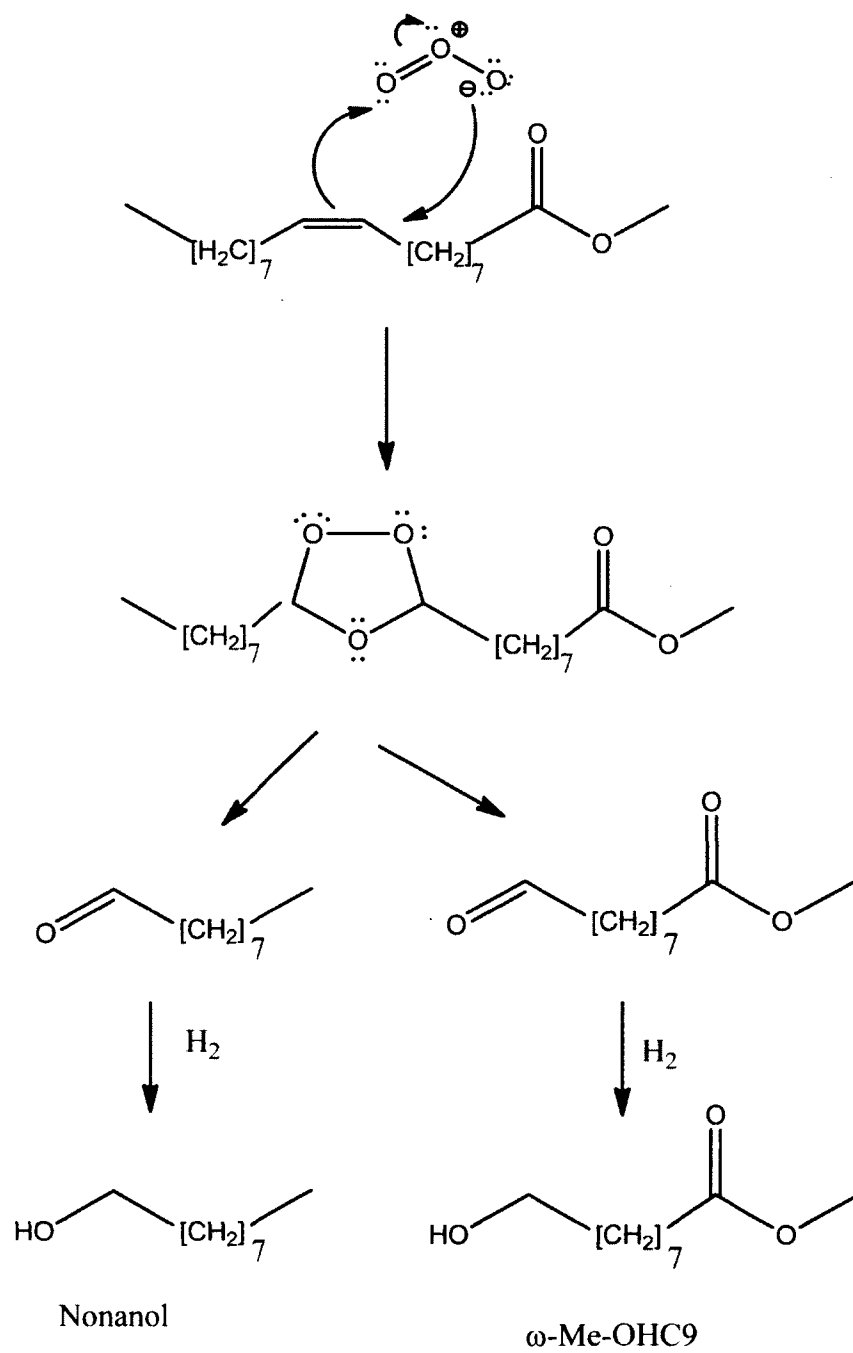
in terms of hydrogenation of unsaturated, cyclic compounds and even heavy aromatic hydrocarbons. Muetterties *et al.* (Muetterties and Bleeke 1979) used the same mechanism for hydrogenation of aromatic hydrocarbons. Siegel *et al.* (Siegel and Smith 1960) also used the Horiuti and Polanyi mechanism for hydrogenation of cyclic olefins in the presence of platinum catalysts.

N-nonanol is the by-product of the process obtained in a moderate yield (78%) and high purity (98%). N-nonanol is an expensive and valuable by-product which was kept for future experiments.

The structure of  $\omega$ -Me-OHC9 was strongly confirmed by  $^1\text{H}$  NMR and further analyzed by mass spectrometry (Appendix A and B). The chemical shifts of  $\omega$ -Me-OHC9 structure obtained are as follows:

$^1\text{H}$  NMR ( $\text{CDCl}_3$ , 400 MHz)  $\delta$  (ppm): 3.63-3.60 (s, 3H,  $\text{OCH}_3$ ), 2.30-2.25 (t, 2H,  $\text{CH}_2\text{OH}$ ), 1.61-1.55 (m, 2H,  $\text{CH}_2\text{COO}$ ) 1.56-1.50 (m, 2H,  $\text{CH}_2\text{CH}_2\text{COO}$ ), 1.29-1.27 (m, 8H,  $\text{CH}_2$ ).

MS (ESI): calculated for  $\text{C}_{10}\text{H}_{20}\text{O}_3$  188.2, found  $m/z$  206.2 ( $[\text{M}+\text{NH}_4]^+$ ).



**Figure 3–2.**  $\omega$ -Me-OHC9 synthesized from methyl oleate via ozonolysis and hydrogenation.

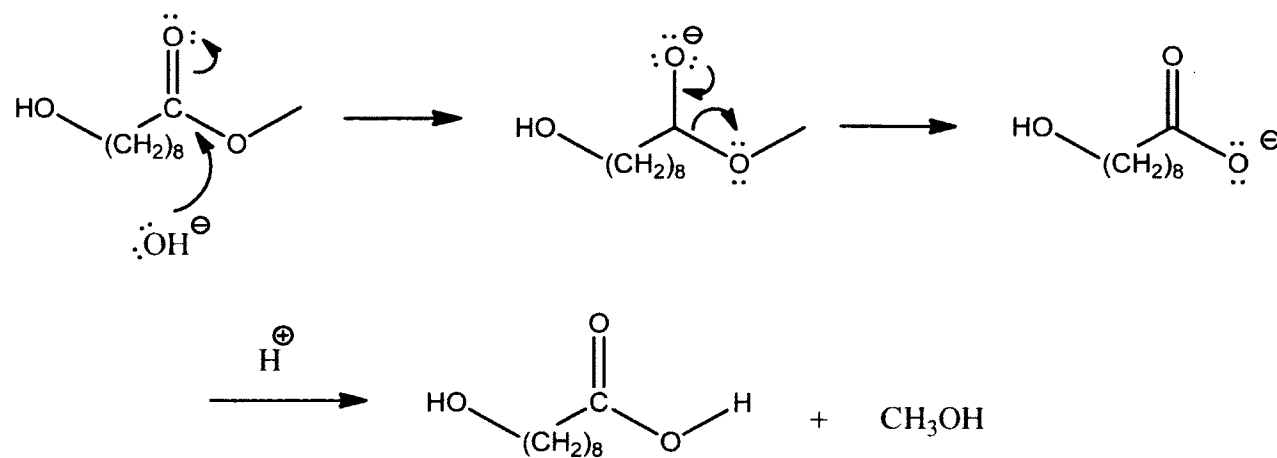
### 3.5.2 9-Hydroxynonanoic acid ( $\omega$ -OHC9)

9-Hydroxynonanoic acid ( $\omega$ -OHC9) was synthesized from  $\omega$ -Me-OHC9 through a saponification reaction. In the saponification process  $\omega$ -Me-OHC9 was hydrolyzed with sodium hydroxide to produce sodium-9-Hydroxynonanoate which can also act as a surfactant. Figure 3-3 shows the mechanism of the saponification reaction of  $\omega$ -Me-OHC9 with sodium hydroxide. In this reaction the nucleophilic hydroxyl group is attacked by the electrophilic carbon atom of  $\omega$ -Me-OHC9. This process leads to a cleavage in the C=C bond and produces a tetrahedral intermediate species. The intermediate molecule then re-forms the C=O by losing the alkoxide anion ( $\text{H}_3\text{C-O}^-$ ) and producing a carboxylic acid. The reaction was relatively high yielded (78%) and the product was obtained with high purity (96.5%).

Saponification by sodium hydroxide is a quite well known reaction in the field of lipid-based compounds. Chu *et al.* (Stoffel, Chu et al. 1959) found saponification a reliable process to form long chain fatty acid methyl esters. Schutter *et al.* (Schutter and Dick 2000) also used the saponification reaction by sodium hydroxide to make fatty acid methyl esters (FAME)s from the corresponding long chain fatty acids.

$^1\text{H}$  NMR ( $\text{CDCl}_3$  400 MHz)  $\delta$  (ppm): 3.65 (t, 2H,  $\text{CH}_2\text{OH}$ ), 2.35 (m, 2H,  $\text{CH}_2\text{COOH}$ ), 1.65 (m, 2H,  $\text{CH}_2\text{CH}_2\text{COOH}$ ), 1.55 (m, 2H,  $\text{CH}_2\text{CH}_2\text{OH}$ ), 1.35 (s, 8H,  $\text{CH}_2$ ).

MS (ESI): calculated for  $\text{C}_9\text{H}_{18}\text{O}_3$  174.2, found  $m/z$  192.2 ( $[\text{M}+\text{NH}_4]^+$ ).



**Figure 3–3.** Synthesis of  $\omega$ -OHC9 from  $\omega$ -Me-OHC9 by saponification.

### 3.5.3 13-Hydroxytridecanoic acid ( $\omega$ -OHC13)

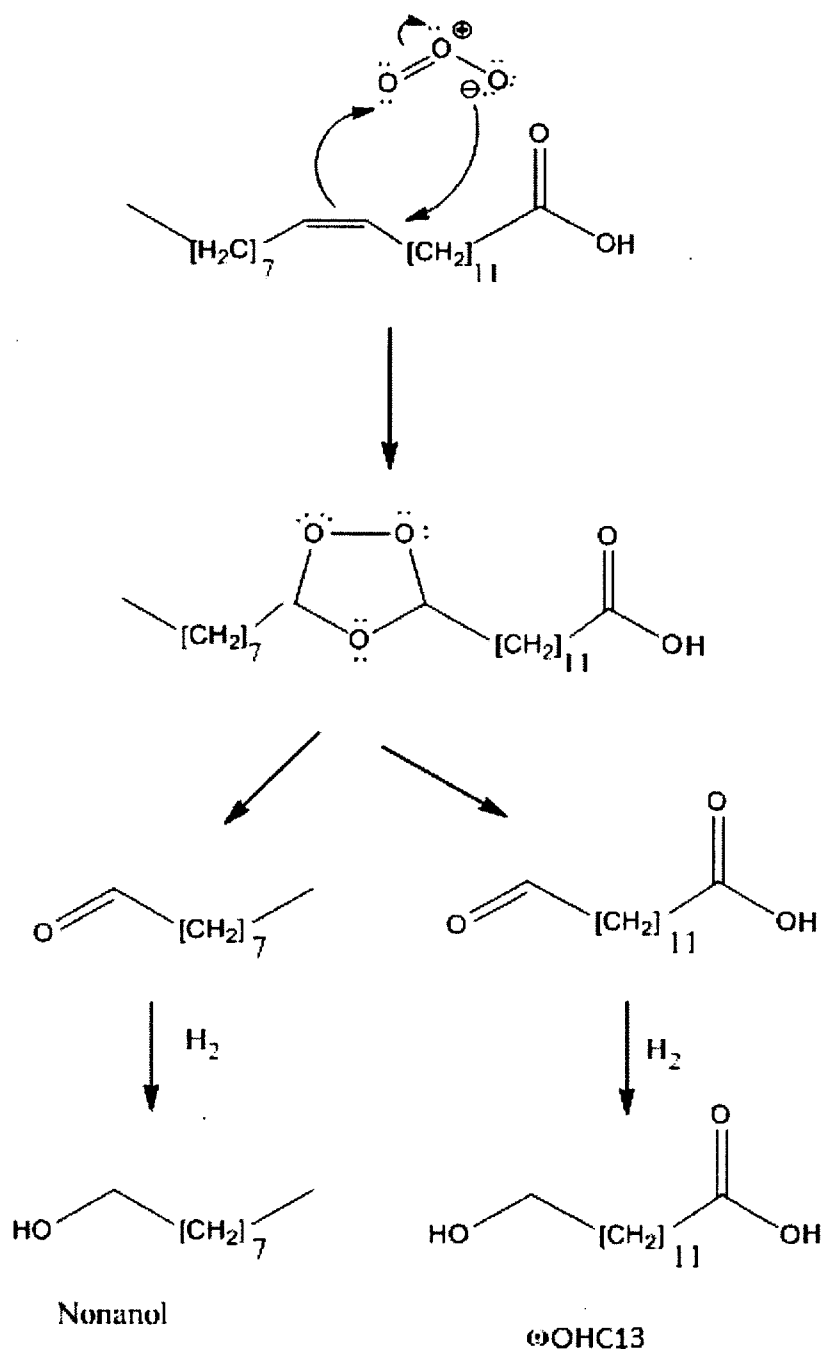
13-hydroxytridecanoic acid ( $\omega$ -OHC13) was synthesized from purified erucic acid following an ozonolysis-reduction procedure. The mechanism of the reaction is the same as discussed in 3.4.1 (Figure 3-2). The yield was moderately high (81%) with high purity (97%) using HPLC calibration curve. N-nonanol was again the side-product which was collected in relatively high yield (85%) and high purity (95%). The schematic synthesis of  $\omega$ -OHC13 is shown in Figure 3-4. The confirmation of structure of  $\omega$ -OHC13 was also obtained by  $^1\text{H}$  NMR and mass spectrum.

$^1\text{H}$  NMR ( $\text{CDCl}_3$ , 400 MHz)  $\delta$  (ppm): 3.63-3.61 (t, 2H,  $\text{CH}_2\text{OH}$ ), 2.32-2.35 (t, 2H,  $\text{CH}_2\text{COO}$ ), 1.63-1.58 (m, 2H,  $\text{CH}_2\text{CH}_2\text{COO}$ ), 1.56-1.53 (m, 2H,  $\text{CH}_2\text{CH}_2\text{OH}$ ), 1.22-1.25 (m, 16H,  $\text{CH}_2$ ).

MS (ESI): calculated for  $\text{C}_{13}\text{H}_{26}\text{O}_3$  230.3, found  $m/z$  248.2 ( $[\text{M}+\text{NH}_4]^+$ ).

### 3.5.4 Methyl-13-Hydroxytridecanoate ( $\omega$ -Me-OHC13)

In order to obtain  $\omega$ -Me-OHC13, methyl erucate was first obtained from erucic acid through an esterification reaction. The mechanism which was used in this study was based on Fischer esterification. Fischer esterification is equilibrium, acid catalyzed reaction of carboxylic acids to synthesize ester-terminated compounds. Figure 3-5 shows the mechanism of the Fischer esterification of erucic acid. As shown in the figure, the electrophilic proton of the acid catalyst attaches to the oxygen atom of the carbonyl group. Afterward, nucleophilic attack of the alcohol produces a tetrahedral intermediate with two equivalent hydroxyl groups.



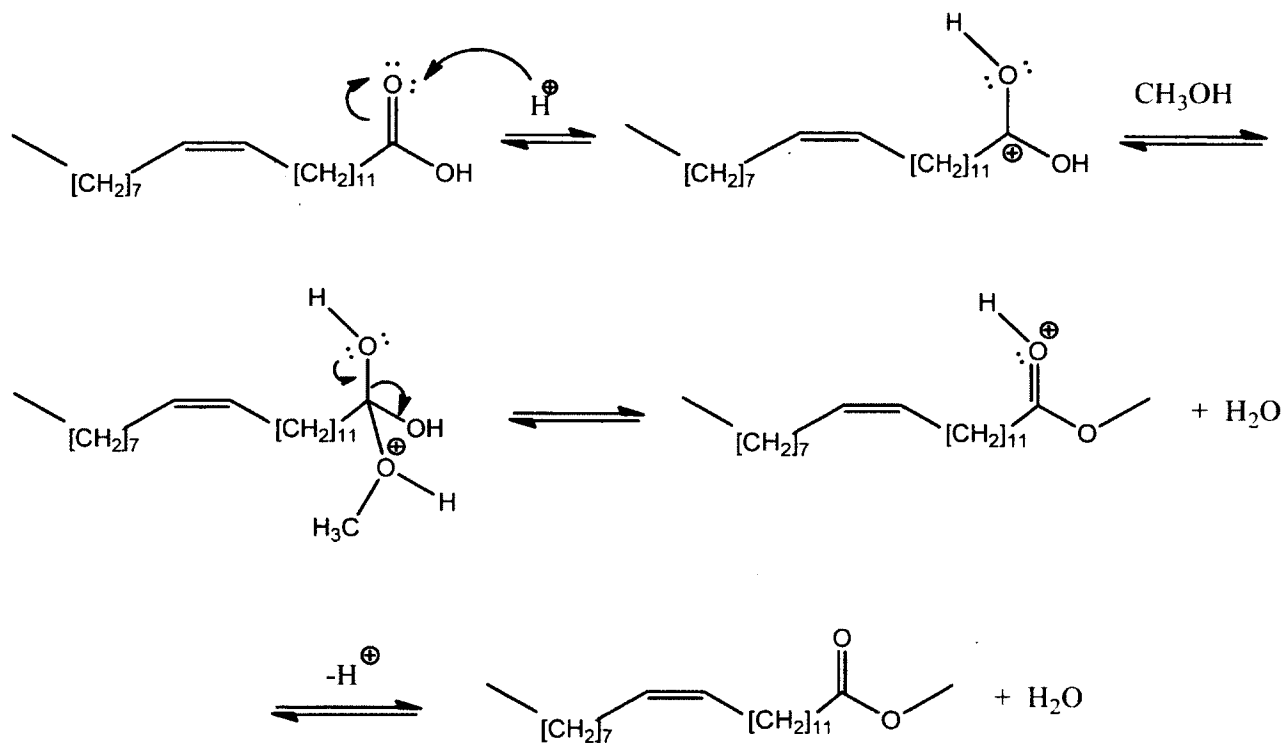
**Figure 3-4.** Synthesis of  $\omega$ -OHC13 from erucic acid via ozonolysis and hydrogenation.

One of the hydroxyl groups then removes by a proton shift to produce an ester molecule as well as water. Since esterification is an equilibrium reaction, the water must be removed from the reaction environment by using drying agents. The esterification reaction occurred in a high yield (94%) as shown in Figure 3-5.

Esterification is also one of the important reactions in biodiesel production from vegetable oils. Zhang *et al.* (Zhang and Jiang 2008) synthesized methyl ester from fatty acids through an acid catalyzed esterification reaction. The reaction proceeded in the presence of methanol and sulphuric acid as catalyst. The esterified product was then utilized as biodiesel. Santos *et al.* (Aranda, Santos et al. 2008) also studied acid catalyzed esterification of palm oil fatty acids. They compared different alcohols and demonstrated that methanol has a higher activity for esterification due to having a shorter chain length and higher polarity than the other alcohols used. Figure 3-6 shows the schematic synthesis of  $\omega$ -Me-OHC13 from methyl erucate by high yielding (82%) ozonolysis-reduction combination reactions. The mechanism of reaction is the same as shown in Figure 3-2. The purity of the product obtained from HPLC was determined to be 98%.

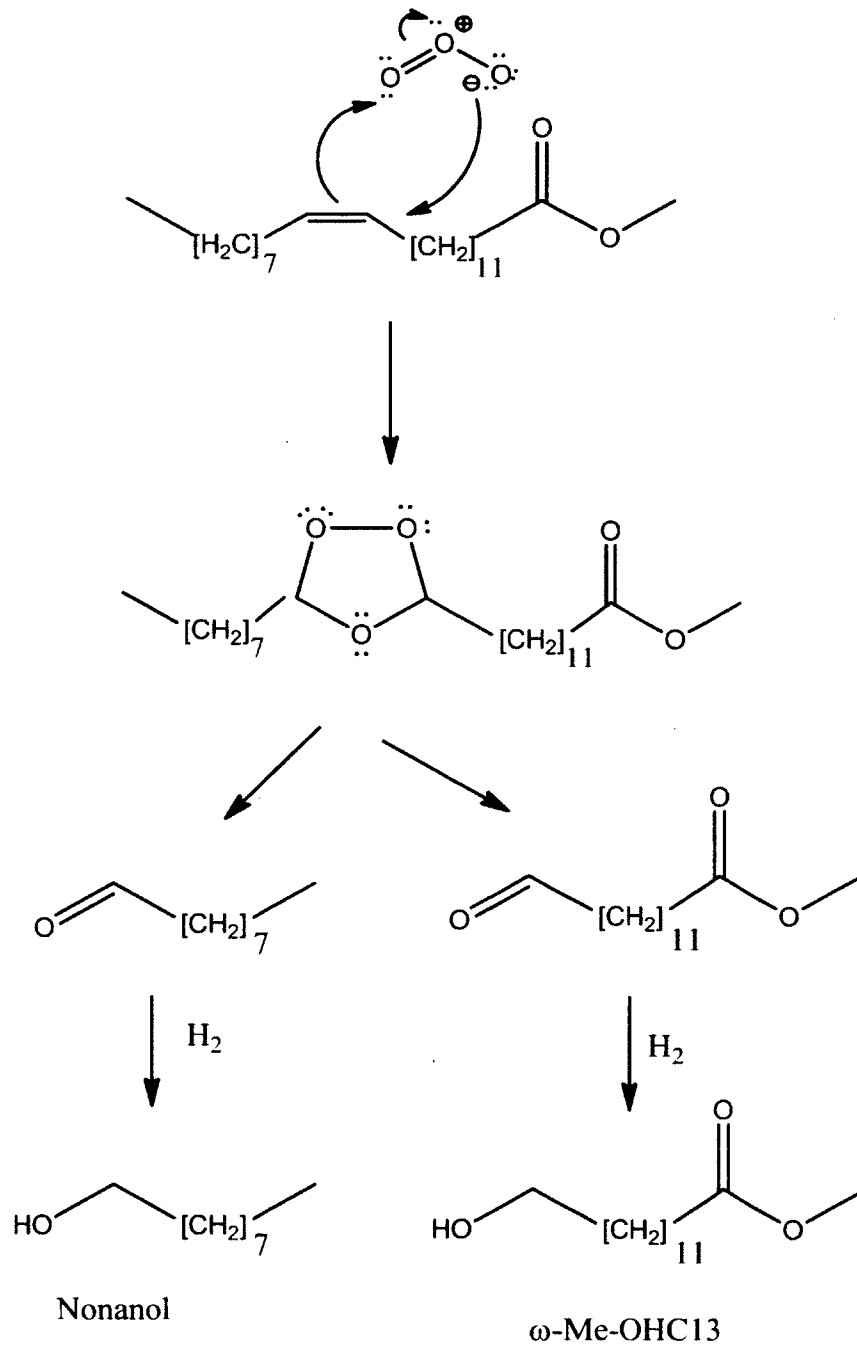
$^1\text{H NMR}$  ( $\text{CDCl}_3$ , 400 MHz)  $\delta$  (ppm): 3.64 (s, 3H,  $\text{OCH}_3$ ), 3.63-3.61 (t, 2H,  $\text{CH}_2\text{OH}$ ), 2.32-2.35 (t, 2H,  $\text{CH}_2\text{COO}$ ), 1.63-1.58 (m, 2H,  $\text{CH}_2\text{CH}_2\text{COO}$ ), 1.56-1.53 (m, 2H,  $\text{CH}_2\text{CH}_2\text{OH}$ ) 1.22-1.25 (m, 18H,  $\text{CH}_2$ ).

MS (ESI): calculated for  $\text{C}_{14}\text{H}_{28}\text{O}_3$  244.2, found  $m/z$  262.2 ( $[\text{M}+\text{NH}_4]^+$ ).



**Figure 3–5.** Synthesis of methyl erucate from erucic acid by Fischer Esterification





**Figure 3–6.** Synthesis of ω-Me-OHC13 from ozonolysis and hydrogenation of methyl erucate

### 3.5.5 Methyl 18-Hydroxyoctadecanoate ( $\omega$ -Me-OHC18)

Methyl 18-hydroxyoctadecanoate ( $\omega$ -Me-OHC18) was synthesized through a cross metathesis reaction between methyl oleate and oleyl alcohol, catalyzed by the second generation Grubbs catalyst. The catalyst consists of N-heterocyclic carbene (NHC) ligands which are large electron donating compounds. The general formula of second generation Grubbs catalyst is  $(\text{NHC})(\text{PCy}_3)(\text{Cl})_2\text{Ru}=\text{CHPh}$  (Cy is cyclohexyl and Ph is phenyl). The metathesis reaction basically relies on an exchange of species between the double bonds. A general mechanism which is well known for the cross metathesis reaction is based on the generation of a cyclic intermediate by attaching the metal ion of the catalyst to one of the unsaturated reactants. The cyclic intermediate then ruptures and attaches to the second reactant at the position of  $\text{C}=\text{C}$ . As such the formation of the cyclic intermediate drives the kinetics of the reaction. Generally, a cross metathesis reaction between two unsaturated molecules results in the production of six possible products, including un-reacted starting material and the various products of the reaction. Recently cross metathesis has become very attractive to chemists due to advantages it confers in the field of “green chemistry”. Metathesis is a clean, catalytic, solvent-free reaction performed under mild conditions. For example, Rybak *et al.* investigated the synthesis of  $\alpha,\omega$ -dicarboxylic acids and esters from unsaturated  $\alpha,\omega$ -diesters by cross metathesis using different catalysts (Rybak and Meier 2007). An exemplary review is provided by J.C. Mol, where the chemical routes to produce unsaturated fatty acid esters from lipid-based compounds are discussed. This publication emphasizes metathesis as a clean, green method useful for the oils and fats industry (Mol 2004).

Figure 3-7 shows the products of the cross metathesis reaction between methyl oleate and oleyl alcohol. The products include: (1) un-reacted methyl oleate, (2) un-reacted oleyl alcohol, (3) 18 carbons alkene, (4) 18 carbons diester, (5) 18 carbons diol and (6) unsaturated ( $\omega$ -Me-OHC18), the desired product. All these by-products are valuable and were collected in high purity. The theoretical yield of the cross metathesis reaction is generally low due to the production of such a multiplicity of by-products. The yield of unsaturated ( $\omega$ -Me-OHC18) was obtained around 40%. The purity of the main product after separation by column chromatography was determined by HPLC to be approximately 99%. Although the metathesis is a low yield reaction, the hydrogenation process was done in a high yield to obtain saturated  $\omega$ -Me-OHC18 (Yield = 88%).  $^1\text{H}$  NMR and mass spectrometry were strong evidence of structure of  $\omega$ -Me-OHC18.

$^1\text{H}$  NMR ( $\text{CDCl}_3$ , 400 MHz)  $\delta$  (ppm): 3.64 (s, 3H,  $\text{OCH}_3$ ), 3.62-3.59 (t, 2H,  $\text{CH}_2\text{OH}$ ), 2.30-2.26 (t, 2H,  $\text{CH}_2\text{COO}$ ), 1.56 (m, 2H,  $\text{CH}_2\text{CH}_2\text{COO}$ ), 1.25-1.23 (m, 26H,  $\text{CH}_2$ ).

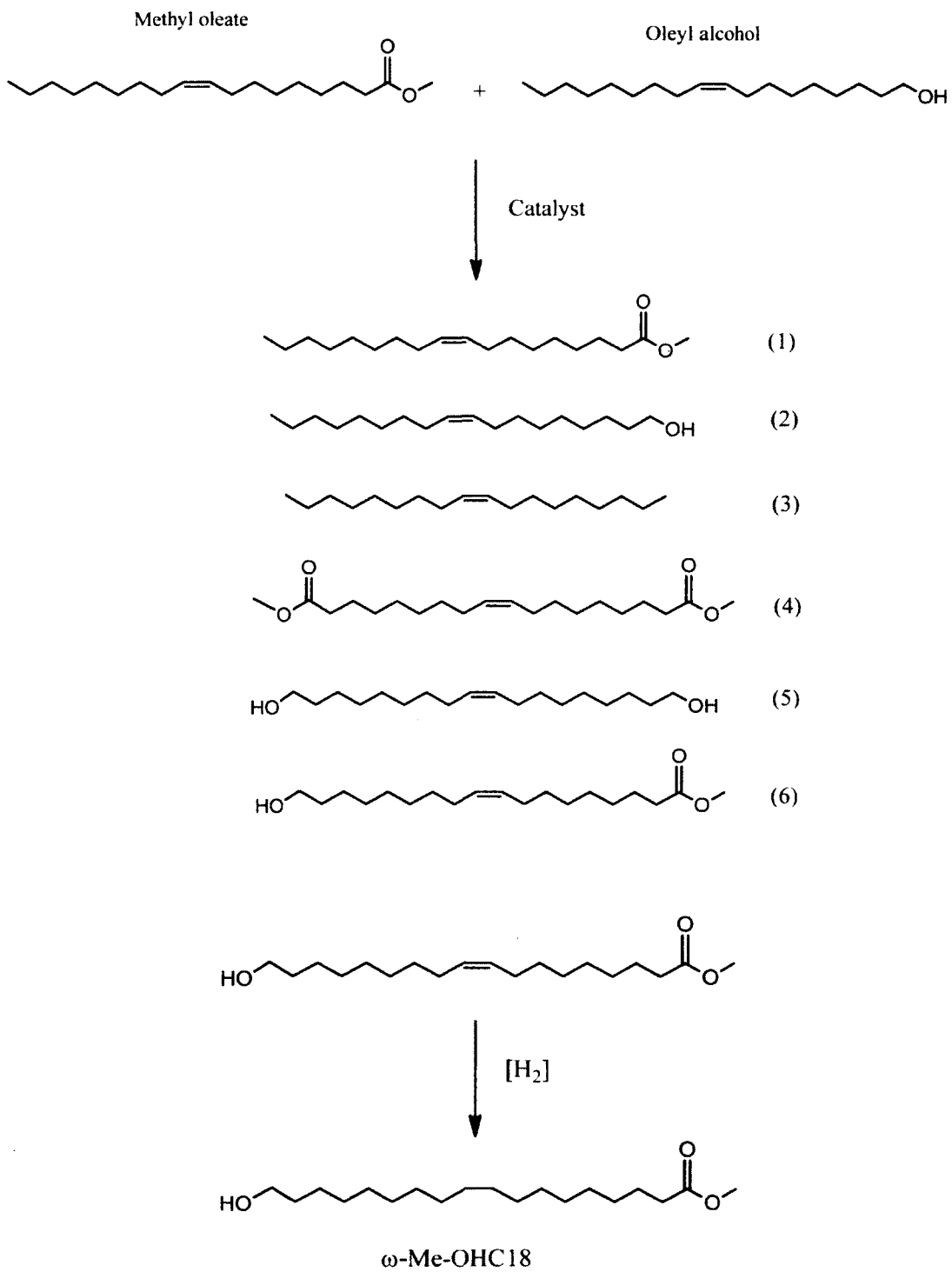
MS (ESI): calculated  $[\text{C}_{19}\text{H}_{38}\text{O}_3] = 314.4$  g/mol, found  $[\text{C}_{19}\text{H}_{38}\text{O}_3 + \text{NH}_4]^+ = 332.4$ .

### 3.5.6 18-Hydroxyoctadecanoic acid ( $\omega$ -OHC18)

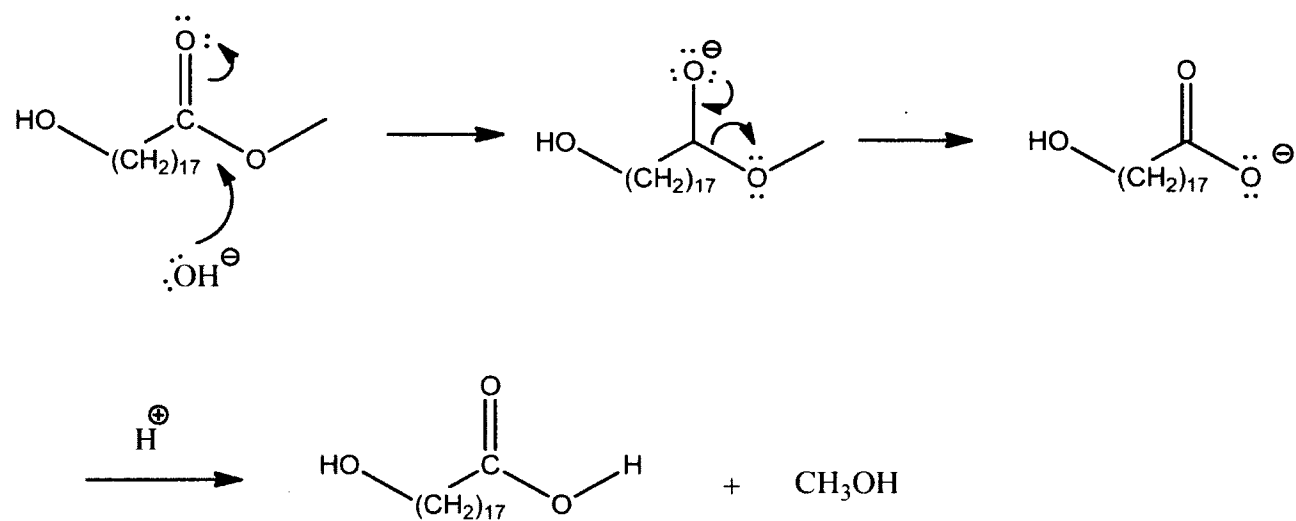
18-hydroxyoctadecanoic acid ( $\omega$ -OHC18) was synthesized through a saponification reaction of  $\omega$ -Me-OHC18 as indicated in Figure 3-8. The mechanism of the reaction is similar to that discussed in 3.4.2. The yield of the reaction was relatively high (80%) and as was purity of the product (97%) obtained from HPLC.

$^1\text{H}$  NMR ( $\text{CDCl}_3$ , 400 MHz)  $\delta$  (ppm): 3.61-3.64 (t, 2H,  $\text{CH}_2\text{OH}$ ) 2.31-2.35 (t, 2H,  $\text{CH}_2\text{COO}$ ), 1.58 (m, 2H,  $\text{CH}_2\text{CH}_2\text{COO}$ ), 1.55-1.53 (m, 2H,  $\text{CH}_2\text{CH}_2\text{OH}$ ), 1.25-1.23 (m, 26H,  $\text{CH}_2$ ).

MS (ESI): calculated  $[\text{C}_{18}\text{H}_{36}\text{O}_3] = 300.4$  g/mol, found  $[\text{C}_{18}\text{H}_{36}\text{O}_3 + \text{NH}_4]^+ = 318.3$  g/mol



**Figure 3–7.** Synthesis of  $\omega$ -Me-OHC18 from methyl oleate and oleyl alcohol using cross metathesis followed by hydrogenation.



**Figure 3–8.** Synthesis of  $\omega$ -OHC18 from  $\omega$ -Me-OHC18 by saponification.

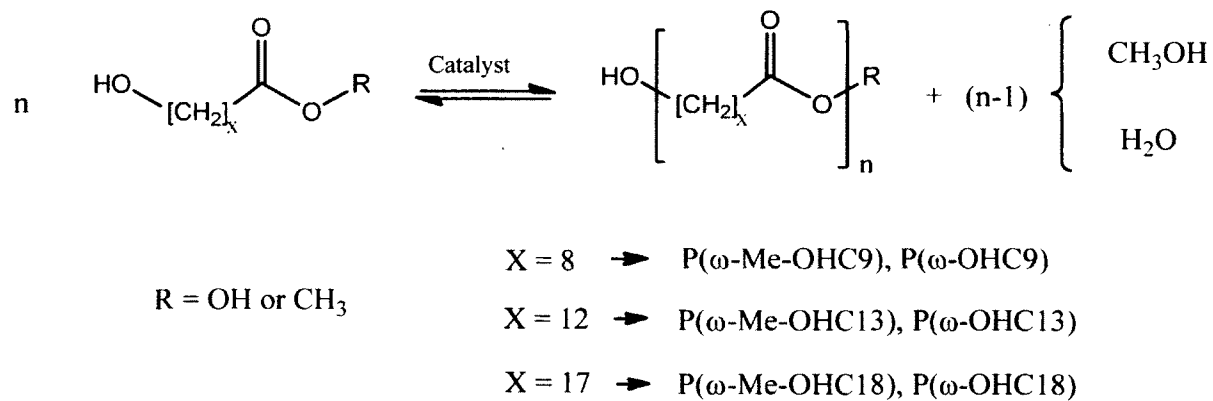
### **3.6 Summary**

All of the monomers produced in this study were of high purity and relatively high yields (purity  $\geq$  95% and yields  $\geq$  80%). They were synthesized from vegetable oil-based compounds employing reproducible reactions. The structure of the monomers was fully characterized by  $^1\text{H}$  NMR and Mass Spectroscopy.

## 4 Melt condensation polymerization of polyesters

### 4.1 Introduction

Polycondensation is a widely used classical polymerization method to synthesize polyesters. As discussed in chapter 2, controlling the polyesterification reaction conditions are crucial for obtaining desirable polyester molar masses and distribution. This chapter discusses the optimization studies on P( $\omega$ -OHFA)s and P(Me- $\omega$ -OHFA)s obtained from  $\omega$ -hydroxyfatty acid monomers. P( $\omega$ -OHFA)s and P(Me- $\omega$ -OHFA)s were prepared by melt polycondensation using titanium (IV) isopropoxide [Ti(OiPr)<sub>4</sub>] catalyst. Figure 4-1 shows the general reaction scheme for the polycondensation of an acid as well as ester terminated monomer prepared from vegetable oil. A series of polycondensation reactions were performed to determine the optimal values for catalyst concentration, reaction time and temperature. The influence of various reaction parameters on the kinetic and thermodynamic aspects of polycondensation is further elucidated. Note, optimization study was performed on each individual parameter as imposed to a time Multi-Carlo type condition of multiple parameters.



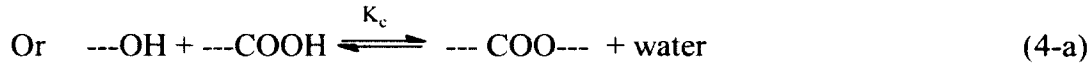
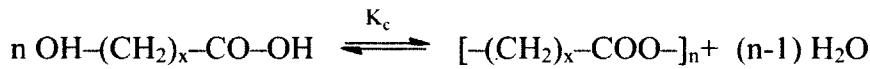
**Figure 4–1.** Reaction scheme for melt polycondensation of P(Me- $\omega$ -OHFA)s and P( $\omega$ -OHFA)s.



## 4.2 Theoretical Background

### 4.2.1 Thermodynamic aspects

For a typical polycondensation of hydroxyl acid, as shown below, the equilibrium constant ( $K_c$ ) is given by equation (4-1) (Duda and Penczek 2002).



$$K_c = \frac{[\text{COO}][\text{H}_2\text{O}]}{[\text{OH}][\text{COOH}]} \quad (4-1)$$

In a bi-functional monomer having both reacting functional groups in the same monomer, at the beginning of reaction:  $[\text{OH}]_0 = [\text{COOH}]_0 = [\text{A}]_0$ , and at equilibrium,  $[\text{OH}] = [\text{COOH}] = [\text{A}]$ .

The concentration of ester group ( $[\text{COO}]$ ) at equilibrium is  $p_c[\text{A}]$  (where  $p_c$  is the extent of the reaction at equilibrium). The concentration of the by-product ( $[\text{H}_2\text{O}]$ ) is also  $p_c[\text{A}]$ . The concentration of hydroxyl  $[\text{OH}]$  and carboxyl group  $[\text{COOH}]$  at equilibrium is given by  $([\text{A}]_0 - p_c[\text{A}]_0)$ . The equilibrium constant of polymerization therefore is given by equation (4-2):

$$K_c = \frac{[\text{COO}][\text{H}_2\text{O}]}{[\text{OH}][\text{COOH}]} = \frac{(p_c[\text{A}]_0)^2}{([\text{A}]_0 - p_c[\text{A}]_0)^2} \quad (4-2)$$

Equation (4-6) then simplifies to:

$$K_c = \frac{(p_c)^2}{(1-p_c)^2} \quad (4-3)$$

Solving for  $p_c$  gives:

$$p_c = \frac{K_c^{1/2}}{1 + K_c^{1/2}} \quad (4-4)$$

Equation (4-4) represents the extent of the reaction as a function of the equilibrium constant.

According to Carothers's equation  $p_c$  is also related to the  $\bar{X}_n$  (equation (4-5)),

$$\bar{X}_n = \frac{1}{1-p} \quad (4-5)$$

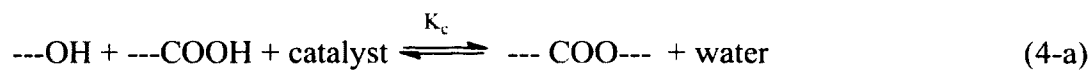
Combining equations (4-4) and (4-5) gives an expression of  $\bar{X}_n$  as a function of  $K_c$ :

$$\bar{X}_n = 1 + K_c^{1/2} \quad (4-6)$$

Polycondensation is a reversible process, and therefore, the value of  $K_c$  should be large enough to obtain high molecular weight polyesters. The  $K_c$  values for polyesterification, however, are generally low (Nisoli, Doherty et al. 2004). So, in order to obtain high degrees of polymerization, the equilibrium is pushed forward by removing the low molecular weight by-products. The majority of polyesters require  $\bar{X}_n \geq 100$  ( $p = 0.99$ ) to exhibit sufficient physical properties, which corresponds to  $K_c \geq 10^4$  (Duda and Penczek 2002).

#### 4.2.2 Kinetics study

The kinetics of the polymerization is studied by considering equation (4-a) again:



$$\text{Rate of reaction} = - \frac{d[\text{OH}]}{dt} = - \frac{d[\text{COOH}]}{dt} = k_r [\text{catalyst}] [\text{OH}] [\text{COOH}] = k [\text{OH}] [\text{COOH}],$$

where  $k = k_r[\text{catalyst}]$ , and  $k_r$  is the reaction rate constant and was obtained at constant temperature.

As discussed before, for a hydroxyacid bi-functional monomer  $[\text{OH}] = [\text{COOH}] = [\text{A}]$  and  $[\text{OH}]_0 = [\text{COOH}]_0 = [\text{A}]_0$  then:

$$-\frac{d[\text{A}]}{dt} = k[\text{A}]^2 \quad \rightarrow \quad \int_{[\text{A}]_0}^{[\text{A}]} \frac{d[\text{A}]}{[\text{A}]^2} = -k \int_0^t dt$$

$$\frac{1}{[\text{A}]} - \frac{1}{[\text{A}]_0} = k t \quad (4-7)$$

The number average degree of polymerization  $\bar{X}_n$  would be given as,

$$\bar{X}_n = \frac{[\text{A}]_0}{[\text{A}]} \quad (4-8)$$

Combining equations (4-7) and (4-8) provides the kinetic equation:

$$\bar{X}_n = 1 + k [\text{A}]_0 t \quad (4-9)$$

Thus, equation (4-9) indicates a linear relationship between  $\bar{X}_n$  and reaction time. The slope gives the reaction rate constant ( $k_r$ ), from equation (4-3).

$$\text{Slope} = k [\text{A}]_0 = k_r [\text{catalyst}] [\text{A}]_0 \quad (4-10)$$

## 4.3 Experimental

### 4.3.1 Materials

Ti(IV) isopropoxide (99.99% purity) and 1-butanol (99.98% purity) was purchased from Sigma-Aldrich. The various monomers ( $\omega$ -OHC9) (96.5% purity), ( $\omega$ -Me-OHC9) (97% purity), ( $\omega$ -OHC13) (97% purity), ( $\omega$ -Me-OHC13) (98% purity), ( $\omega$ -OHC18) (97% purity) and ( $\omega$ -Me-OHC18) (99% purity) were synthesized from vegetable oil (refer to chapter 3).

#### 4.3.2 Melt polycondensation of P( $\omega$ -OHFA)s and P( $\omega$ -Me-OHFA)s

Polyesterification was conducted in a stainless steel reactor equipped with a mechanical stirrer, nitrogen inlet, gas outlet, a thermocouple and pressure gauge. The monomer (10 g) and a predetermined amount of catalyst solution (10 mg/mL Ti(OiPr)<sub>4</sub> in 1-butanol) was transferred into the reactor. In the first polymerization phase (esterification/transesterification), the reaction mixture was initially heated at 150°C for three hours with continuous stirring under N<sub>2</sub> flow at atmospheric pressure. The temperature was subsequently raised and maintained at 180°C for 2 hrs, followed by another 2 hrs at 200°C under the same reaction conditions. Except for  $\omega$ -Me-OHC9, because of its low thermal stability (~130°C), the reaction was initiated at 120°C for an hour before applying elevated temperature cycles. In the second phase (polycondensation), traces of water/methanol were removed from the reaction medium to ensure high molecular weight products. This was achieved by (i) raising the temperature to 220°C and maintaining it for 4 hours, (ii) placing the contents of the reactor under reduced pressure (<0.1 torr), (iii) increasing the speed of mixing (iv) maintaining the reaction conditions while samples were taken every hour. The polycondensation was further continued for another two hours at 220°C under vacuum. Samples were measured in duplicates at regular intervals using GPC to determine the evolution of molecular weights and distributions.

The optimization study on catalyst concentration was carried out by the performing melt polycondensation using a series of catalyst concentrations, ranging between 50 to 500 ppm.

The polycondensation at the optimum catalyst concentration was also performed in duplicates so as to determine the reproducibility of the experiments.

### 4.3.3 Characterization techniques

#### 4.3.3.1 Gel permeation chromatography

Gel Permeation Chromatography (GPC) was used to determine the number average molecular weight ( $\bar{M}_n$ ), weight-average molecular weight ( $\bar{M}_w$ ) and polydispersity index (the distribution of molecular mass,  $PDI = \bar{M}_w/\bar{M}_n$ ). GPC tests were carried out on a Waters Alliance (Milford, MA, USA) e2695 pump, Waters 2414 refractive index detector and a Styragel HR5E column (5 mm). Chloroform was used as eluent with a flow rate of 0.5 mL/min. The sample was made with a concentration of 2 mg/mL, and the injection volume was 30 ml for each sample. Polystyrene (PS, #140) standards were used to calibrate the curve. All the GPC analyses were done in duplicate to assess the uncertainties. The polymer structures were also confirmed by  $^1H$  NMR (refer to chapter 3 for  $^1HNMR$  details).

## 4.4 Results and discussions

### 4.4.1 Characterization of P( $\omega$ -OHFA)s and P(Me- $\omega$ -OHFA)s

The structures of P( $\omega$ -OHFA)s and P(Me- $\omega$ -OHFA)s were analyzed by  $^1H$  NMR spectroscopy. The  $^1H$  NMR spectra of each polymer sample is shown in Appendix A.

The  $^1H$  NMR spectra of P( $\omega$ -OHFA)s and P(Me- $\omega$ -OHFA)s when compared to their respective monomers reveals disappearance of peaks at 3.50 - 3.70 ppm corresponding to protons from the end methyl group, the hydrogen from the hydroxyl group as well as the carbon atom associated with the hydroxyl group. The spectra also indicate appearance of a new peak at a chemical shift value of 4.10 ppm, which was assigned to the protons from the methylene group attached to the ester linkage.

***P( $\omega$ -OHC9) and P( $\omega$ -Me-OHC9)***

$^1\text{H}$  NMR (CDCl<sub>3</sub> 400MHz)  $\delta$  (ppm): 1.20-1.34 (m, 10H, CH<sub>2</sub>), 1.6-1.64 (m, 2H, CH<sub>2</sub>CH<sub>2</sub>COO), 2.28-2.36 (t, 2H, CH<sub>2</sub>COO), 4.06-4.09 (2H, CH<sub>2</sub>O)

***P( $\omega$ -OHC13) and P( $\omega$ -Me-OHC13)***

$^1\text{H}$  NMR (CDCl<sub>3</sub> 400MHz)  $\delta$  (ppm): 1.29-1.31 (m, 18H, CH<sub>2</sub>), 1.6-1.66 (m, 2H, CH<sub>2</sub>CH<sub>2</sub>COO), 2.29-2.33 (t, 2H, CH<sub>2</sub>COO), 4.06-4.09 (2H, CH<sub>2</sub>O)

***P( $\omega$ -OHC18) and P( $\omega$ -Me-OHC18)***

$^1\text{H}$  NMR (CDCl<sub>3</sub> 400MHz)  $\delta$  (ppm): 1.28-1.33 (m, 28H, CH<sub>2</sub>), 1.59-1.66 (m, 2H, CH<sub>2</sub>CH<sub>2</sub>COO), 2.29-2.36 (t, 2H, CH<sub>2</sub>COO), 4.06-4.10 (2H, CH<sub>2</sub>O)

#### **4.4.2 Optimization results**

The polymer chain lengths and distribution plays a key role in determining its physical properties. It has been shown before that for polyesters prepared by melt polycondensation, the catalyst concentration, reaction time and reaction temperature controls its molecular size and distribution (Liu, Liu et al. 2011). Hence, for ( $\omega$ -OHFA)s and ( $\omega$ -Me-OHFA)s, the reaction conditions were optimized for the catalyst amount, time and temperature in order to obtain P( $\omega$ -OHFA)s and P( $\omega$ -Me-OHFA)s with molecular weights suitable for desired applications.

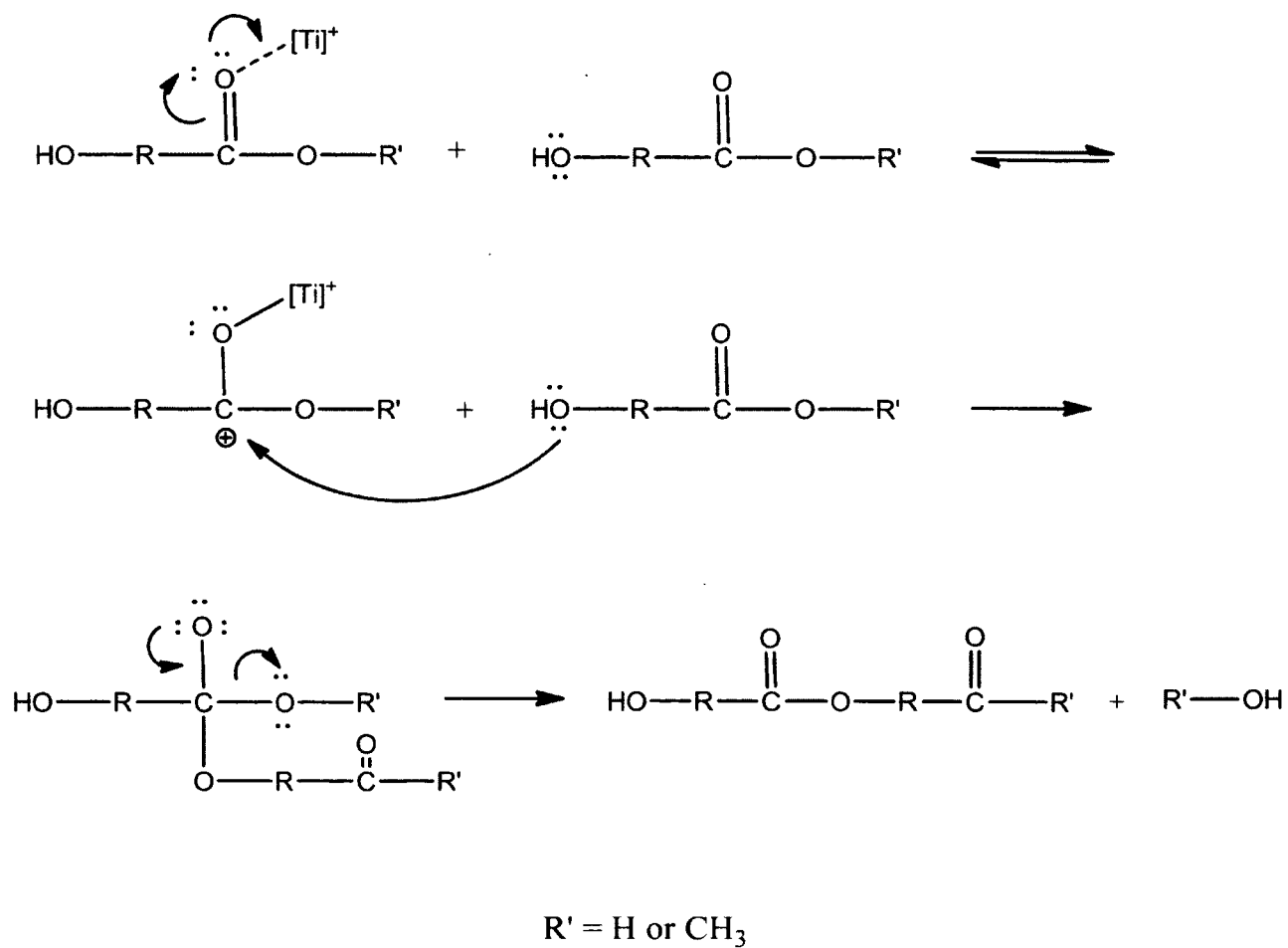
##### **4.4.2.1 Influence of catalyst concentration**

For polycondensation, the action of catalyst has been explained mostly using the Ravindranath mechanism (MacDonald 2002) (refer to chapter 2 for further explanation). Assuming a similar

mechanism for P( $\omega$ -OHFA)s and P( $\omega$ -Me-OHFA)s, the catalytic mechanism of polymerization for  $\omega$ -OHFA monomers could be explained as follows (Figure 4-2).

In the primary step, the catalyst metal ion coordinates to the carbonyl oxygen bond. This decreases the electron density of the carbonyl carbon atom and facilitates a nucleophilic attack. The hydroxyl end group of a different polymer chain then attacks the nucleophilic carbonyl carbon, generating an ester bond. The metal catalyst undergoes an intramolecular rearrangement before it is regenerated.

Figure 4-3 (a) to (c) shows the variation of  $\bar{M}_n$  and PDI with catalyst concentration for P( $\omega$ -OHFA)s and P( $\omega$ -Me-OHFA)s. As can be seen in Figure 4-3 (a), for P( $\omega$ -OHC9) and P( $\omega$ -Me-OHC9), with increasing catalyst concentration,  $\bar{M}_n$  initially increases, reaches a maximum and thereafter decreases.  $\bar{M}_n$  varied in a similar manner for other monomers as well (Figures 4-3 (b), (c)). Similar findings have been reported in the literature for polyesters. For example, for the polycondensation of poly(ethylene terephthalate) (PET) using antimony catalyst, Duh (Duh 2002) observed a similar trend, and the maximum value for molecular weight was obtained for 150 ppm catalyst concentration.

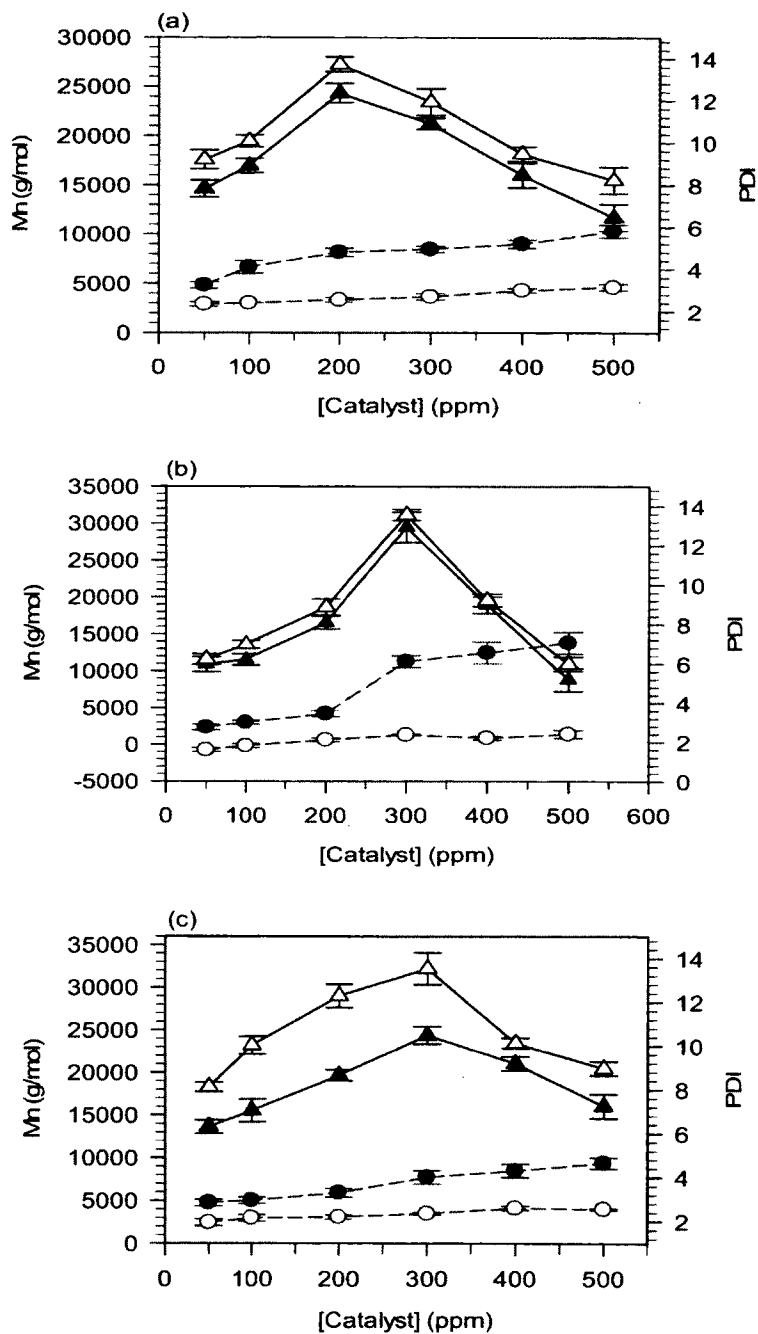


**Figure 4–2.** Mechanism of catalytic polycondensation of  $\omega$ -OHFAs and  $\omega$ -Me-OHFAs



The reduction in molecular weights beyond the optimal catalyst concentration was attributed to the cleavage of ester bond linkages constituting the polymer backbone by excess catalyst ions. During polycondensation, with increasing molecular weight the acid/ester/hydroxyl end group concentration decreases. The excess catalyst ions would therefore attack the pre-existing ester linkages resulting in chain cleavage (Shah, Bhatta et al. 1984).

The PDI values increased with increasing catalyst amounts for all the polyesters (Figure 4-3). For P( $\omega$ -OHC9), the maximum  $\bar{M}_n$  value (24,321 g/mol) is obtained at 200 ppm and is considered as the optimal catalyst amount for polycondensation. Table 4-1 lists the optimum catalyst contents for the various P( $\omega$ -OHFA)s and P( $\omega$ -Me-OHFA)s. As can be seen from Table 4-1, both P( $\omega$ -OHC9) and P( $\omega$ -Me-OHC9) have the same optimal catalyst concentration(200 ppm). This is again true in the case of P( $\omega$ -OHC18) and P( $\omega$ -Me-OHC18), as well as for P( $\omega$ -OHC13) and P( $\omega$ -Me-OHC13). Thus, for P( $\omega$ -OHFA)s prepared from monomers of the chain lengths, the optimal catalyst amount is unaffected by the type of carboxyl end group functionality of the reacting monomers.



**Figure 4-3.** Variation of  $\bar{M}_n$  and PDI as a function of catalyst concentration (a) P( $\omega$ -OHC9) and P( $\omega$ -Me-OHC9), (b) P( $\omega$ -OHC13) and P( $\omega$ -Me-OHC13), (c) P( $\omega$ -OHC18) and P( $\omega$ -Me-OHC18). Symbols are: ( $\Delta$ ,  $\blacktriangle$ )  $\bar{M}_n$  of P( $\omega$ -Me-OHFA) and P( $\omega$ -OHFA), respectively, ( $\circ$ ,  $\bullet$ ):

PDI of P( $\omega$ -Me-OHFA) and P( $\omega$ -OHFA), respectively.

**Table 4-1.**  $\bar{M}_w$ ,  $\bar{M}_n$  and PDI obtained at the optimum catalyst concentrations for P( $\omega$ -OHFA) and

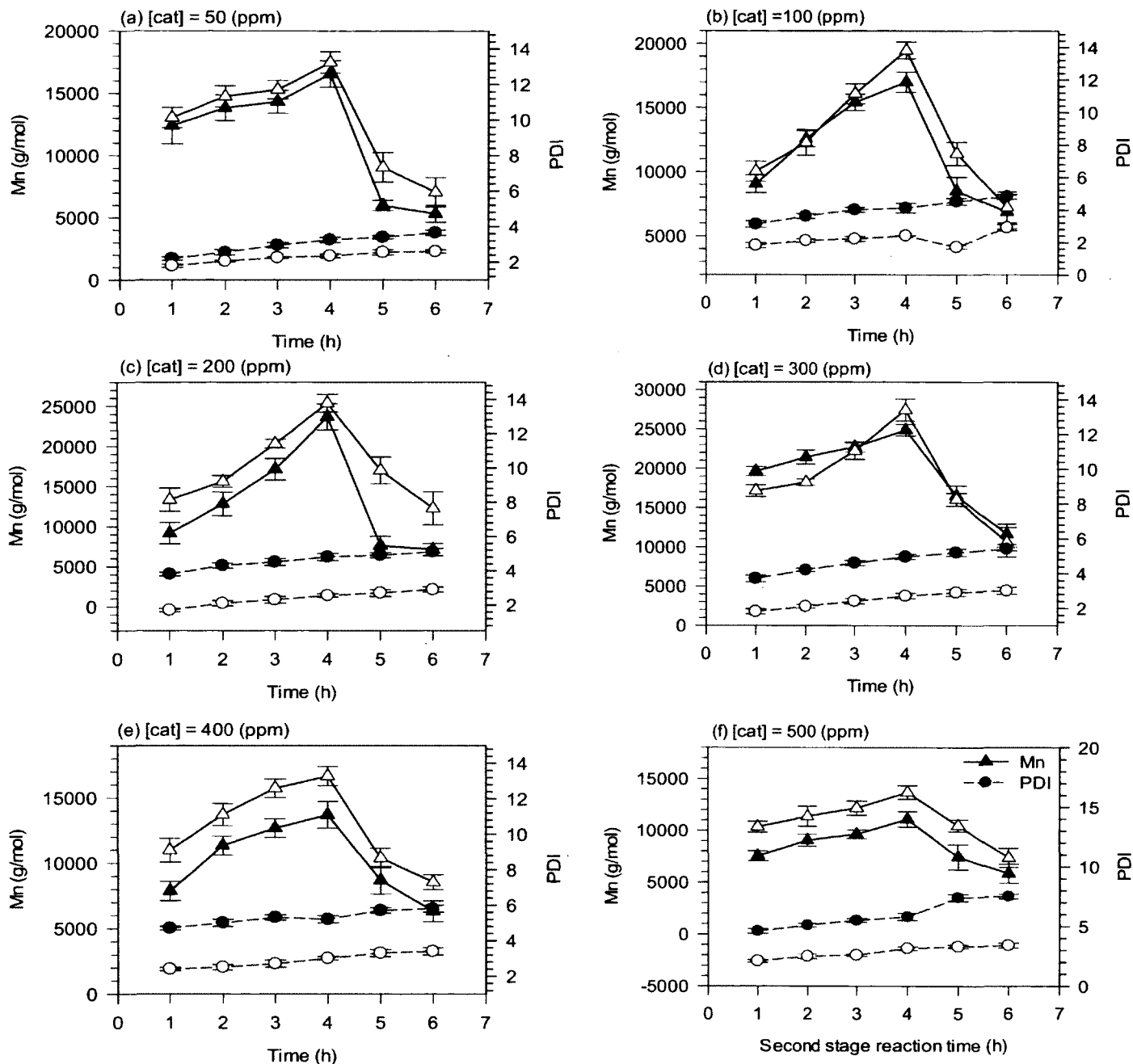
P( $\omega$ -Me-OHFA)

	<b>Polyesters</b>	<b>Optimum [Catalyst] (ppm)</b>	$\bar{M}_w$ (g/mol)	$\bar{M}_n$ (g/mol)	<b>PDI</b>
<b>Acid terminated polymers</b>	P( $\omega$ -OHC9)	200	115720 $\pm$ 1050	24321 $\pm$ 987	4.8 $\pm$ 0.2
	P( $\omega$ -OHC13)	300	180777 $\pm$ 5800	29469 $\pm$ 1397	6.1 $\pm$ 0.3
	P( $\omega$ -OHC18)	300	102288 $\pm$ 2640	27469 $\pm$ 905	4.0 $\pm$ 0.3
<b>Ester terminated polymers</b>	P( $\omega$ -Me-OHC9)	200	72788 $\pm$ 2300	28470 $\pm$ 761	2.5 $\pm$ 0.1
	P( $\omega$ -Me-OHC13)	300	78495 $\pm$ 3690	30377 $\pm$ 975	2.4 $\pm$ 0.0
	P( $\omega$ -Me-OHC18)	300	82040 $\pm$ 1820	34779 $\pm$ 528	2.3 $\pm$ 0.0

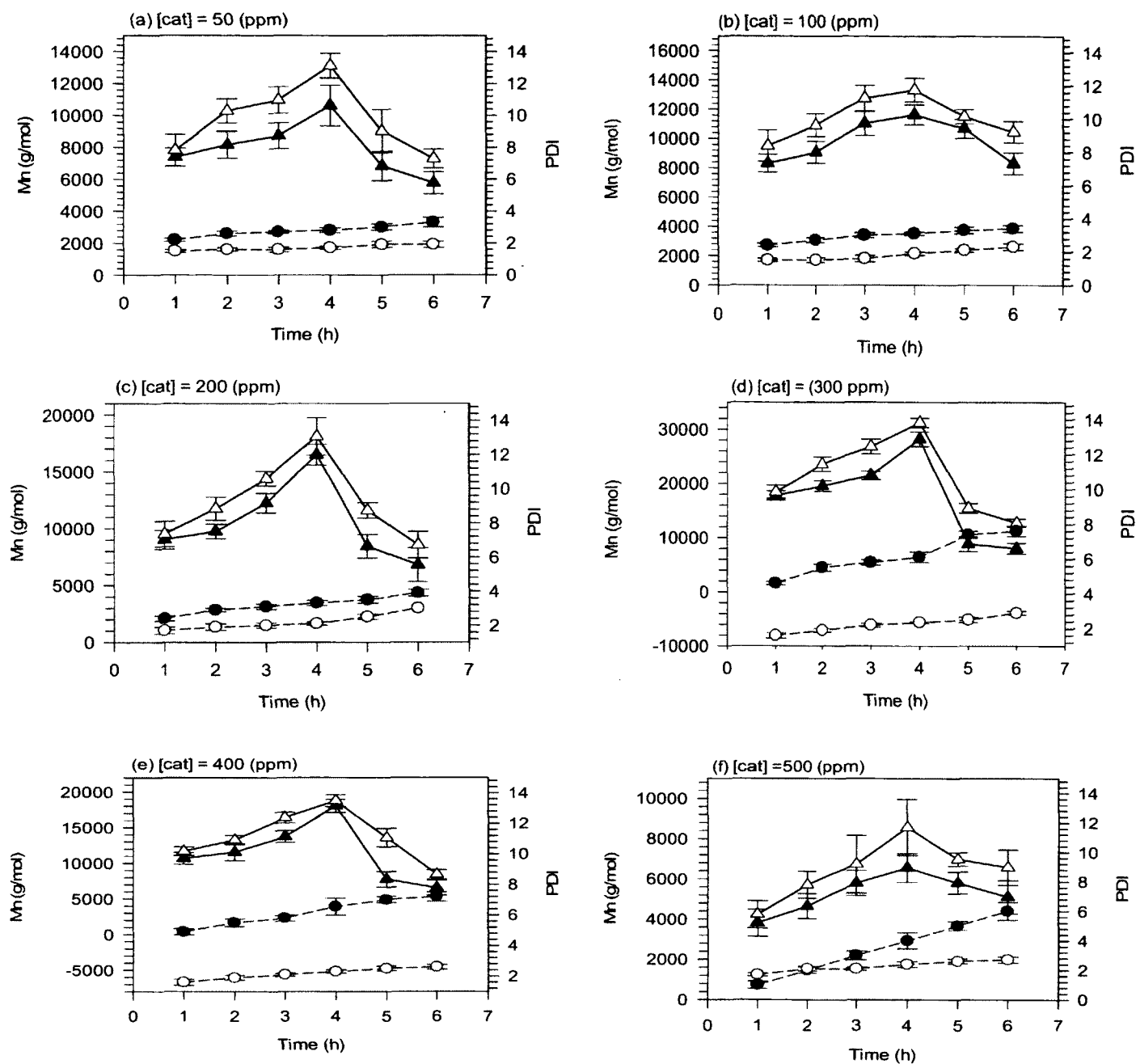
#### 4.4.2.2 Reaction time kinetic analysis

The reaction time was optimized to obtain high molecular weight polyesters, and further to investigate the kinetics of polycondensation. Optimization of the reaction time for maximum molecular weight was performed for the second phase (polycondensation) of polymerization. This was done by increasing the reaction time up to 6 hours at 220°C, for each individual catalyst concentrations ranging from 50 to 500 ppm. The polyester molecular weight and distribution was measured at every hour by GPC analysis. Figures 4-4 (a-f) to 4-6 (a-f) show the variation in  $\bar{M}_n$  and PDI with phase two reaction times for P( $\omega$ -OHFA) and P( $\omega$ -Me-OHFA)s at different catalyst concentrations. The  $\bar{M}_n$  values increased initially with reaction time, until 4 hours, and thereafter decreased for all polyesters. The observed decrease beyond 4 hours can be attributed to the thermal degradation of the polyesters at prolonged reaction times, which is also clear from the  $\bar{M}_n$  values from Tables 4-2 (a) and (b).

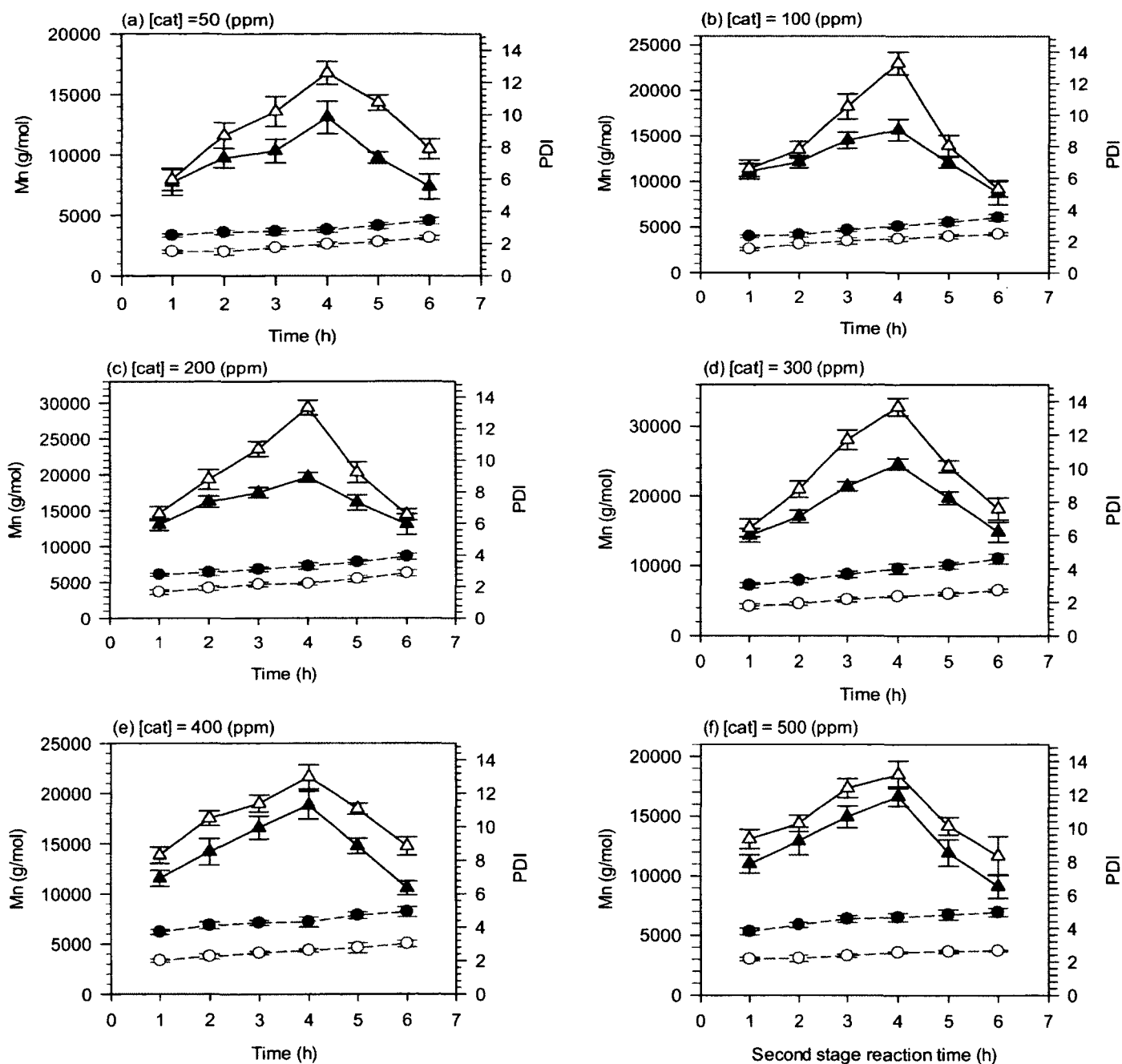
As seen from the Figures 4-4 (a-f) to 4-6 (a-f), the maximum  $\bar{M}_n$  is obtained after 4 hours at 220°C for all polyesters, irrespective of their monomer chain lengths. However, the values of  $\bar{M}_n$  were higher for ester derived polyesters compared to those prepared from the acid terminated monomers, in all cases. The effect of ester/acid terminal functional groups on polycondensation was further investigated using kinetic analysis.



**Figure 4-4.** (a) to (f).  $\bar{M}_n$  and PDI as a function of reaction time during the second phase of the polymerization at different catalyst concentrations (50-500 ppm). Symbols are: ( $\Delta$ ,  $\blacktriangle$ )  $\bar{M}_n$  of P( $\omega$ -Me-OHC9) and P( $\omega$ -OHC9), respectively. ( $\circ$ ,  $\bullet$ ): PDI of P( $\omega$ -Me-OHC9) and P( $\omega$ -OHC9), respectively.



**Figure 4-5.** (a) to (f)  $\bar{M}_n$  and PDI as a function of reaction time during the second phase of the polymerization at different catalyst concentrations (50-500 ppm). Symbols are: ( $\Delta, \blacktriangle$ )  $\bar{M}_n$  of P( $\omega$ -Me-OHC13) and P( $\omega$ -OHC13), respectively. ( $\circ, \bullet$ ): PDI of P( $\omega$ -Me-OHC13) and P( $\omega$ -OHC13), respectively.



**Figure 4-6.** (a) to (f)  $\bar{M}_n$  and PDI as a function of reaction time during the second phase of the polymerization at different catalyst concentrations (50-500 ppm). Symbols are: ( $\Delta$ ,  $\blacktriangle$ )  $\bar{M}_n$  of P( $\omega$ -Me-OHC18) and P( $\omega$ -OHC18), respectively. ( $\circ$ ,  $\bullet$ ): PDI of P( $\omega$ -Me-OHC18) and P( $\omega$ -OHC18), respectively.



***Kinetic studies of P( $\omega$ -OHFA)s and P( $\omega$ -Me-OHFA)s***

The reaction kinetics were studied for each type of P( $\omega$ -OHFA)s and P( $\omega$ -Me-OHFA)s. Polycondensation reactions corresponding to the optimal catalyst quantity for each kind of acid/ester derived monomer has been considered. Thus, for P( $\omega$ -OHC13), P( $\omega$ -Me-OHC13), P( $\omega$ -OHC18), and, P( $\omega$ -Me-OHC18), polymerization at 300 ppm catalyst concentration was considered, and the kinetic studies of P( $\omega$ -OHC9) and P( $\omega$ -Me-OHC9) was performed for polycondensation at 200 ppm catalyst concentration. Polycondensation for a total reaction time up to 11 hours was considered for the analysis.

The rate equation, as discussed earlier under section (4.1.2) is given by equation (4-9)

$$\bar{X}_n = 1 + k [A]_0 t \quad (4-9)$$

Table 4-2(a) and (b) summarizes the cumulative values from experimental and the kinetic model for P( $\omega$ -OHC9) and P( $\omega$ -Me-OHC9). Values of  $\bar{M}_w$ ,  $\bar{M}_n$ ,  $\bar{M}_w/\bar{M}_n$  and PDI were obtained from GPC analysis.  $\bar{X}_n$  (Exp) was obtained from equation (4-8) whereas  $\bar{X}_n$  (Calc) was achieved from kinetic rate equation (4-9).

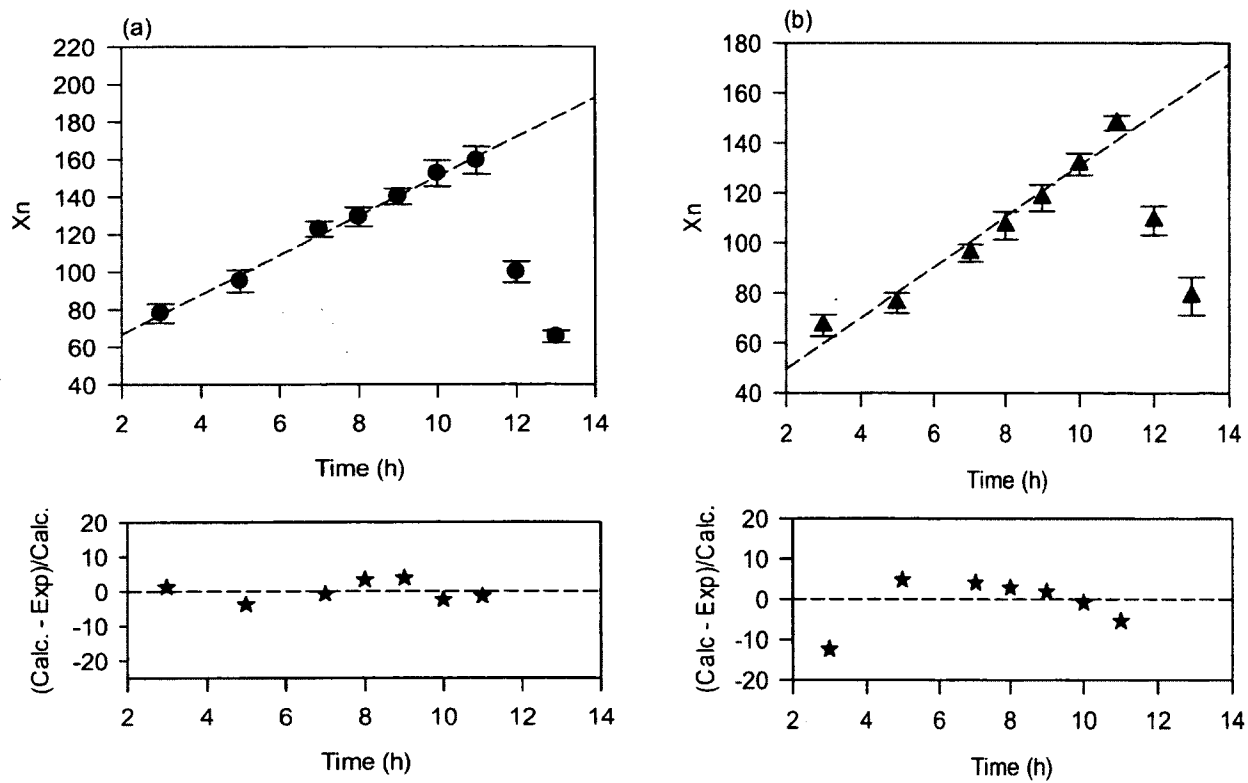
**Table 4-2.** Experimental (exp) and mathematical (calc) results obtained from the kinetic analysis of (a) P( $\omega$ -OHC9). (b) P( $\omega$ -Me-OHC9).  $M_0=156$  g/mol.

(a)	Time (h)	Temp. (°C)	$\bar{M}_w$ (g/mol)	$\bar{M}_n$ (g/mol)	PDI	$\bar{X}_n$ (Exp)	$\bar{X}_n$ (Calc)	p
<b>First phase</b>	3	150	30672 $\pm$ 2893	12164 $\pm$ 1328	2.2 $\pm$ 0.1	77.9	90.4	0.988
	2	180	38221 $\pm$ 2271	14820 $\pm$ 1480	2.3 $\pm$ 0.2	95	102.6	0.990
	2	200	46911 $\pm$ 3103	19137 $\pm$ 1336	2.6 $\pm$ 0.1	122.6	114.7	0.991
<b>Second phase</b>	1	220	52893 $\pm$ 3005	20140 $\pm$ 675	3.3 $\pm$ 0.2	129.1	120.8	0.991
	1	220	70473 $\pm$ 3501	21860 $\pm$ 980	3.8 $\pm$ 0.1	140.1	126.9	0.991
	1	220	89245 $\pm$ 5021	23788 $\pm$ 1120	4.3 $\pm$ 0.1	152.4	133.0	0.992
	1	220	115720 $\pm$ 1050	24851 $\pm$ 987	4.8 $\pm$ 0.2	159.3	139.0	0.992
	1	220	69798 $\pm$ 3749	15572 $\pm$ 1020	4.9 $\pm$ 0.1	99.8	90.4	0.988
	1	220	52602 $\pm$ 3366	10205 $\pm$ 760	5.1 $\pm$ 0.2	65.4	102.6	0.984

(b)	Time (h)	Temp (°C)	$\bar{M}_w$ (g/mol)	$\bar{M}_n$ (g/mol)	PDI	$\bar{X}_n$ (Exp)	$\bar{X}_n$ (Calc)	p
<b>First phase</b>	3	150	22767 $\pm$ 3779	10452 $\pm$ 1145	2.2 $\pm$ 0.1	67.2	59.6	0.9851
	2	180	31190 $\pm$ 3690	11844 $\pm$ 830	2.3 $\pm$ 0.1	76.8	79.8	0.9868
	2	200	40442 $\pm$ 4387	14918 $\pm$ 615	2.5 $\pm$ 0.1	96.9	100	0.9896
<b>Second phase</b>	1	220	46254 $\pm$ 5267	16690 $\pm$ 870	2.6 $\pm$ 0.2	107.1	110.1	0.9907
	1	220	51654 $\pm$ 3894	18413 $\pm$ 1015	2.6 $\pm$ 0.1	118.4	120.2	0.9915
	1	220	61589 $\pm$ 3425	20438 $\pm$ 965	2.7 $\pm$ 0.2	131.5	130.3	0.9924
	1	220	72604 $\pm$ 6693	28470 $\pm$ 760	2.5 $\pm$ 0.1	176.5	140.4	0.9932
	1	220	51935 $\pm$ 4823	16996 $\pm$ 1665	3.3 $\pm$ 0.2	108.9	168.7	0.9908
	1	220	46175 $\pm$ 3135	12276 $\pm$ 2060	3.4 $\pm$ 0.1	78.7	180.6	0.9872

As seen from Tables 4-2 (a) and (b) this corresponds to the second phase of polycondensation reaction, giving the maximum  $\bar{X}_n$  (Exp) at 159 and 176.5 respectively, for P( $\omega$ -OHC9) and P( $\omega$ -Me-OHC9). This also substantiates our selection of the phase two reaction stage for studying the reaction kinetics. This stage also has high monomer degree of conversion, i.e., from 98 – 99 %. For P( $\omega$ -OHC9) and P( $\omega$ -Me-OHC9), Figures 4-7(a) and (b) represent the linear fit ( $R^2 > 0.9945$ ) for  $\bar{X}_n$  (Exp) versus total reaction times, i.e., reaction times combined for phase one and two. The residual plots are also given. The  $\bar{X}_n$  (Exp) values deviates from linearity, for both the initial and at late stages of reaction. The percentages of residual values are found to vary within  $\pm 10\%$  error.

The polycondensation rate is generally affected by different factors, such as the reactivity of functional groups, reaction temperature, mass transfer limitations, as well as by the rate of removal of the reaction by-products. A comparison between the linear behaviour for (P( $\omega$ -OHC9) and P( $\omega$ -Me-OHC9) as a function of reaction time is given by Figure 4-8. The  $\bar{X}_n$  values for P( $\omega$ -OHC9) are initially higher than P( $\omega$ -Me-OHC9). This is attributed to the larger extent of the reaction between the highly polar carboxylic acid (COOH) and hydroxyl group (OH) (esterification) compared with the relatively less polar ester and hydroxyl group (OH) in P( $\omega$ -Me-OHC9). At the beginning ( $t=3$  h) of polymerization of P( $\omega$ -OHC9) and P( $\omega$ -Me-OHC9) in which the viscosity of reaction system was low, the reaction rate was dominated by the reactivity of functional groups.



**Figure 4–7.** Linear performance of experimental  $\bar{X}_n$  as a function of reaction time for (a)  $P(\omega\text{-OHC9})$  and (b)  $P(\omega\text{-Me-OHC9})$ , respectively. (★) percentage residual values, ( $R^2 > 0.9945$ ).

By increasing the reaction time ( $t=3-8$  hours), the  $\bar{X}_n$  linearly increased with an increased reaction time despite the reaction temperature changing from 150 to 200°C. The reaction rate of polymerization of P( $\omega$ -Me-OHC9) was higher than that of P( $\omega$ -OHC9). This might be because the dominating factors in this phase were mass transfer, as opposed to reactivity of functional groups when the  $\bar{X}_n$  increased, the viscosity of reaction mixtures also increased. However, due to having a terminal carboxyl acid group, P( $\omega$ -OHC9) is able to create stronger hydrogen-bonding between the polymer chains than P( $\omega$ -Me-OHC9). This leads to a higher viscosity in P( $\omega$ -OHC9), and a more significant limitation to mass transfer. Furthermore, the terminal carboxyl acid group also has stronger hydrogen-bonding with water, the by-product from the reaction of  $\omega$ -OHC9, increasing the difficulty to remove water, and decreasing the reactivity of the carboxyl acid groups. These two factors eventually lead to a decreased reaction rate of  $\omega$ -OHC9.

In the second phase ( $t = 8 - 11$  h) where the vacuum was applied, there was not a clear change in the reaction rate of P( $\omega$ -OHC9), but an obvious increase in the reaction rate of P( $\omega$ -Me-OHC9). In this phase, applied vacuum could increase the removal rate of by-products. At the same time, when vacuum was applied, the free volume of the reaction mixture increased and caused a decrease in viscosity, which could also increase the removal of by-products. Because of the hydrogen-bonding in P( $\omega$ -OHC9), the effect of vacuum on the polymerization of ( $\omega$ -OHC9) was not clearly shown.

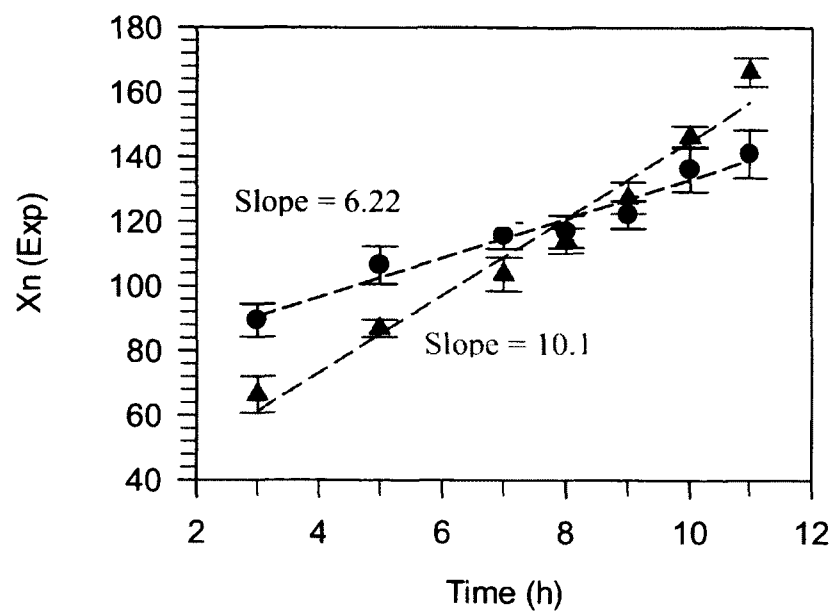
Another factor that can affect the reaction rate is related to some secondary reactions that could occur at random stages of the polymerization process. Secondary reactions are involved with mostly the degradation of functional groups. Decarboxylation, for example, is one of the reactions that could take place during polymerization, releasing CO<sub>2</sub>. Carboxylic acid terminal groups are more likely to undergo decarboxylation compared to ester groups. Therefore, the

reactive carboxylic acid functional group becomes inactive and consequently the rate of reaction is lowered compared to the reaction rate of ester compounds as shown in Figure 4-8.

***Kinetic study of P( $\omega$ -OHC13) and P( $\omega$ -Me-OHC13)***

Tables 4-3 (a) and (b) indicate the quantitative results of polycondensation for  $\omega$ -OHC13 and  $\omega$ -Me-OHC13. A linear relationship ( $R^2 > 0.9827$ ) in P( $\omega$ -OHC13) and P( $\omega$ -Me-OHC13) with respect to reaction time is also seen in Figures 4-9 (a) and (b). The percentage residual values were within  $\pm 15\%$  error, respectively for P( $\omega$ -OHC13) and P( $\omega$ -Me-OHC13).

The polycondensation reaction rates of P( $\omega$ -OHC13) and P( $\omega$ -Me-OHC13) are also compared in Figure 4-10. The slope values are higher for P( $\omega$ -Me-OHC13) suggesting a relatively higher reaction rate than compared to that of P( $\omega$ -OHC13). This result is similar to the earlier findings for P( $\omega$ -OHC9) and P( $\omega$ -Me-OHC9).



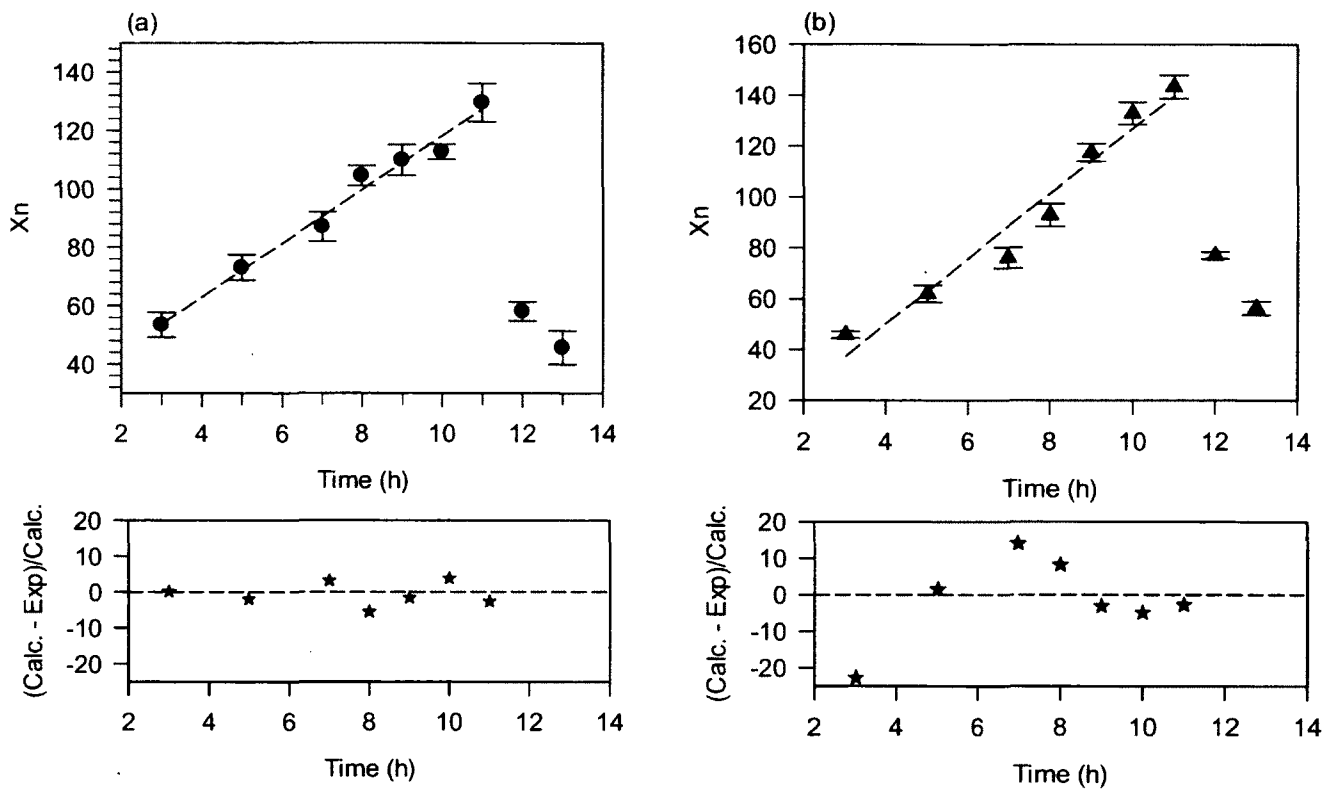
**Figure 4-8.** Comparison of kinetic study between P( $\omega$ -OHC9),(●), and P( $\omega$ -Me-OHC9),(▲)

**Table 4-3.** Experimental (exp) and mathematical (calc) results obtained from the kinetic analysis of (a)P( $\omega$ -OHC13) and (b)P( $\omega$ -Me-OHC13).  $M_0 = 212$  g/mol.

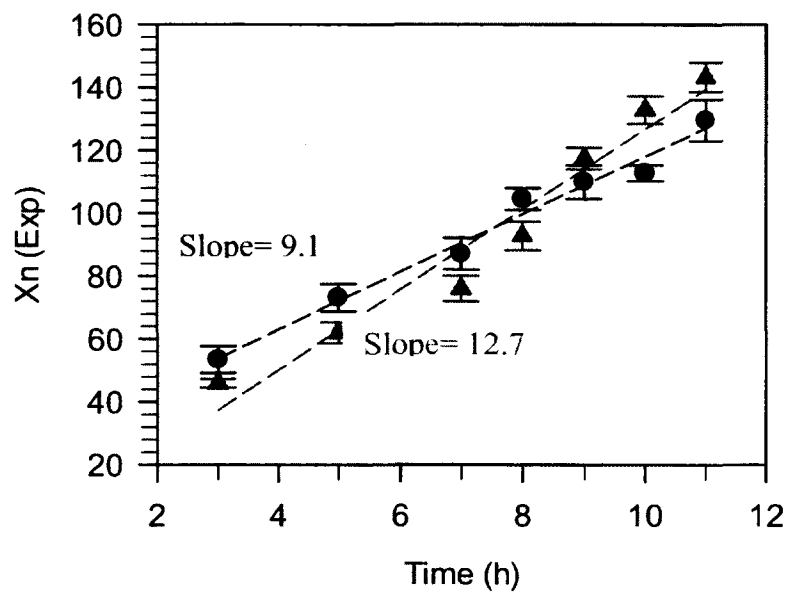
(a)	Time (h)	Temp (°C)	$\bar{M}_w$	$\bar{M}_n$	PDI	$\bar{X}_n$ (Exp)	$\bar{X}_n$ (Calc)	p
<b>First phase</b>	3	150	25199 $\pm$ 4311	11325 $\pm$ 895	2.2 $\pm$ 0.1	54.6	53.5	0.981
	2	180	34486 $\pm$ 4086	15499 $\pm$ 920	2.2 $\pm$ 0.1	69.3	71.7	0.985
	2	200	47984 $\pm$ 4959	18455 $\pm$ 1069	2.6 $\pm$ 0.1	73.4	89.9	0.986
<b>Second phase</b>	1	220	63702 $\pm$ 5768	22157 $\pm$ 734	2.8 $\pm$ 0.1	74.3	99.0	0.986
	1	220	75697 $\pm$ 6924	23291 $\pm$ 1121	3.2 $\pm$ 0.1	81.6	108.1	0.987
	1	220	86054 $\pm$ 6818	23904 $\pm$ 542	3.6 $\pm$ 0.1	114.4	117.2	0.99
	1	220	164131 $\pm$ 12429	27469 $\pm$ 1397	5.9 $\pm$ 0.2	148	126.3	0.994
	1	220	70706 $\pm$ 5933	12296 $\pm$ 684	5.7 $\pm$ 0.1	35	135.4	0.972
	1	220	53628 $\pm$ 6295	9662 $\pm$ 1215	5.5 $\pm$ 0.2	24.7	144.5	0.957

(b)	Time (h)	Temp (°C)	$\bar{M}_w$	$\bar{M}_n$	PDI	$\bar{X}_n$ (Exp)	$\bar{X}_n$ (Calc)	p
<b>First phase</b>	3	150	15793 $\pm$ 4119	9719 $\pm$ 591	1.6 $\pm$ 0.1	45.8	37.3	0.976
	2	180	21661 $\pm$ 4012	13128 $\pm$ 700	1.6 $\pm$ 0.1	61.9	62.8	0.983
	2	200	28190 $\pm$ 3927	16109 $\pm$ 866	1.7 $\pm$ 0.1	75.9	88.3	0.986
<b>Second phase</b>	1	220	35908 $\pm$ 5962	19675 $\pm$ 950	1.8 $\pm$ 0.2	92.8	101.4	0.988
	1	220	46053 $\pm$ 4659	24893 $\pm$ 735	1.8 $\pm$ 0.1	117.4	113.9	0.991
	1	220	53512 $\pm$ 4111	28164 $\pm$ 930	1.9 $\pm$ 0.1	132.8	126.6	0.992
	1	220	72147 $\pm$ 6247	30377 $\pm$ 975	2.3 $\pm$ 0.1	143.2	139.4	0.992
	1	220	24054 $\pm$ 4928	9719 $\pm$ 599	2.4 $\pm$ 0.1	77	152.1	0.987
	1	220	32820 $\pm$ 3282	13128 $\pm$ 566	2.5 $\pm$ 0.1	56.3	164.9	0.983





**Figure 4-9.** Linear performance of experimental  $\bar{X}_n$  as a function of reaction time for (a) P( $\omega$ -OHC13) and (b) P( $\omega$ -Me-OHC13), respectively. (★) percentage residual values, ( $R^2 > 0.9827$ ).



**Figure 4–10.** Comparison of kinetic study between (●) P( $\omega$ -OHC13) and (▲) P( $\omega$ -Me-OHC13).

***Reaction kinetics for P( $\omega$ -OHC18) and P( $\omega$ -Me-OHC18)***

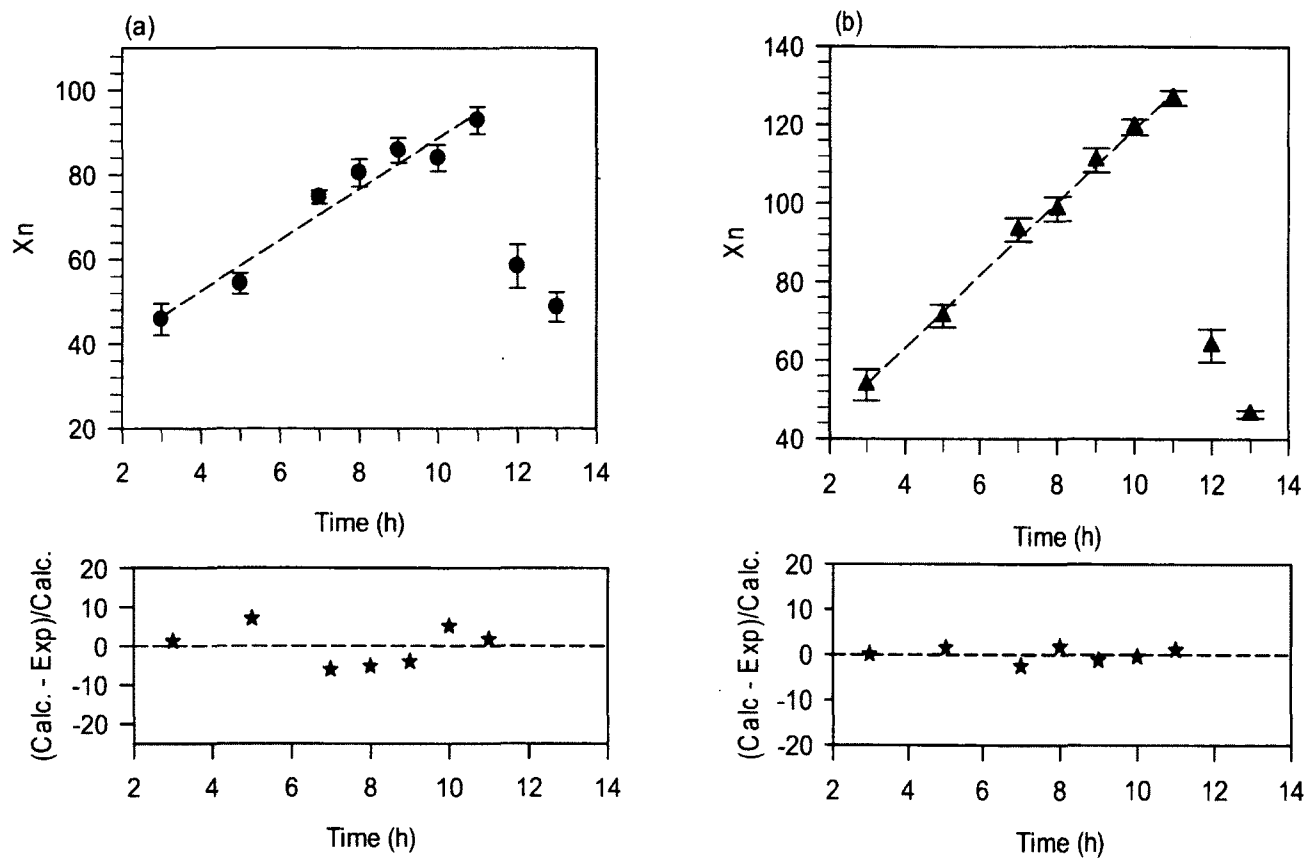
Tables 4-4 (a) and (b) demonstrate the quantitative results for polycondensation of  $\omega$ -OHC18 and  $\omega$ -Me-OHC18. Similar to earlier discussed polyesters, P( $\omega$ -OHC18) and P( $\omega$ -Me-OHC18), also exhibit a linear relationship ( $R^2 > 0.9831$ ) between  $\bar{X}_n$  and reaction time (Figure 4-11 (a) and (b)). The percentage residual values are within  $\pm 10\%$  error for P( $\omega$ -Me-OHC18) and P( $\omega$ -OHC18). The reaction rates, given by the slope values (Figure 4-12) are also higher for P( $\omega$ -Me-OHC18) compared to those for P( $\omega$ -OHC18), and a similar explanation holds as well.

The rate constant values ( $k_r$ ) for the polyesters are calculated by substituting for  $[A]_0$ , the initial concentration of functional groups and the optimal value for catalyst concentration into equation (4-10). Table 4-5 represents the values of reaction rate constant for each individual acid and ester terminated polymers. As can be seen from Table 4-5, the values of reaction rate constant for methyl ester terminated polyesters are higher than the acid terminated polyesters. This could be explained by the relatively higher reactivity for terminal carboxyl ester groups in the reacting monomers compared to the carboxyl acid terminal groups. Another possible reason for this observation could be related to the relative ability of the carboxyl acid/ester groups to attach to the catalyst metal ion  $[Ti^+]$ . Based on the proposed mechanism of polycondensation catalysis (Figure 4-3), in an acid terminated molecule the reaction between nucleophilic oxygen atoms of carbonyl group with  $[Ti^+]$  is not easy, because the carbonyl is already involved in strong hydrogen bonding with (OH) group. In contrast, in an ester terminated molecule the carbonyl group is connected to a methyl group ( $CH_3$ ) which is more likely to react with the (OH) group of the closest monomeric chain to produce methanol as a by-product.

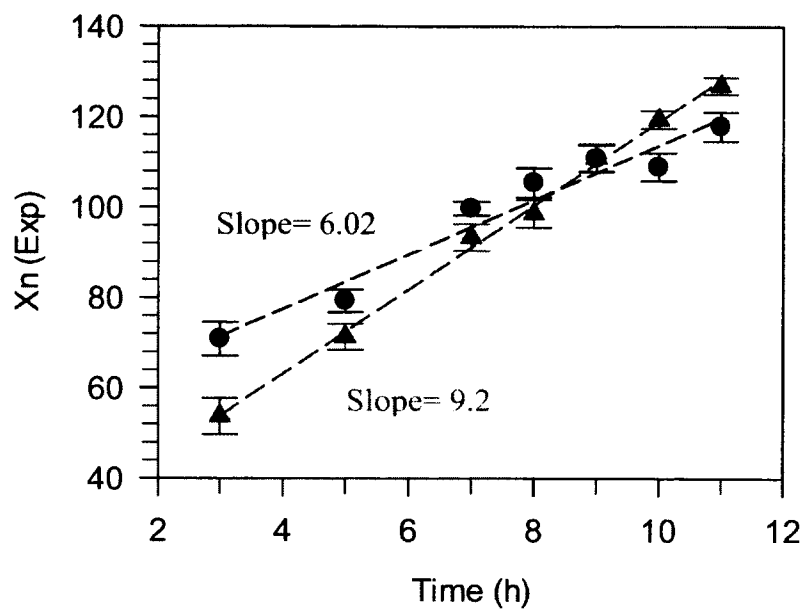
**Table 4-4.** Experimental (exp) and mathematical (calc) data of (a)P( $\omega$ -OHC18) and (b) P( $\omega$ -Me-OHC18).  $M_0 = 282$  g/mol.

(a)	Time (h)	Temp (°C)	$\bar{M}_w$	$\bar{M}_n$	PDI	$\bar{X}_n$ (Exp)	$\bar{X}_n$ (Calc)	p
First phase	3	150	26615 $\pm$ 4154	11325 $\pm$ 1050	2.3 $\pm$ 0.1	45.8	46.3	0.9782
	2	180	38361 $\pm$ 4350	15499 $\pm$ 702	2.4 $\pm$ 0.1	54.2	58.4	0.9816
	2	200	47061 $\pm$ 3639	18455 $\pm$ 433	2.5 $\pm$ 0.1	74.6	70.4	0.9866
Second phase	1	220	68687 $\pm$ 4295	22157 $\pm$ 915	3.1 $\pm$ 0.1	80.4	76.4	0.9876
	1	220	80937 $\pm$ 3788	23291 $\pm$ 829	3.4 $\pm$ 0.1	85.7	82.4	0.9883
	1	220	95018 $\pm$ 5222	23904 $\pm$ 872	3.9 $\pm$ 0.1	83.9	88.5	0.9881
	1	220	118806 $\pm$ 12961	27469 $\pm$ 905	4.3 $\pm$ 0.1	92.8	94.5	0.9892
	1	220	472853 $\pm$ 6457	11325 $\pm$ 1447	4.1 $\pm$ 0.1	58.3	100.5	0.9829
	1	220	64710 $\pm$ 7636	15499 $\pm$ 974	4.1 $\pm$ 0.1	48.7	106.5	0.9795

(b)	Time (h)	Temp (°C)	$\bar{M}_w$	$\bar{M}_n$	PDI	$\bar{X}_n$ (Exp)	$\bar{X}_n$ (Calc)	p
First phase	3	150	24615 $\pm$ 5196	15147 $\pm$ 1122	1.6 $\pm$ 0.1	53.7	53.8	0.9814
	2	180	34181 $\pm$ 4231	20106 $\pm$ 811	1.7 $\pm$ 0.1	71.2	72.4	0.9860
	2	200	48021 $\pm$ 2202	26313 $\pm$ 836	1.8 $\pm$ 0.1	93.3	91.0	0.9893
Second phase	1	220	52120 $\pm$ 4205	27797 $\pm$ 854	1.8 $\pm$ 0.1	98.5	100.0	0.9899
	1	220	61806 $\pm$ 5603	31294 $\pm$ 860	1.9 $\pm$ 0.1	110.9	109.6	0.9910
	1	220	68200 $\pm$ 6713	33679 $\pm$ 561	2.0 $\pm$ 0.1	119.4	118.9	0.9916
	1	220	84975 $\pm$ 8793	34779 $\pm$ 528	2.3 $\pm$ 0.1	126.8	128.2	0.9921
	1	220	45025 $\pm$ 3750	18010 $\pm$ 1182	2.5 $\pm$ 0.1	63.8	137.5	0.9843
	1	220	32696 $\pm$ 4486	13078 $\pm$ 573	2.5 $\pm$ 0.1	46.3	146.8	0.9784



**Figure 4-11.** Linear relationship between  $\bar{X}_n$  and reaction time for (a)  $P(\omega\text{-OHC18})$  and (b)  $P(\omega\text{-Me-OHC18})$ , ( $R^2 > 0.9831$ ).



**Figure 4–12.** Comparison of kinetic study between (●) P(ω-OHC18) and (▲) P(ω-Me-OHC18).

For P( $\omega$ -OHFA) and P( $\omega$ -Me-OHFA) the values of equilibrium constant ( $K_c$ ) for the polycondensation process which corresponds to the maximum  $\bar{X}_n$  are calculated using equation (4-6) and is given by Table 4-5. As can be seen in the table,  $K_c \geq 10^4$  obtained for all P( $\omega$ -Me-OHFA)s and P( $\omega$ -OHFA)s, suggesting that the reactions have been performed under conditions sufficient for obtaining high molecular weight products.

#### 4.4.2.3 Effect of Temperature on polycondensation

The temperature of the second phase of the polymerization (at optimal catalyst concentrations) was increased from 220 °C to 230°C, 240 °C and 250 °C at regular intervals of every 1 hour. Figures 4-13 (a) to (c) demonstrate the effect of increasing temperature on  $\bar{M}_n$  and PDI for P( $\omega$ -Me-OHFA)s and P( $\omega$ -OHFA)s. The different  $\bar{M}_n$  and PDI values for each pair of acid/ester terminated polyesters are listed in Table 4-7.  $\bar{M}_n$  decreased with increasing reaction temperature beyond 220 °C for both acid as well as ester derived polyesters. Polyesters formed at temperatures higher than 220 °C also demonstrated broader molecular weight distributions. The samples at these higher temperatures had a charred appearance and most of them were not completely soluble in chloroform. The above findings suggest possible thermal degradation of the samples at higher reaction temperatures, leading to depolymerisation and subsequent unwanted side reactions. At higher temperatures, side reactions such as backbiting or cross-linking have been observed for polyesters (Quan 2005; Gupta and Kumar 2007).

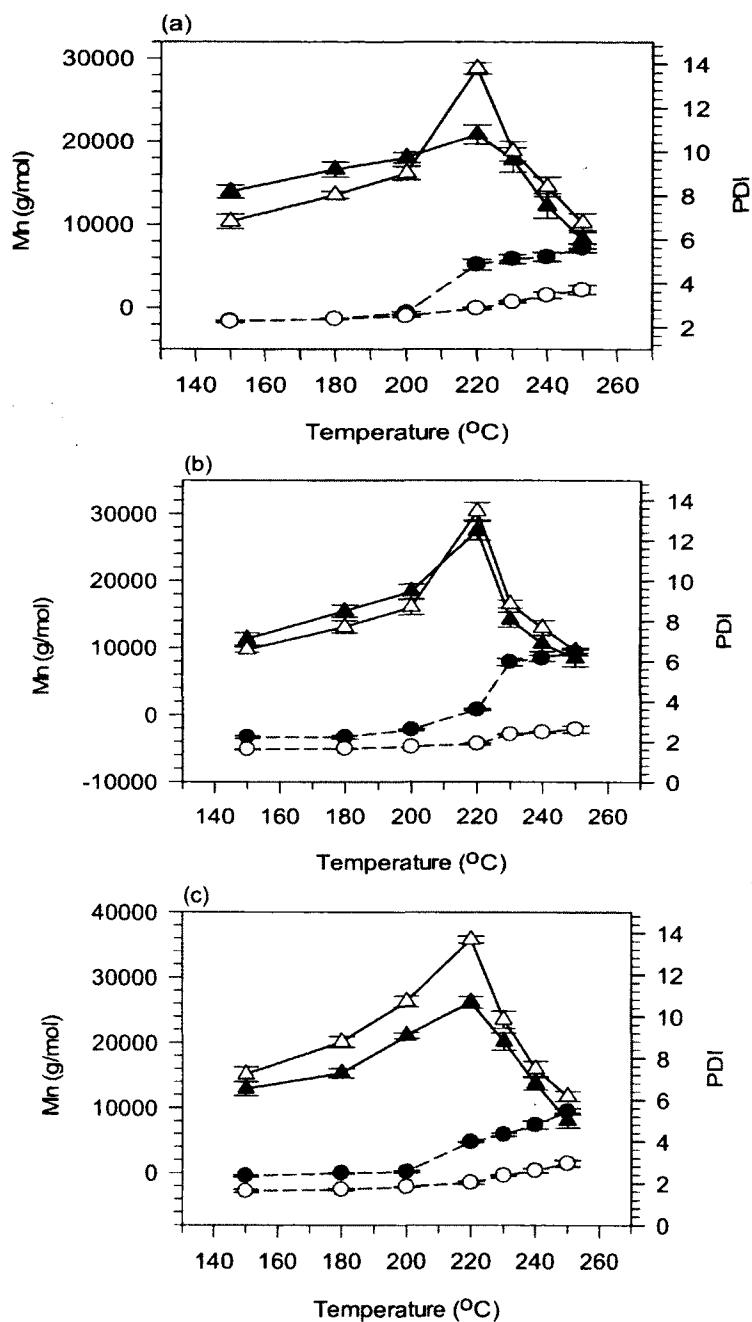
**Table 4-5.** Reaction rate and equilibrium constant of polycondensation of acid and ester terminated polymers

Polymers	Acid terminated		Methyl ester terminated	
	$k_r \times 10^4$ ( $L^2 \text{ mol}^{-1} \text{ h}^{-1}$ )	$K_c \times 10^4$	$k_r \times 10^4$ ( $L^2 \text{ mol}^{-1} \text{ h}^{-1}$ )	$K_c \times 10^4$
<b>P(<math>\omega</math>-C9)</b>	15	1.9	24	2.5
<b>P(<math>\omega</math>-C13)</b>	20	2.0	29	2.2
<b>P(<math>\omega</math>-C18)</b>	17	1.0	27	1.6



**Table 4-6.**  $\bar{M}_n$  and PDI values of P( $\omega$ -OHFA)s and P( $\omega$ -Me-OHFA)s versus temperature

		$\bar{M}_n$ (g/mol)	PDI	$\bar{M}_n$ (g/mol)	PDI
Time (h)	Temperature (°C)	<b>P(<math>\omega</math>-OHC9)</b>		<b>P(<math>\omega</math>-Me-OHC9)</b>	
3	150	14000 $\pm$ 793	2.2 $\pm$ 0.1	10350 $\pm$ 870	2.2 $\pm$ 0.05
2	180	16600 $\pm$ 930	2.3 $\pm$ 0.1	13500 $\pm$ 415	2.3 $\pm$ 0.02
2	200	18040 $\pm$ 640	2.6 $\pm$ 0.1	16200 $\pm$ 813	2.5 $\pm$ 0.05
4	220	20800 $\pm$ 1150	4.8 $\pm$ 0.2	28470 $\pm$ 761	2.8 $\pm$ 0.05
1	230	16270 $\pm$ 1400	5.1 $\pm$ 0.2	18800 $\pm$ 1190	3.1 $\pm$ 0.05
1	240	12240 $\pm$ 1470	5.2 $\pm$ 0.2	14500 $\pm$ 1180	3.4 $\pm$ 0.1
1	250	8220 $\pm$ 1095	5.6 $\pm$ 0.2	10100 $\pm$ 1135	3.7 $\pm$ 0.2
		<b>P(<math>\omega</math>-OHC13)</b>		<b>P(<math>\omega</math>-Me-OHC13)</b>	
3	150	11300 $\pm$ 900	2.2 $\pm$ 0.1	9720 $\pm$ 400	1.6 $\pm$ 0.02
2	180	15500 $\pm$ 920	2.2 $\pm$ 0.1	13130 $\pm$ 930	1.6 $\pm$ 0.01
2	200	18450 $\pm$ 1069	2.6 $\pm$ 0.1	16110 $\pm$ 1150	1.7 $\pm$ 0.01
4	220	27480 $\pm$ 1397	3.6 $\pm$ 0.1	30377 $\pm$ 975	1.9 $\pm$ 0.05
1	230	14200 $\pm$ 1124	5.9 $\pm$ 0.2	16550 $\pm$ 590	2.3 $\pm$ 0.02
1	240	10660 $\pm$ 1215	6.1 $\pm$ 0.2	13000 $\pm$ 1100	2.5 $\pm$ 0.05
1	250	8450 $\pm$ 1250	6.4 $\pm$ 0.2	9600 $\pm$ 405	2.6 $\pm$ 0.1
		<b>P(<math>\omega</math>-OHC18)</b>		<b>P(<math>\omega</math>-Me-OHC18)</b>	
3	150	12900 $\pm$ 1050	2.3 $\pm$ 0.1	15150 $\pm$ 1120	1.6 $\pm$ 0.07
2	180	15300 $\pm$ 700	2.4 $\pm$ 0.1	20106 $\pm$ 810	1.7 $\pm$ 0.05
2	200	21060 $\pm$ 430	2.5 $\pm$ 0.1	26300 $\pm$ 840	1.8 $\pm$ 0.02
4	220	26190 $\pm$ 905	3.9 $\pm$ 0.1	34779 $\pm$ 528	2.0 $\pm$ 0.07
1	230	20160 $\pm$ 1300	4.3 $\pm$ 0.1	23520 $\pm$ 1300	2.3 $\pm$ 0.05
1	240	13700 $\pm$ 974	4.8 $\pm$ 0.2	16000 $\pm$ 1170	2.6 $\pm$ 0.1
1	250	8067 $\pm$ 1160	5.4 $\pm$ 0.1	11700 $\pm$ 750	2.9 $\pm$ 0.1



**Figure 4-13.**  $\bar{M}_n$  and PDI as function of temperature of (a) P( $\omega$ -OHC9) and P( $\omega$ -Me-OHC9), (b) P( $\omega$ -OHC13) and P( $\omega$ -Me-OHC13), (c) P( $\omega$ -OHC18) and P( $\omega$ -Me-OHC18). Symbols are: ( $\Delta$ ,  $\blacktriangle$ )  $\bar{M}_n$  of P( $\omega$ -Me-OHC13) and P( $\omega$ -OHC13), respectively. ( $\circ$ ,  $\bullet$ ): PDI of P( $\omega$ -Me-OHC13) and P( $\omega$ -OHC13), respectively.

#### 4.5 Summary

Acid and ester terminated P( $\omega$ -C9), P( $\omega$ -C13) and P( $\omega$ -C18) were successfully synthesized through melt polycondensation reactions catalyzed by [Ti(OiPr)<sub>4</sub>]. The effect of reaction conditions such as catalyst concentration, reaction time and temperature were considered in order to optimize the polycondensation process so as to achieve high molecular weight polyesters. For both ester and acid derived P( $\omega$ -OHFA)s, the optimal conditions included a two phase polycondensation reaction at the highest temperature of 220 °C for up to 4 hours using a catalyst amount between 200-300 ppm. A comparison of the rate constant for acid and ester terminated polymers revealed that polymerization was faster for ester terminated monomers.

## **5 Physical properties of aliphatic polyesters: Influence of monomer chain length on structure and physical functionality**

### **5.1 Introduction**

Thermoplastics are polymers used in a wide variety of applications depending on their physical properties such as thermal stability, strength, melting temperature etc.(Margolis 1985; MacDermott and Shenoy 1997). Recently, the need for alternatives to polymers made from petroleum has become very important amid rising global concerns about renewability and environmental impact. For example, polyethylene (PE) which is used in a broad range of applications, owing its desirable physical properties, has raised widespread concerns. Very slow biodegradation process and persistence in the environment for example, results in the accumulation of very large amounts of plastic that is a source of major environment contamination(Malpass 2010). Biodegradable aliphatic polyesters such as poly(lactic acid) (PLA), poly(glycolide acid) (PGA) are potential alternatives to thermoplastics made from petroleum. However, their use is limited due to the insufficiency of some of their thermal and mechanical properties (Cai, Yao et al. 2002). The molecular weight of aliphatic polyester and the length of its monomeric unit are key factors defining its crystal structure, thermal properties, and strength. The principal cause of the poor performance of PLA and PGA, for example, is considered to be their short monomeric unit length.

The physical properties of bio-based aliphatic polyesters can be somehow improved by blending, copolymerization and sometimes high branching (Albertsson and Varma 2002). However, a comprehensive understanding of the effect of the several factors determining the material's

properties, such as molar mass, distribution of polymeric chains, chemical composition of the repeating units, crystallinity, and the presence of polar functional groups, is required in order to design bio-based materials which can compare with conventional thermoplastics. It is therefore of primary importance to understand the relationships between the structure of both the monomer and polymer, and the physical properties, i.e., functionality, of the materials.

In the present study, several ester and acid terminated polymers, namely, poly( $\omega$ -hydroxy methyl esters) (P( $\omega$ -Me-OHFA)s) and poly( $\omega$ -hydroxyfatty acid) (P( $\omega$ -OHFA)s), have been investigated. The polyesters of the present study were prepared with different fatty acid chain length (FA= C9, C13 and C18) each in different molecular weights (Chapter 4). The thermal stability, and melting and crystallization behaviour of the P( $\omega$ -Me-OHFA) polyesters were investigated by thermal gravimetric analysis (TGA) and differential scanning calorimetry (DSC), respectively. Their viscoelastic and tensile properties were tested by a dynamic mechanical analyzer (DMA) and a Texture Analyzer, respectively. The crystalline structure and polymorphism of the cast P( $\omega$ -Me-OHFA) films were examined by wide-angle x-ray diffraction (WAXD). The effects of the average number molecular weight ( $\bar{M}_n$ ) and monomeric unit length ( $n$ , in carbon atoms) on the physical properties are examined and discussed.

## 5.2 Experimental

P( $\omega$ -OHC9), P( $\omega$ -Me-OHC9), P( $\omega$ -OHC13), P( $\omega$ -Me-OHC13), P( $\omega$ -OHC18) and P( $\omega$ -Me-OHC18) were prepared through a melt polycondensation catalyzed by Ti(IV) isopropoxide [Ti(OiPr)<sub>4</sub>]. The synthesis procedure was discussed in chapter 4, in details. All the samples have been fully characterized in terms of chemical structure and physical properties. The detailed analysis of the molecular weight and molecular weight distribution of the P( $\omega$ -OHFA)s, the acid

terminated materials, indicated relatively low average number molecular weight and very high PDI (4 to 6). As a consequence, it was not possible to process them in to useable films. Furthermore, preliminary analysis of the physical properties of the P( $\omega$ -OHFA)s, indicated very poor functionality compared to the P( $\omega$ -Me-OHFA)s suggesting that they may not be optimal for practical applications. The acid terminated polymers are therefore not presented.

### **5.3 Characterization techniques for physical properties**

#### **5.3.1 Thermogravimetric analysis**

Thermogravimetric Analysis (TGA) is commonly used to test the thermal stability of materials. This technique monitors the weight change as a function of temperature. TGA and its derivative (DTG) allow for the tracking of decomposition temperatures and the decomposition stages of the materials at each stage. TGA also record the volatilization of any moisture or solvent in a specimen at an earlier stage than the decomposition of the polymer. For optimal TGA results, test samples should be dried before testing.

TGA was carried out on the synthesized polyesters using a Q500 (TA instrument, Newcastle, DE, USA) following the ASTM D3850-94 standard. Polymer samples of ~10 mg were evenly spread in the platinum pan and heated under dry nitrogen at a constant rate of 10 °C/min from room temperature to 600 °C.

#### **5.3.2 Wide-angle X-ray diffraction**

Wide-angle X-ray diffraction (WAXD) was carried out at room temperature (~ 22 °C) on an EMPYREAN diffractometer system (PANalytical, The Netherlands) equipped with a Cu-K $\alpha$  radiation source ( $\lambda = 1.540598 \text{ \AA}$ ) and a PIXcel-3D<sup>TM</sup> area detector. The 2 $\theta$ -scanning range was from 3° to 90°. 3313 points were collected in 45 min in this process. The WAXD patterns were

recorded at 45 kV and at 40 mA. The data were processed and analyzed using the Panalytical's X'Pert HighScore V3.0 software.

### 5.3.2.1 X-ray data analysis and polymorphism of aliphatic compounds

The WAXD lines of the polyester's patterns were indexed and their crystal structure determined with the help of comparative data mined from the literature. The common crystal structure models of aliphatic compounds were established in numerous studies. The molecules take different orientations relative to their neighbours by rotation around their long axis, forming different crystal structure symmetries of the methylene subcells (Larsson 1994). Three basic symmetries, commonly denoted as  $\alpha$ ,  $\beta'$  and  $\beta$ , are described in the literature (Larsson 1986). Molecular packing within a unit cell is the main difference between the  $\alpha$ -,  $\beta'$ - and  $\beta$ - forms. The chains of the  $\alpha$ - polymorph pack in a hexagonal symmetry and is characterized by one strong wide-angle line in the WAXD pattern at a lattice spacing of  $d_{hkl} \sim 4.2$  Å, originating from the ( $h=1, k=0, l=0$ ) basal plane reflection, here noted  $100_{\alpha}$ . Recall that the  $hkl$  values are the Miller indices of the ( $hkl$ ) family of planes with  $d_{hkl}$ -spacing. The common subcell packing of the  $\beta'$ -polymorph is orthorhombic, with the alternate acyl chains packing in planes almost perpendicular to each other ( $O_{\perp}$ ), and is characterized by two strong wide-angle lines at lattice spacings of 4.2– 4.3 Å originating from the  $110_{\beta'}$  reflection and 3.7 – 3.9 Å originating from the  $200_{\beta'}$  reflection. The hydrocarbon chains of the  $\beta$ -polymorph are commonly packed parallel to each other in a triclinic (or monoclinic, if the angles  $\alpha$  and  $\gamma$  are 90 °C) parallel subcell ( $T_{||}$ ). The  $\beta$ -form is characterized in the wide-angle region by a lattice spacing of  $\sim 4.6$  Å originating from the  $010_{\beta}$  reflection and a number of other strong lines around 3.6 – 3.9 Å. The  $\beta$ -polymorph is

the most stable crystal form, with the highest melting temperature, and the  $\alpha$ -polymorph is the least stable crystal form, with the lowest melting temperature (Ghotra, Dyal et al. 2002; Timms 2003).

### 5.3.3 Differential scanning calorimetry (DSC)

DSC is used to measure the temperature and the heat flow associated with the thermal phase transitions of materials. DSC is commonly used to test the melting ( $T_m$ ), crystallization ( $T_c$ ) and eventually, the glass transition ( $T_g$ ) temperatures of polymers.

DSC analysis was carried out on a Q200 (TA instrument, Newcastle, DE, U.S.A.) equipped with a refrigerated cooling system (RCS 90, TA Instruments) under a nitrogen flow of 50mL/min. Approximately 5.0 – 6.0 ( $\pm 0.1$ ) mg of sample was placed and hermetically sealed in an aluminum DSC pan. The “TA Universal Analysis” software v5.4.0 together with a method developed by our group (Bouzidi, Boodhoo et al. 2005) was used to analyze the data and extract the main characteristics of the thermal transitions, such as onset, offset, and peak temperatures ( $T_{on}$ ,  $T_{off}$ ,  $T_{c,m}$ , respectively), full width at half maximum (FWHM) and crystallization or melting enthalpy,  $\Delta H_{c,m}$ .

The sample was first equilibrated at 0 °C and heated to 130 °C at a constant rate of 3.0 °C/min (first heating cycle), and held at that temperature for 10 min to erase the thermal history. The sample was then cooled down to -90 °C with a cooling rate of 3 °C/min and subsequently reheated to 130 °C at the same rate (second heating cycle). During the heating process, measurements were performed with modulation amplitude of 1 °C/min and a modulation period of 60 s. The modulation process permits the separation of the total heat flow into its reversing and non-reversing contributions. This method confers benefits such as increasing the sensitivity



for detecting weak and complex transitions especially for detecting the glass transition and measuring the glass transition temperature ( $T_g$ ).  $T_g$  can be better discerned in the reversing heat flow upon its availability.

The measurements were performed following the ASTM E1356-03 standard procedure.

#### 5.3.4 Dynamic Mechanical Analysis

Dynamic mechanical analysis (DMA) is an analytical technique in which an oscillating force is applied to a sample and the resultant response is analyzed. The response of the material is measured as a function of both oscillatory frequency and temperature. Stress is the sinusoidal force which is applied to deform the sample. Strain is the amount by which the sample is deformed. Storage, loss modulus and damping are parameters that have been widely used in order to study the viscoelastic properties of polymeric material.

The viscoelastic properties of P( $\omega$ -Me-OHFA)s, were tested by a DMA, model Q800 (TA Instruments, Newcastle, DA), equipped with a liquid nitrogen cooling system. The sample was cut into a rectangular shape (17.5 mm  $\times$  13 mm  $\times$  0.6 mm) and analyzed in the single cantilever mode. The sample was heated under a constant rate of 1  $^{\circ}$ C/min over a temperature range of -100  $^{\circ}$ C to 60  $^{\circ}$ C. The measurements were performed at a frequency of 1 Hz and fixed oscillation displacement of 20  $\mu$ m following the ASTM E1640-99 standard.

For a viscoelastic material, the modulus is a complex quantity  $E^*$ , defined as follow:

$$E^* = E' + iE'' \quad (5-1)$$

The complex modulus (equation 5-1) consists of real and imaginary parts. The real part (storage modulus) describes the ability of the material to store potential energy and release it upon deformation. The imaginary portion (loss modulus) is associated with energy dissipation in the form of heat upon deformation.

The storage modulus ( $E'$ ) is a measure of the elastic response of the material, and the loss modulus ( $E''$ ) is the measure of the viscous response of the material.  $E'$  and  $E''$  are defined as follow:

$$E' = \frac{\sigma}{\varepsilon} \cos \delta \quad (5-2)$$

$$E'' = \frac{\sigma}{\varepsilon} \sin \delta \quad (5-3)$$

Where  $\sigma$  is the stress,  $\varepsilon$  is the strain, and  $\delta$  is the phase angle.

Damping is a dimensionless quantity, so-called Tan ( $\delta$ ), obtained by the ratio of loss to storage modulus ( $E''/E'$ ) and is a measure of how well a polymeric material can dissipate energy. Tan  $\delta$  ranges from zero for an ideal elastic material to infinity for an ideal viscous liquid. Larger values of tan  $\delta$  and  $E''$  indicate that greater deformation energy is dissipated as heat (Chartoff, Menczel et al. 2009). Tan  $\delta$  varies with the temperature and frequency.

DMA is particularly suitable to measure  $T_g$  of polymers.  $T_g$  is the temperature where polymer transforms from a hard- and glassy-like state to a flexible and rubbery-like state. When the temperature is below  $T_g$ , the molecules of the polymer have little relative mobility and high amount of storage modulus. When the temperature is above  $T_g$ , the molecular chains are allowed to slide past each other when a force is applied and the amount of absorbed energy can be dissipated through the chains movements. Note that Tan  $\delta$  is maximum at the glass transition point.

### 5.3.5 Tensile Analysis

The measurements of tensile strength and strain were obtained using a Texture Analyzer (TA HD, Texture Technologies Corp, NJ, USA) equipped with a 2-kg load cell. Tensile analysis is a

technique in which the material is subjected to a uniaxial tension until ruptured. Mechanical properties such as ultimate tensile strength, maximum elongation and Young's modulus are measured using tensile test. Tensile stress and strain are defined as the following:

$$\text{Tensile Stress: } \sigma = \frac{F}{A_0} \quad (5-4)$$

$$\text{Tensile Strain: } \varepsilon = \frac{\Delta L}{L_0} \quad (5-5)$$

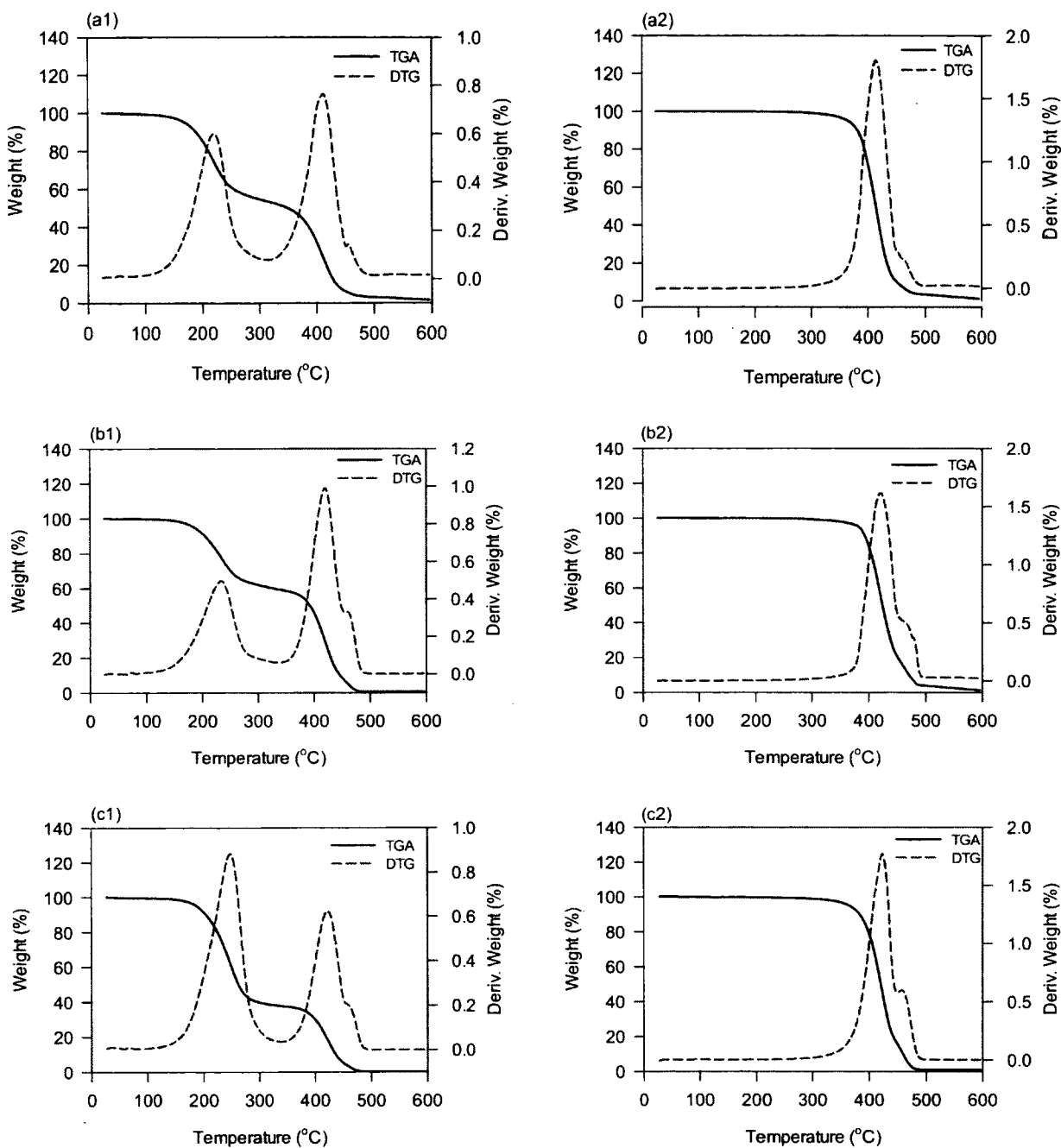
Where  $F$  is the applied force;  $A_0$  is the initial cross-sectional area;  $L_0$  is the initial length and  $\Delta L$  is the change of the length of the object. Young's modulus, which is also known as tensile modulus, can be calculated by dividing the tensile strength by the tensile strain. It is experimentally determined by the slope of the stress versus strain curve obtained from the tensile test.

## 5.4 Result and discussion

### 5.4.1 Thermal stability of the polyesters

The decomposition temperatures of P( $\omega$ -Me-OHFA) samples were studied by TGA and its first derivative (DTG). Figures 5-1 (a<sub>1</sub>) to (c<sub>1</sub>) display typical TGA and DTG traces of the  $\omega$ -Me-OHFA monomers and Figures 5-1 (a<sub>2</sub>) to (c<sub>2</sub>) those of their respective P( $\omega$ -Me-OHFA) polymer samples with the highest  $\bar{M}_n$ . Table 5-1 lists the values of the onset temperature of degradation as defined at 1% weight loss ( $T_{d(on)}$ ) and temperature at maximum of the first DTG peak ( $T_{d(max)}$ ) for each P( $\omega$ -Me-OHFA)s with different  $\bar{M}_n$ . As can be seen in Figure 5-1, the polyesters undergo similar decomposition paths but degrade quite differently from the monomers. The DTG of the monomers (dashed curve in Figure 5-1(a<sub>1</sub>-c<sub>1</sub>)) display two resolved

peaks (at  $\sim 221.1 \pm 3.6$  and  $414.3 \pm 2.7$  °C) and a very apparent shoulder (at  $\sim 458 \pm 3.5$  °C), evidencing a three- stage thermal degradation process. In contrast, the DTG of the polyesters (dashed curve in Figure 5-1(a<sub>2</sub> –c<sub>2</sub>)) demonstrate one prominent peak (at  $\sim 420 \pm 2.0$  °C) followed by a shoulder (at  $\sim 466 \pm 2.8$  °C), indicating a two-stage degradation process. The monomers were expected to show a degradation process with at least two stages as they consist of two functional end groups (hydroxyl and methyl ester) plus a moderately long linear chain (C9, C13 and C18) made of methylene groups. As illustrated in Figures 5-1(a<sub>2</sub>-c<sub>2</sub>), the P( $\omega$ -Me-OHFA)s displayed a two- stage thermal degradation process. The first stage of degradation of P( $\omega$ -Me-OHFA) samples is reminiscent of that of high thermal stability polyethylene (HDPE) but its temperature at maximum rate degradation is lower (430 °C compared to 470°C for HDPE) (Mengeloglu and Karakus 2008). Nevertheless, P( $\omega$ -Me-OHFA)s demonstrated an overall very good thermal stability as evidenced by their high  $T_d(on)$  and  $T_{d(max)}$  values which span from 310 to 344 °C and from 417 to 431 °C, respectively, for the samples with the highest  $\bar{M}_n$  (Table 5-1). The polyesters of this study compare favorably in terms of thermal stability with similar biodegradable aliphatic polyester reported in the literature. Chrissafis *et al.* (Chrissafis, Paraskevopoulos et al. 2006) reported that the biodegradable aliphatic poly(propylene succinate) has a relatively high thermal stability with a DTG evidencing a  $T_{d(max)}$  at around 404 °C and degrades in a single stage process. A high thermal stability with a single thermal degradation stage and a DTG peak at  $\sim 380$ °C was also reported for aliphatic polyesters based on poly( $\epsilon$ -caprolactone) copolyesters (Liu, Qian et al. 2006).



**Figure 5–1.** TGA and DTG traces of (a<sub>1</sub>) ( $\omega$ -Me-OHC9), (b<sub>1</sub>) ( $\omega$ -Me-OHC13) and (c<sub>1</sub>) ( $\omega$ -Me-OHC18). TGA and DTG traces of (a<sub>2</sub>) P( $\omega$ -Me-OHC9), and (b<sub>2</sub>) P( $\omega$ -Me-OHC13), and (c<sub>2</sub>) P( $\omega$ -Me-OHC18).

**Table 5-1.** Average number of molecular weight  $\bar{M}_n$ , Onset temperature of degradation,  $T_d(on)$ , and DTG peak maximum temperature,  $T_{d(max)}$ , of the P( $\omega$ -Me-OHFA)s.

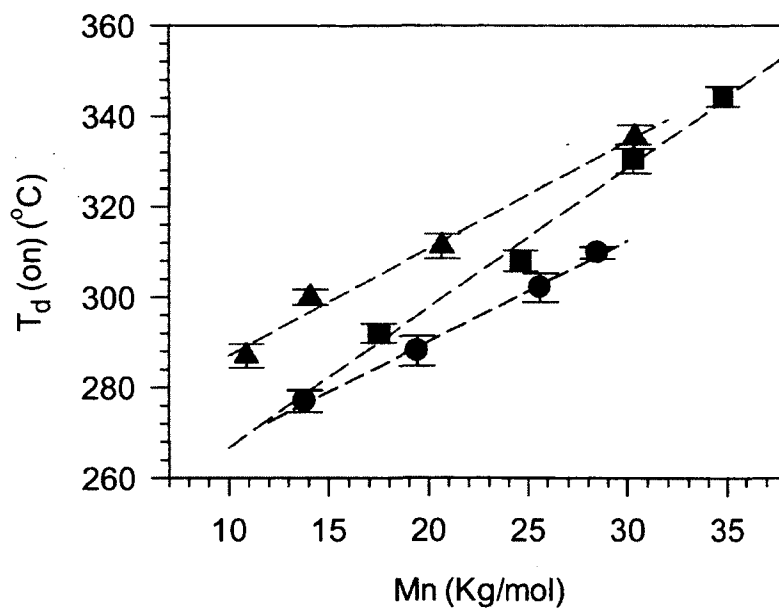
Entry	$\bar{M}_n$ (g/mol)	$T_d(on)$ (°C)	$T_{d(max)}$ (°C)
P( $\omega$ -Me-OHC9)	13831 $\pm$ 988	277.0 $\pm$ 2.4	411.5 $\pm$ 1.9
	19438 $\pm$ 1015	288.1 $\pm$ 3.3	412.4 $\pm$ 1.6
	25633 $\pm$ 946	302.1 $\pm$ 3.2	415.4 $\pm$ 1.6
	28470 $\pm$ 761	309.8 $\pm$ 1.3	416.5 $\pm$ 2.0
P( $\omega$ -Me-OHC13)	10889 $\pm$ 1022	287.0 $\pm$ 2.6	419.9 $\pm$ 2.8
	14109 $\pm$ 866	300.0 $\pm$ 1.7	420.9 $\pm$ 2.7
	20675 $\pm$ 930	311.2 $\pm$ 2.7	423.9 $\pm$ 2.4
	30377 $\pm$ 975	335.4 $\pm$ 2.6	425.6 $\pm$ 2.1
P( $\omega$ -Me-OHC18)	17506 $\pm$ 1044	29.20 $\pm$ 2.1	424.6 $\pm$ 1.4
	24616 $\pm$ 836	302.9 $\pm$ 2.3	426.2 $\pm$ 1.6
	30294 $\pm$ 860	330.6 $\pm$ 3.2	427.8 $\pm$ 1.7
	34779 $\pm$ 528	344.3 $\pm$ 2.2	430.8 $\pm$ 1.5

The effect of variation of two main parameters,  $\bar{M}_n$  and monomeric unit length, on thermal stability was studied as follows:

#### 5.4.1.1 Effect of molecular weight on thermal stability

Figure 5-2 displays  $T_d(on)$  as a function  $\bar{M}_n$  for the P( $\omega$ -Me-OHFA)s. As can be seen,  $T_d(on)$  scales linearly ( $R^2 > 0.9945$ ) with,  $\bar{M}_n$  in the range of the molecular weights considered in the study. Because the thermal degradation of the polyesters starts by the decomposition of ester groups, this increase in onset of degradation may be related to the increase of ester bond density as a consequence of increasing  $\bar{M}_n$  (Chrissafis, Paraskevopoulos et al. 2006). One can however notice that  $\frac{d(T_d(on))}{d\bar{M}_n}$ , the rate of increase of  $T_d(on)$ , as a function of  $\bar{M}_n$  for P( $\omega$ -Me-OHC18) ( $3.3 \pm 0.4$  °C per kg/mol.) is higher than for P( $\omega$ -Me-OHC9) and P( $\omega$ -Me-OHC13) which is practically the same ( $2.2 \pm 0.1$  °C per kg/mol.). This suggests that bond density effect is probably balanced by the limiting size effect of the monomeric unit constituting the polyester.

Note that for a given monomeric unit,  $T_{d(max)}$  of P( $\omega$ -Me-OHFA) samples was not significantly affected by  $\bar{M}_n$ . This finding is in agreement with what was reported in the literature for similar materials such as P( $\omega$ -OHC14) (Liu, Liu et al. 2011).



**Figure 5–2.** Onset temperature of degradation ( $T_d(on)$ ) as a function  $\bar{M}_n$  for P( $\omega$ -Me-OHC9), (●), P( $\omega$ -Me-OHC13), (▲), and P( $\omega$ -Me-OHC18), (■). Dashed lines are linear fits ( $R^2 > 0.9945$ ).

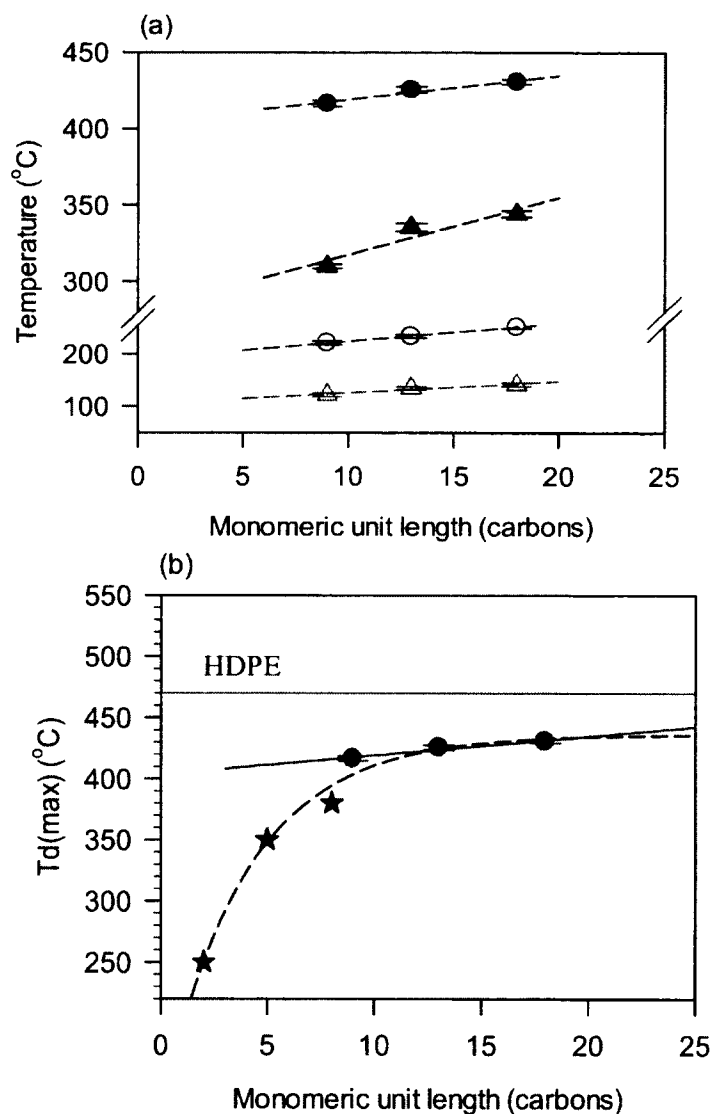


#### 5.4.1.2 Effect of monomeric unit length on thermal stability

The effect of the length of the monomeric repeating unit ( $n$ , in carbon atoms) on  $T_{d(on)}$  and  $T_{d(max)}$  of the  $\omega$ -Me-OHFA monomers and P( $\omega$ -Me-OHFA)s is shown in Figure 5-3(a). Note that the data shown in Figure 5-3(a) are those of the polymers with the highest  $\bar{M}_n$  and the trends observed are typical of all the polyesters with similar  $\bar{M}_n$ . As can be seen; both on  $T_{d(on)}$  and  $T_{d(max)}$  temperatures scale apparently linearly with number of carbons in the range of lengths examined in this study. One can note that the increase in stability of the polymers as a function of monomer length mirrors the variation in stability of the constituting monomers themselves. This is understandable as the most effective structural contribution to the stability of polyesters is correlated to the linear  $-(CH_2)_n-$  segments. It has been well established that polymers with longer hydrocarbon chains are more stable and degrade at higher temperature than shorter ones (Chartoff, Menczel et al. 2009). In the case of polyesters which provide an ester linkage, most of the delay in thermal degradation process is attributed to the hydrophobic nature of the methylene chains. The increase in thermal stability could be attributed to the increase of the hydrophobic character of the fatty acid chain, Van der Waals interactions as well as the availability of more sites which accumulate energy before cleavage as the number of  $(CH_2)$  groups increases.

It is well known that polyesters with short monomeric lengths have poor thermal stability. For example, polyesters such as PGA with one  $(CH_2)$  groups has poor thermal stability with  $T_{d(max)} = 250$  °C (Madhavan Nampoothiri, Nair et al. 2010), poly(caprolactone) with four  $(CH_2)$  groups are more stable and demonstrate  $T_{d(max)}$  up to 350°C (Labet and Thielemans 2009) and poly(nonanolactone) with eight  $(CH_2)$  groups is even more stable demonstrating a  $T_{d(max)}$  at around

380°C (Liu, Kong et al. 2008). These data from the literature were plotted (★ in Figure 5-3(b)) together with the  $T_{d(\max)}$  values obtained for the polyesters of the present study (● in Figure 5-3(b)). The general trend ( $T_{d(\max)}$  versus carbon numbers) depicts an exponential rise to a maximum, with a plateau estimated at ~ 436 °C. This suggests that there is a limit to the increase in stability with increasing number of CH<sub>2</sub> groups in the monomeric unit. The comparison of this limit temperature to the decomposition temperature of high density polyethylene (HDPE), an example of a polymer with very long hydrocarbon chains, which is ~ 470 °C (Mengelolu and Karakus 2008), suggests that it is the competition between the hydrophobic character, Van der Waals attractive interactions and ester bonds that determine the stability of the polyesters.



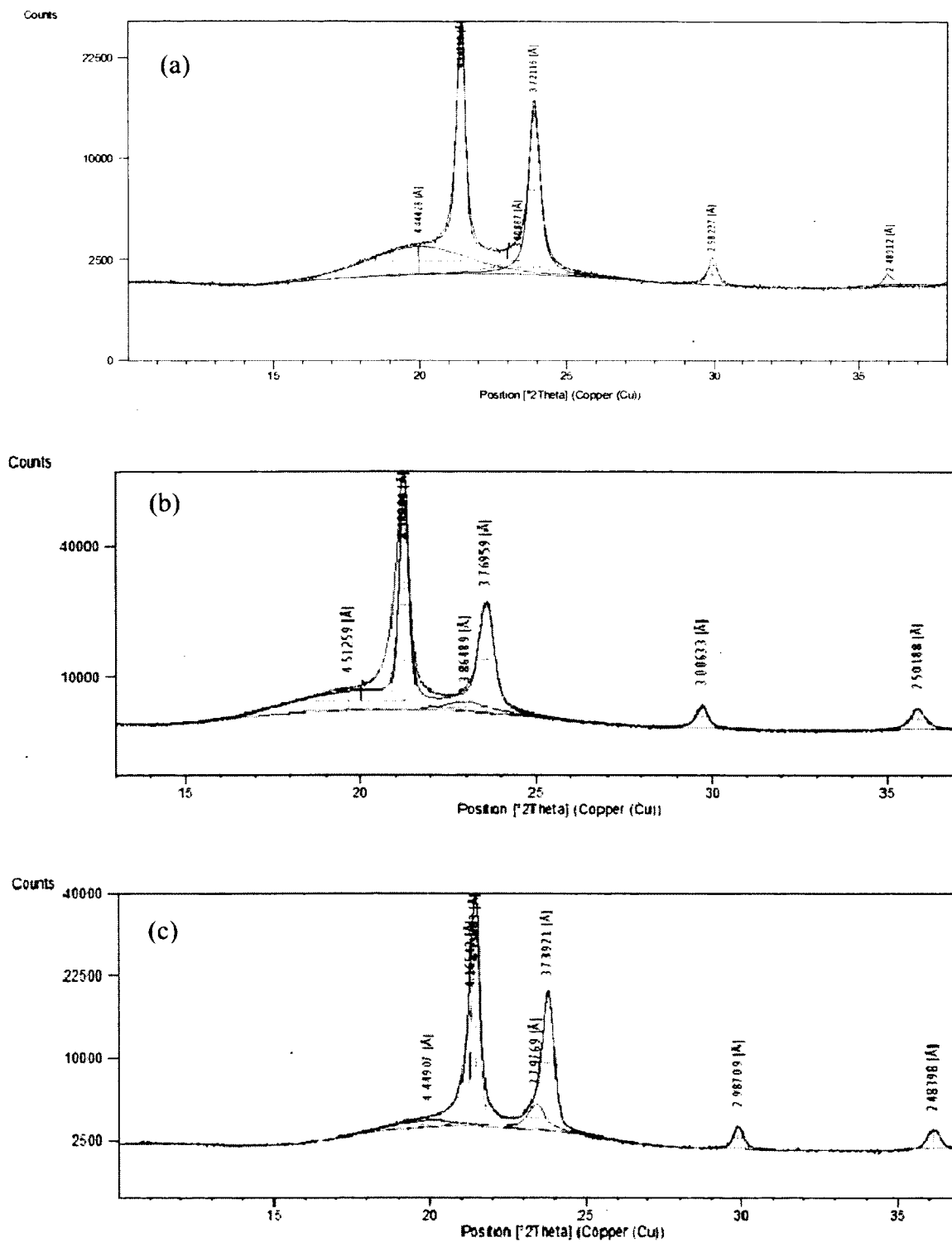
**Figure 5–3.**(a) Characteristic thermal degradation temperatures of monomers (Onset temperature of degradation ( $T_d(on)$ ) and leading DTG peak temperature ( $T_{d(max)}$ ) of monomers ( $\Delta$  and  $\circ$ , respectively), and polymers with the maximum  $\bar{M}_n$  ( $\blacktriangle$  and  $\bullet$ ) as a function of monomeric unit length ( $n$ , carbon atoms). (b)  $T_{d(max)}$  as a function of monomeric unit length ( $n$ , carbon atoms) of P( $\omega$ -Me-OHFA)s ( $\bullet$ ) and of polyesters from the literature measured at the same conditions<sup>1</sup> ( $\star$ ).

<sup>1</sup>Madhavan Nampoothiri, Nair et al. 2010, Liu, Kong et al. 2008, Mengeloglu and Karakus 2008

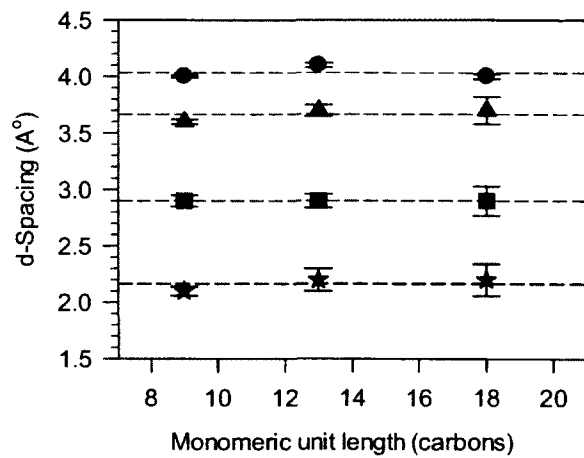
#### 5.4.2 Crystalline structure of P( $\omega$ -Me-OHFA)s

The crystalline structure of the P( $\omega$ -Me-OHFA) samples was investigated by wide-angle X-ray diffraction (WAXD). The WAXD patterns of P( $\omega$ -Me-OHC9), P( $\omega$ -Me-OHC13) and P( $\omega$ -Me-OHC18) are shown in Figure 5-4 (a) to (c), respectively. The d-spacing of the crystal peaks for the three polymers are presented in Figure 5-5. The experimental WAXD profiles of all the P( $\omega$ -Me-OHFA) samples consisted of four resolved diffraction peaks, characteristic of a large crystalline phase, superimposed to a relatively small wide halo, indicative of the presence of an amorphous phase. As can be seen, all demonstrated similar WAXD spectra indicating that they crystallized in similar crystal forms. The analysis of the WAXD patterns was performed with a fitting module of HighScore Version 3.0. The initial positions of the peaks were selected at the maximum height of the well-resolved WAXD peaks. The amorphous contribution was added in the form of two wide lines (centered at  $\sim 3.8$  and  $4.6$  Å) as typically done for semi-crystalline polymers (Murthy and Minor 1990). The observed intensities were evaluated by integrating the crystalline peaks observed in the WAXD profiles.

The sharp diffraction peaks observed in the WAXD patterns of the P( $\omega$ -Me-OHFA)s (Figure 5-4 (a)–(c)) are characteristic of the common orthorhombic methylene subcell packing, normally known as the  $\beta'$ -form. The two very intense lines at positions  $21.29$   $^{\circ}[2\theta]$  (d-spacings of  $4.18 \pm 0.02$  Å) and  $24.22$   $^{\circ}[2\theta]$  (d-spacings of  $3.69 \pm 0.05$  Å) originated from the  $110_{\beta'}$  and  $200_{\beta'}$  reflections of the orthorhombic symmetry, respectively. The weaker peaks at d-spacings of  $2.99 \pm 0.01$  Å and  $2.50 \pm 0.03$  Å originated from the  $210_{\beta'}$  and  $020_{\beta'}$  reflections of the orthorhombic symmetry, respectively.



**Figure 5-4.** WAXD patterns of (a) P( $\omega$ -Me-OHC9), (b) P( $\omega$ -Me-OHC13) and (c) P( $\omega$ -Me-OHC18)



**Figure 5–5.** d-spacing of the P( $\omega$ -Me-OHFA)s in the range of  $2\theta= 3-90^\circ$  as a function of the number of carbon atoms in the monomeric unit.

The WAXD patterns obtained for the P( $\omega$ -Me-OHFA)s are reminiscent of that obtained for melt crystallized polyethylene (PE) (Bunn 1939) and their crystal structure resembles that of PE. This indicates that the crystallinity of P( $\omega$ -Me-OHFA)s is driven by the van der Waals interaction, similarly to PE, which crystallizes by folding into an orthorhombic unit cell in order to maximize the van der Waals interactions between the chains. However, the dipole–dipole interactions of the C-O bonds in the ester linkages play an important role in the crystal packing as revealed by conformational analysis of polyesters and should not be ignored (Bittiger, Marchessault et al. 1970; Hu and Dorset 1990).

The degree of crystallinity (volume fraction of the crystalline phase in a polymer),  $X_c$ , was determined from WAXD patterns as the ratio of the area of the crystalline peaks to the total area. The values of  $X_c$ (%) obtained for the P( $\omega$ -Me-OHFA)s are listed in Table 5-2. The values of  $X_c$ (%) are relatively high and range from 50% to 78% for the P( $\omega$ -Me-OHFA)s, depending on the type of polymer and  $\bar{M}_n$ .

#### 5.4.2.1 Effect of molecular weight on crystalline structure

As discussed above (Section 5-4), all the P( $\omega$ -Me-OHFA)s demonstrated similar WAXD spectra indicating that their crystal structure was not affected by molecular weight. The same orthorhombic symmetry was obtained for all samples independently of  $\bar{M}_n$ . However, the amount of crystal phase was significantly affected by molecular weight. The degree of crystallinity,  $X_c$ (%), of the P( $\omega$ -Me-OHFA)s is listed in (Table 5-2). Figure 5-6 represents  $X_c$ (%) as a function of  $\bar{M}_n$  for the different polyesters. Indeed, as shown in Table 5-2, lower

degrees of crystallinity were obtained for higher  $\bar{M}_n$  for any P( $\omega$ -Me-OHFA) with a given monomer. Furthermore,  $X_c(\%)$  decreased linearly as  $\bar{M}_n$  was increased (Figure 5-6). This is attributable to the fact that lower molecular weight polymers crystallize relatively more easily and allow a higher degree of crystallinity than higher ones because of higher chain mobility (Tung and Buckser 1958; Zen, Saphiannikova et al. 2006; Peponi, Navarro-Baena et al. 2012). The linear trend may be the result of the additive nature of this effect in the range of molecular weights considered here.

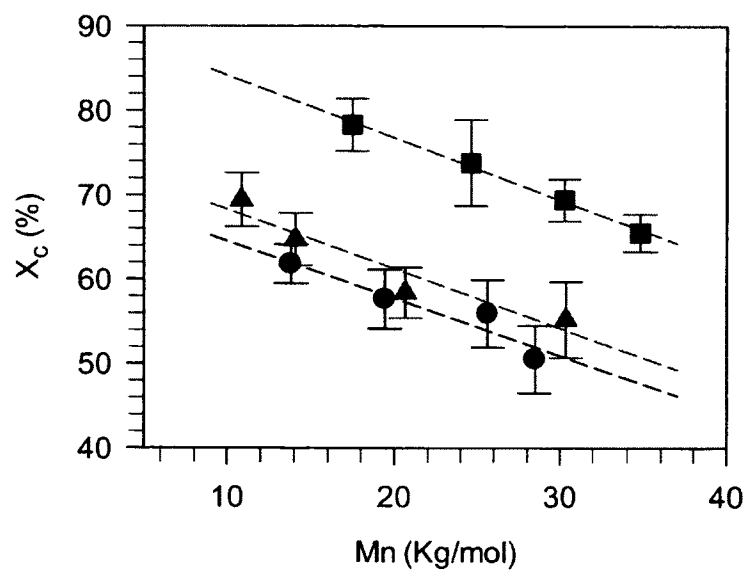
#### 5.4.2.2 Effect of monomeric unit length on crystallinity

The degree of crystallinity increased significantly with the length of the repeating units in all the P( $\omega$ -Me-OHFA) samples (Table 5-2). This is expected because long linear methylene segments provide significant crystallinity in polyesters (Trzaskowski, Quinzler et al. 2011). There are several factors that affect crystallinity: (i) linearity of the polymer (ii) intermolecular forces and (iii) arrangement of side groups in the polymer backbone. In the case of the P( $\omega$ -Me-OHFA)s which are linear polymers without side groups in the backbone, the intramolecular forces are an important factor affecting the degree of crystallinity. An increase in the number of  $-(CH_2)-$  groups in the repeating unit increases the Van der Waals attractive forces which in turn increase the degree of crystallinity and enhance the stability of the crystals.



**Table 5-2.** Degree of crystallinity  $X_c$  (%) of P( $\omega$ -Me-OHFA)s as a function of  $\bar{M}_n$ 

Entry	$\bar{M}_n$ (g/mol)	$X_c$ (%)
P( $\omega$ -Me-OHC9)	13831 $\pm$ 988	61.8 $\pm$ 2.3
	19438 $\pm$ 1015	57.6 $\pm$ 3.5
	25633 $\pm$ 946	55.9 $\pm$ 4.0
	28470 $\pm$ 761	50.5 $\pm$ 4.0
P( $\omega$ -Me-OHC13)	10889 $\pm$ 1022	69.4 $\pm$ 3.2
	14109 $\pm$ 866	64.7 $\pm$ 3.1
	20675 $\pm$ 930	57.4 $\pm$ 3.0
	30377 $\pm$ 975	55.2 $\pm$ 4.5
P( $\omega$ -Me-OHC18)	17506 $\pm$ 1044	78.3 $\pm$ 3.1
	24616 $\pm$ 836	73.8 $\pm$ 5.1
	30294 $\pm$ 860	69.4 $\pm$ 2.5
	34779 $\pm$ 528	65.5 $\pm$ 2.2

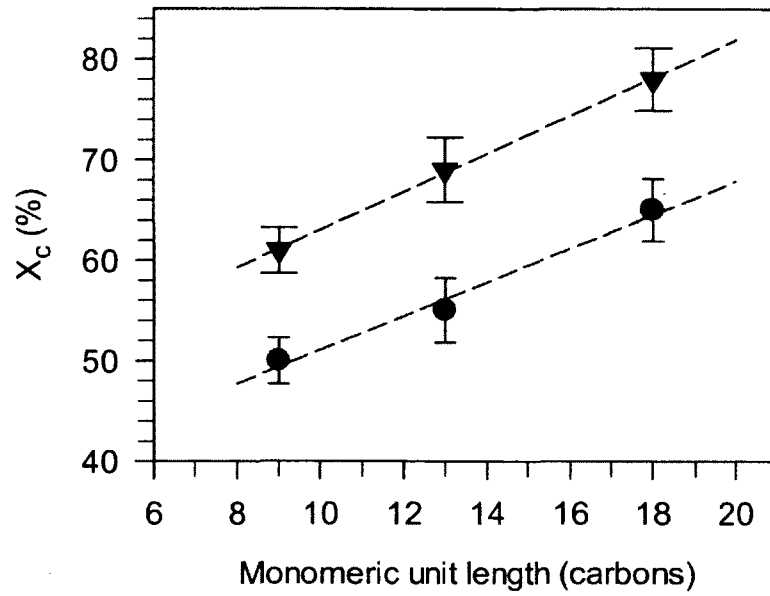


**Figure 5-6.** Degree of crystallinity  $X_c$  (%) as a function of  $\bar{M}_n$  for P( $\omega$ -Me-OHC9), (●), P( $\omega$ -Me-OHC13), (▲), and P( $\omega$ -Me-OHC18), (■).

The linear trend which is observed in the  $X_c$  versus the number of carbons in the monomeric unit for the P( $\omega$ -Me-OHFA) samples with the highest and lowest  $\bar{M}_n$  shown in Figure 5-7 is common to all the examined polyesters with similar  $\bar{M}_n$ . The linear trend observed in the  $n = [9 - 18]$  range may be attributed to a concurrent specific increase of the intermolecular forces due to an additive contribution of the (CH<sub>2</sub>) groups. The additivity of the contributions may only hold as long as this contribution is dominating. This can be only resolved with additional studies that are out of the scope of this work.

#### 5.4.3 Crystallization and melting behaviour studied by DSC

The DSC cooling and second heating cycles for the samples with the highest  $\bar{M}_n$  are shown in Figure 5-8 (a), (b) and (c) for P( $\omega$ -Me-OHC9), P( $\omega$ -Me-OHC13) and P( $\omega$ -Me-OHC18), respectively. The DSC characteristic data (temperature and enthalpy) of the different cycles are listed in Table 5-3. Note that the thermograms shown in Figure 5-8 are representative of all the P( $\omega$ -Me-OHFA)s of this study. As can be seen, the cooling and heating thermograms of the P( $\omega$ -Me-OHFA)s presented each a single narrow exotherm and a single endotherm, respectively. The crystallization and melting peaks are both intense and narrow (FWHM= 2–4 °C) indicating high crystallinity materials and very homogeneous phases. This is consistent with the WAXD results which evidenced very high crystalline materials. No glass transition was observed in either the DSC cooling or heating cycles.

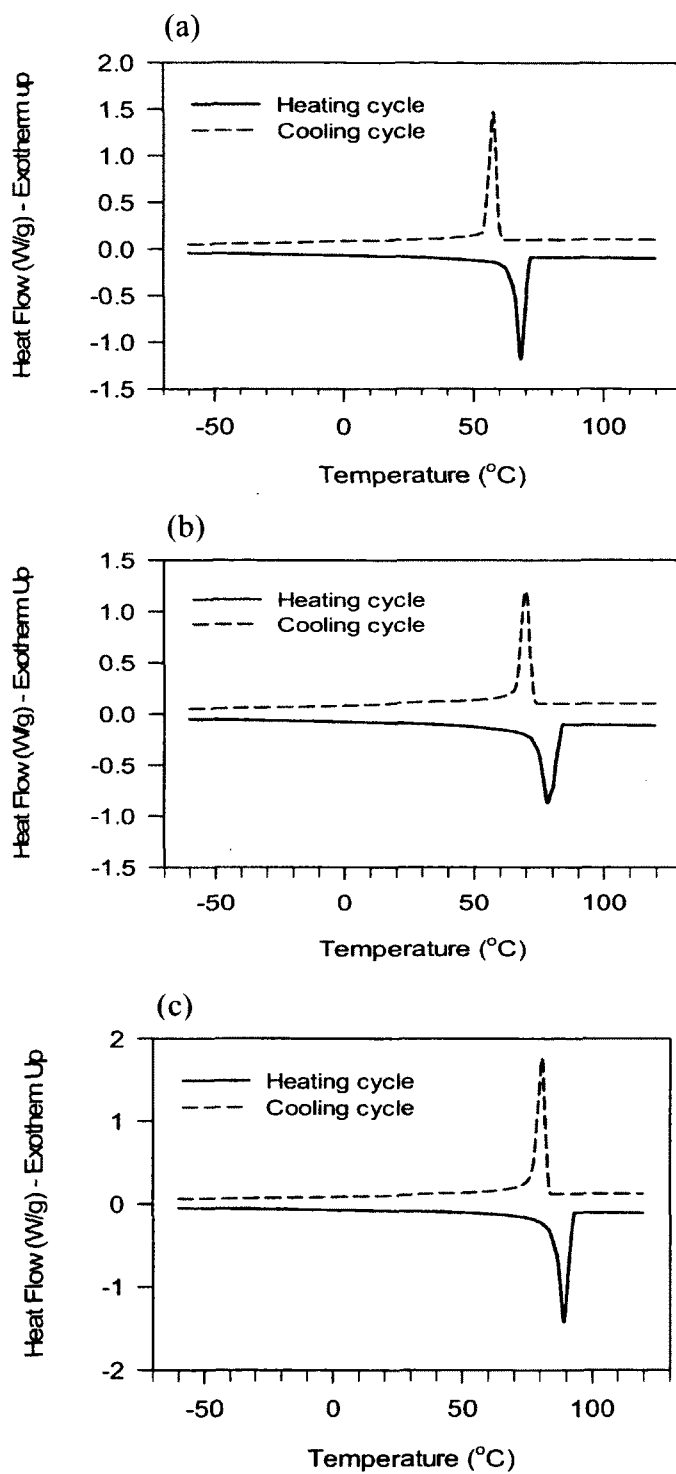


**Figure 5–7.** Degree of crystallinity as a function of length of monomers of the P( $\omega$ -Me-OHFA) samples with the lowest (▼) and highest (●)  $\bar{M}_n$



**Table 5-3.** Thermal characteristic parameters of P( $\omega$ -Me-OHFA)s obtained by DSC. Average number of molecular weight,  $\bar{M}_n$ , onset,  $T_{on}$ , offset,  $T_{off}$  and peak temperature of melting,  $T_m$ , and crystallization,  $T_c$ , and enthalpy of melting,  $\Delta H_m$ , and crystallization,  $\Delta H_c$ . Subscripts 1 and 2 denote first and second heating cycles, respectively. The uncertainties attached to the characteristic temperatures and enthalpies are better than 0.5 °C and 8 J/g, respectively.

Entry	$\bar{M}_n$ (g/mol)	First heating				Second heating				Cooling			
		$T_{on}$ (°C)	$T_{off}$ (°C)	$T_m$ (°C)	$\Delta H_m$ (J/g)	$T_{on}$ (°C)	$T_{off}$ (°C)	$T_m$ (°C)	$\Delta H_m$ (J/g)	$T_{on}$ (°C)	$T_{off}$ (°C)	$T_c$ (°C)	$\Delta H_c$ (J/g)
P( $\omega$ -Me-OHC9)	13831	62.8	68.8	67.0	133	62.9	68.9	66.1	134	55.2	53.1	54.4	135
	19438	59.2	70.6	66.7	133	60.6	69.5	68.8	132	57.6	54.8	55.2	134
	25633	65.1	70.0	68.0	131	60.9	71.2	67.8	132	60.0	55.3	57.2	132
	28470	66.1	73.0	69.3	131	64.9	72.7	69.3	129	59.8	54.4	58.6	134
P( $\omega$ -Me-OHC13)	10889	74.5	82.6	79.7	143	74.1	82.7	78.3	145	72.7	66.2	70.1	144
	14109	75.0	82.9	76.4	145	74.5	82.6	76.7	144	72.6	66.6	69.8	142
	20675	74.9	83.7	78.8	139	73.1	84.4	78.8	138	75.2	67.4	71.9	134
	30377	77.6	84.4	79.4	131	72.1	83.3	79.8	133	71.7	64.2	70.1	141
P( $\omega$ -Me-OHC18)	17506	85.4	92.6	89.2	188	84.8	92.7	89.5	182	83.8	78.0	81.2	185
	24616	85.0	93.0	90.0	179	84.9	93.0	90.0	178	83.6	78.0	80.1	181
	30294	83.9	92.1	89.1	181	84.1	92.5	89.4	182	82.9	77.2	80.5	181
	34779	84.4	92.9	91.5	163	84.2	92.2	90.2	161	81.0	79.2	81.9	166



**Figure 5–8.** DSC thermograms of (a) P( $\omega$ -Me-OHC9), (b) P( $\omega$ -Me-OHC13) and (c) P( $\omega$ -Me-OHC18) obtained with heating and cooling rate of 3  $^{\circ}$ C/min

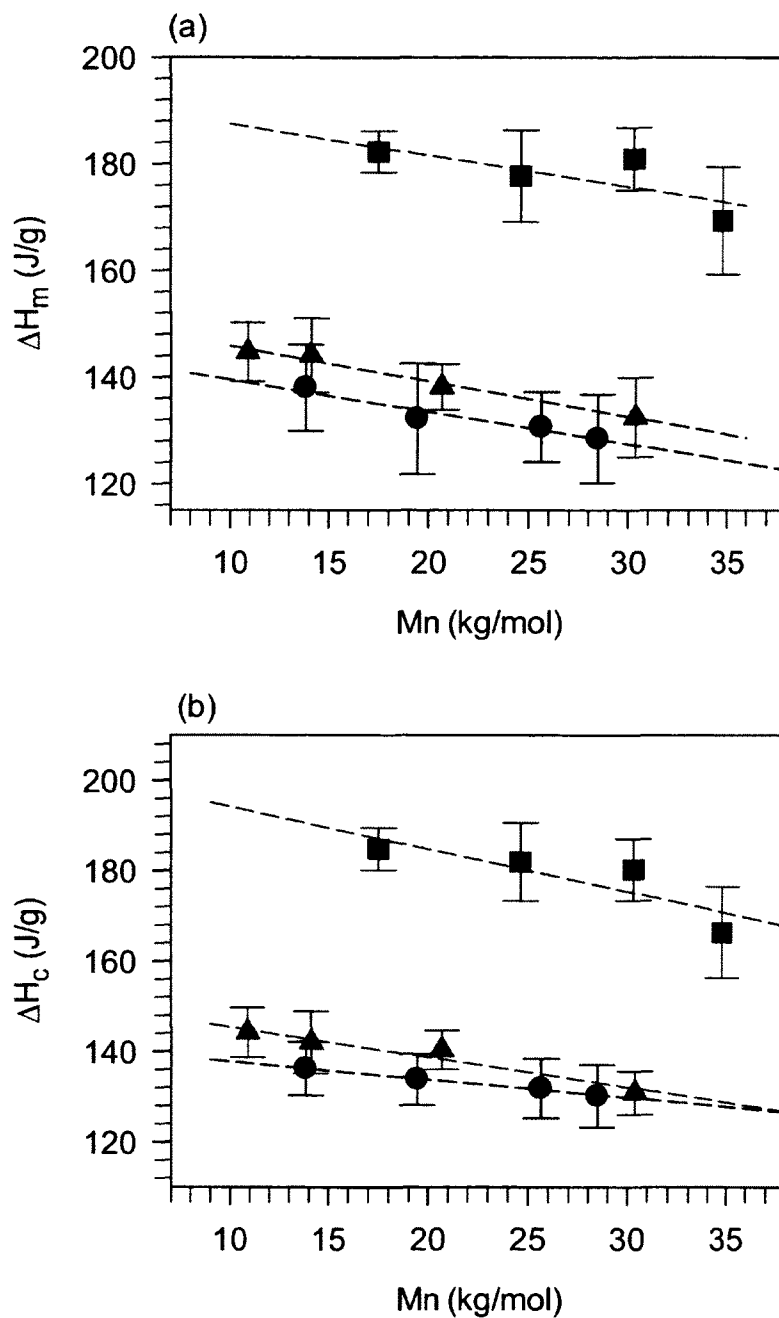
#### 5.4.3.1 Effect of molecular weight on thermal transitions

The average molecular weight,  $\bar{M}_n$ , did not affect  $T_m$  and  $T_c$  of the P( $\omega$ -Me-OHFA)s. This is understandable because all the polyesters crystallized in the same  $\beta'$ -polymorphic form independently of molecular weight as evidenced by WAXD. The enthalpies of melting,  $\Delta H_m$ , and crystallization,  $\Delta H_c$ , were only slightly, affected by molecular weight (Table 5-3 and Figure 5-9 (a) and (b)). Differences in enthalpy cannot be ascertained as they are close to the uncertainty attached to the measurement of the enthalpy changes.

#### 5.4.3.2 Effect of monomeric unit length on thermal transitions

Figure 5-10 (a) and (b) displays the characteristic temperatures (onset,  $T_{on}$ , offset,  $T_{off}$  and peak temperature,  $T_{m,c}$ ) of melting and crystallization of the polymers, as a function of  $n$ , the number of carbons in the monomer. As can be seen, all characteristic temperatures show a linear increase ( $R^2 > 0.9783$ ) as a function of  $n$  with similar slopes ( $2.2 \pm 0.1$  °C per carbon atom) for both melting and crystallization. The linear trend still holds when values of  $T_m$  mined from the literature, such as for PCL, a five carbon long unit with  $T_m = 60$  °C (Hutmacher, Schantz et al. 2001) and for poly(9-hydroxynonaic acid), a nine carbons long unit with  $T_m = 70$  °C (Liu, Kong et al. 2008), are added to the graph (Figure 5-10 (c)). The increase of  $T_m$  with the increase of the monomeric segment length is evidence of the significant improvement of the stability of the polyesters' crystal forms.





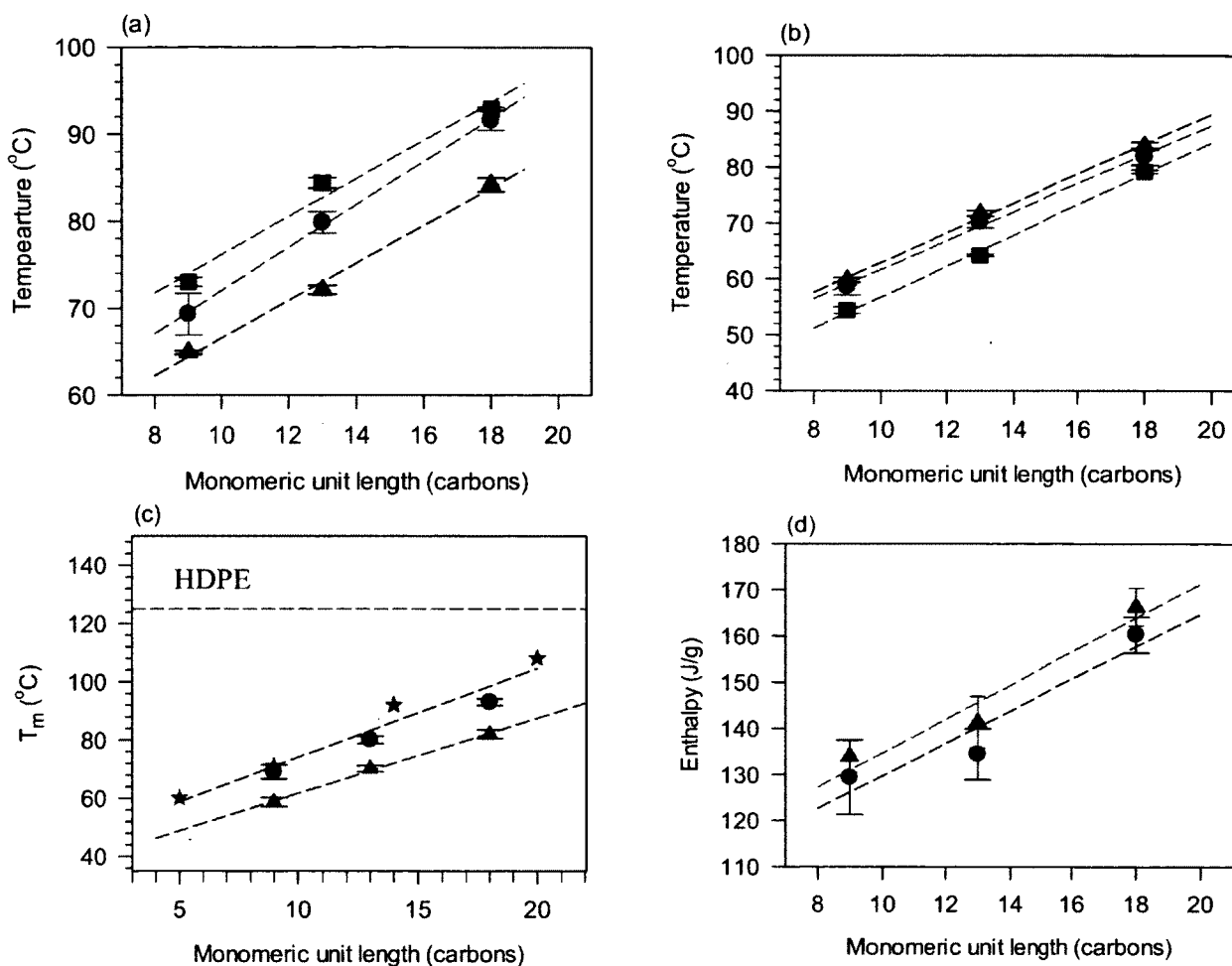
**Figure 5-9.** Enthalpies of (a) melting and (b) crystallization of the P( $\omega$ -Me-OHFA)s as a function of  $\bar{M}_n$ . P( $\omega$ -Me-OHC9): (●), P( $\omega$ -Me-OHC13): (▲) and P( $\omega$ -Me-OHC18): (■).

The trend observed in  $T_m$  and  $T_c$  versus the monomeric unit length appears to be due, at least in the examined [9–18] range, to a cumulative effect of the (CH<sub>2</sub>) groups contributions which increased accordingly the Van der Waals intramolecular attractive forces. These forces together with the dipole-dipole interactions are mainly responsible for crystallization and define the crystal structure and crystal stability of the polyesters.

Both  $\Delta H_m$  and  $\Delta H_c$  also increased linearly ( $R^2 > 0.9080$ ) with monomeric unit length (Figure 5-3(d)) indicating that higher energy was needed to melt or crystallize the polymers with longer monomers. This is consistent with the trend observed in the variation of  $X_c(\%)$  of the polymers versus  $n$  as measured by WAXD (Figure 5-7, Section 5-4). The strong correlation between the enthalpy ( $\Delta H_m, \Delta H_c$ ) and  $X_c(\%)$  can be easily demonstrated by the plot of the enthalpy versus  $X_c(\%)$  curve (figure not shown).

#### 5.4.4 Mechanical properties of P( $\omega$ -Me-OHFA)s by DMA

Figure 5-11 (a) to (c) display storage modulus,  $E'$ , loss modulus,  $E''$ , and  $\tan(\delta)$  for P( $\omega$ -Me-OHC9), P( $\omega$ -Me-OHC13) and P( $\omega$ -Me-OHC18) with the highest molecular weight, respectively. As can be seen from Figure 5-11, at the glass transition temperature (the maximum peak of  $\tan \delta$  curve), the storage modulus decreases dramatically and the loss modulus reaches a maximum. Storage modulus ( $E'$ ) and  $T_g$  are the most important parameters obtained from DMA for characterizing semi-crystalline polymeric materials. The effect of  $\bar{M}_n$  and of the length of the monomeric units on both  $E'$  and  $T_g$  were considered as follows.



**Figure 5–10.** Onset; (▲), offset; (■) and peak temperature (●) of (a) melting and (b) crystallization of P( $\omega$ -Me-OHFA)s. (c) Melting; (●) and crystallization (▲) temperature of P( $\omega$ -Me-OHFA)s; (★) represent peak temperature of melting,  $T_m$ , of aliphatic polyesters mined from the literature<sup>2</sup>. (d) Enthalpies of melting (●) and crystallization (▲) as a function of the number of carbons in the monomeric unit.

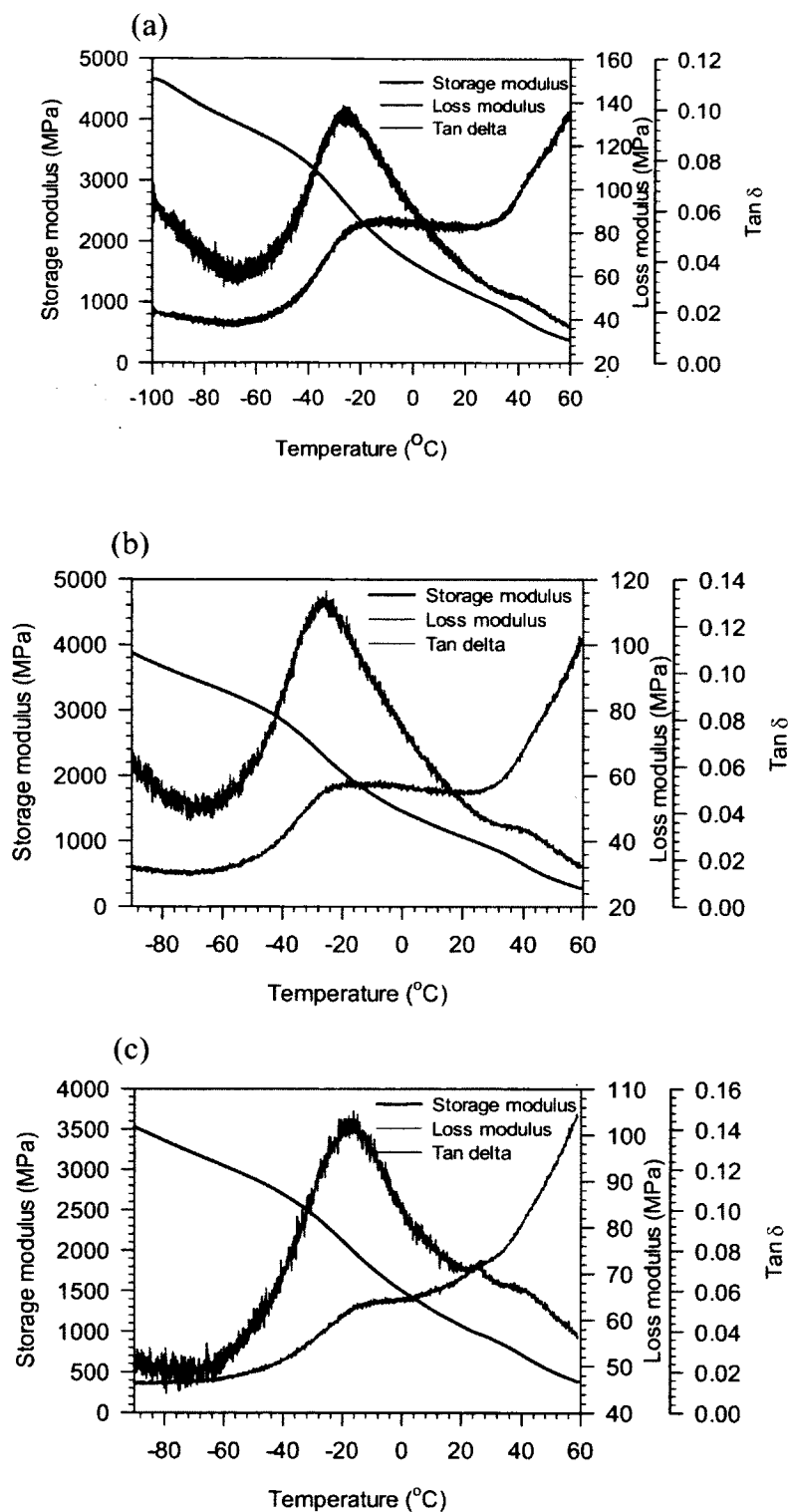
<sup>2</sup>Hutmacher, D. W., T. Schantz, et al. (2001). "Mechanical properties and cell cultural response of polycaprolactone scaffolds designed and fabricated via fused deposition modeling." *Journal of biomedical materials research* **55**(2): 203-216.

Liu, G., X. Kong, et al. (2008). "Production of 9-hydroxynonanoic acid from methyl oleate and conversion into lactone monomers for the synthesis of biodegradable polylactones." *Biomacromolecules* **9**(3): 949-953.

Liu, C., F. Liu, et al. (2011). "Polymers from Fatty Acids: Poly ( -hydroxyl tetradecanoic acid) Synthesis and Physico-Mechanical Studies." *Biomacromolecules*.

#### 5.4.4.1 Effect of molecular weight on storage modulus

Figure 5-12 displays storage modulus of P( $\omega$ -Me-OHC9), P( $\omega$ -Me-OHC13) and P( $\omega$ -Me-OHC18) as a function of  $\bar{M}_n$ , obtained at 37 °C, a temperature suitable for biomedical applications. The decrease observed in E' as  $\bar{M}_n$  was increased can be explained by the higher crystallinity of the samples with lower molecular weight. It is commonly known that mechanical properties of semi-crystalline thermoplastics depend strongly on their crystallinity (Talbot, Springer et al. 1987). The link between crystallinity and storage modulus in polyesters has been specifically reported in a number of publications. Focarete *et al.* (Letizia Focarete, Scandola et al. 2001) observed that high storage modulus of poly(pentadecalactone) is related to its high crystallinity. Cai *et al.* (Cai, Liu et al. 2010) also reported a decrease in storage modulus of poly(pentadecalactone) when molecular weight was increased. This is understandable because sample with greater crystalline fraction absorb and store more energy.



**Figure 5–11.** Storage modulus, loss modulus and  $\tan \delta$  versus  $T$  curves of (a) P( $\omega$ -Me-OHC9), (b) P( $\omega$ -Me-OHC13) and (c) P( $\omega$ -Me-OHC18) obtained from DMA.

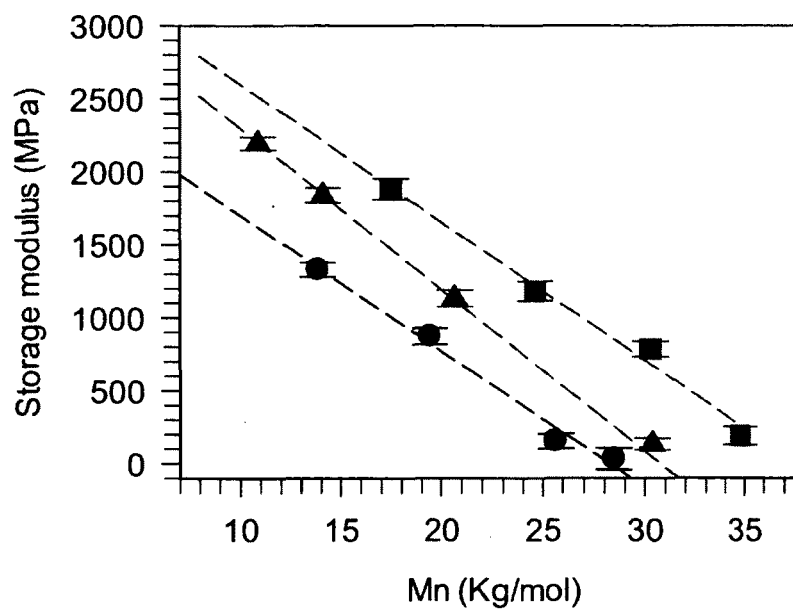
The linear trend ( $R^2 > 0.9824$ ) observed in  $E'$  as a function of  $\bar{M}_n$  clearly mirror the trend observed in  $X_c(\%)$  (Figure 5-6) indicating a strong correlation. One may be therefore able to estimate modulus values of P( $\omega$ -Me-OHFA)s from crystallinity values at least in the range of molecular weights presented in this study. Note that generally, the relation between storage modulus and crystallinity is not as straight forward and it is difficult to estimate quantitatively the storage modulus from only crystallinity measurement.

#### 5.4.4.2 Effect of monomer unit length on storage modulus

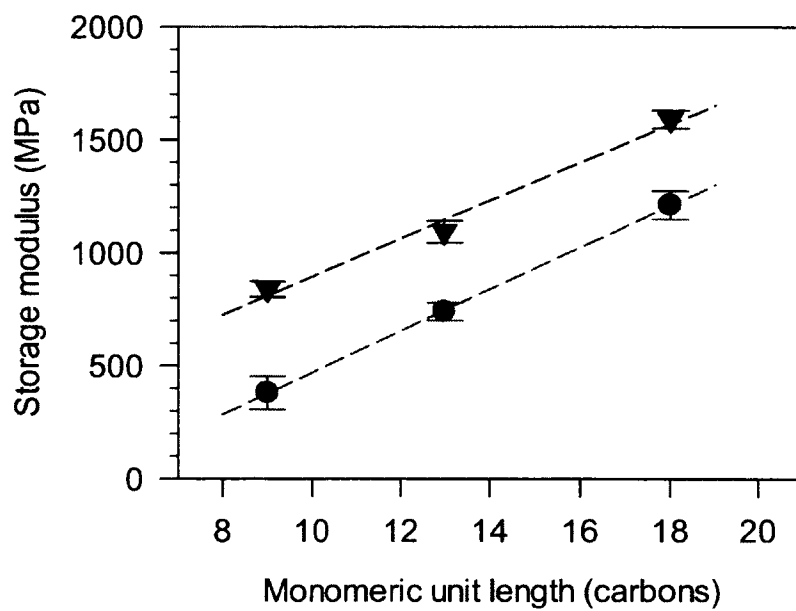
Figure 5-13 shows  $E'$  of the P( $\omega$ -Me-OHFA)s as a function of monomeric unit length for the lowest and highest  $\bar{M}_n$  at 37 °C. This trend is displayed by all the polymers with similar  $\bar{M}_n$ .  $E'$  is also strongly correlated to the degree of crystallinity as evident from the  $X_c(\%)$  versus  $\bar{M}_n$  curves (Figure 5-7) as a function of length of monomers. Such correlations have been reported for ethylene vinyl acetate copolymers as well as PCL (Wurm, Merzlyakov et al. 1999; Sung, Kum et al. 2005).

#### 5.4.5 Glass transition temperature

Glass transition temperature ( $T_g$ ) is one of the most fundamental measurements in polymer applications because it reveals how the polymer behaves under ambient temperature conditions. The glass transition temperature is a function of chain flexibility. Glass transition occurs when there is enough vibrational (thermal) energy in the material to create sufficient chain movements. Glass transition temperature can be readily obtained from DMA, unlike DSC. Note that even when DSC is able to detect the glass transition,  $T_g$  obtained from DMA is typically not the same because of the different testing mechanisms.



**Figure 5-12.** Storage modulus of P( $\omega$ -Me-OHC9), (●), P( $\omega$ -Me-OHC13), (▲), and P( $\omega$ -Me-OHC18), (■), as a function of  $\bar{M}_n$



**Figure 5–13.** Storage modulus as a function of monomeric unit length at 37°C of P( $\omega$ -Me-OHFA)s with lowest  $\bar{M}_n$  (▼) and highest  $\bar{M}_n$  (●).



DMA tests the mechanical response of the polymer chains during the transition and is therefore much more sensitive to the changes in chain flexibility than DSC. As discussed before (Section 5-5) DSC was not able to detect the glass transition in the P( $\omega$ -Me-OHFA) samples of this study not only because of the relative lack of sensitivity to the glass transition but particularly due to the very high crystallinity of the polymers. The changes in heat capacity during the glass transition measured in DSC tests have probably been overwhelmed by the changes due to the crystallization and melting transitions.

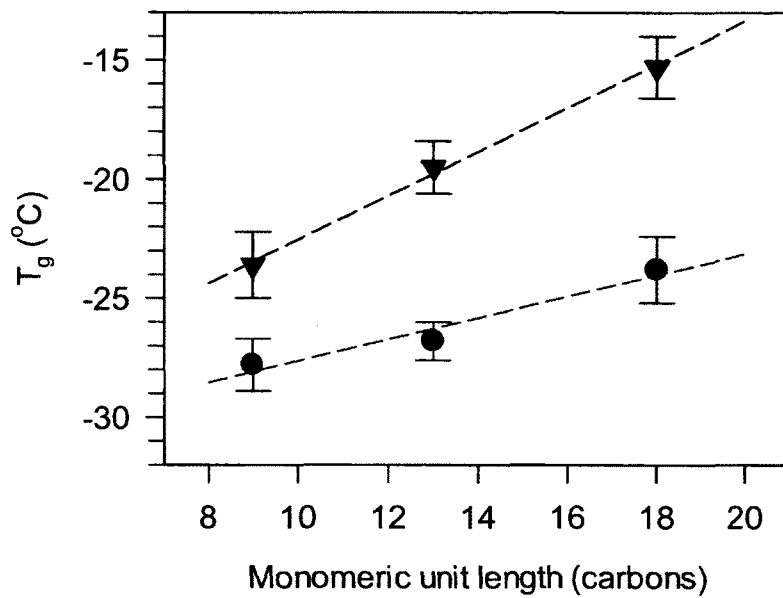
Table 5-4 lists the values of  $T_g$  for the P( $\omega$ -Me-OHFA)s. The relatively low values of the glass transition temperature can be related to the high degree of crystallinity of the polymers.

#### 5.4.5.1 Effect of monomeric unit length on $T_g$

Figure 5-14 displays the variation of  $T_g$  as a function of the length of monomeric units for the P( $\omega$ -Me-OHFA)s with the lowest and highest  $\bar{M}_n$ . It shows that when the number of carbons in the monomer increased from 9 to 18,  $T_g$  increased linearly from -24 °C to -15 °C. As indicated before,  $T_g$  is affected by the degree of crystallinity in the polymer structure. Interestingly, the trend is the same as that of the  $X_c(\%)$  (Figure 5-11). In fact, the more the percent crystallinity the more energy (heat) is required to make the transition from the glassy state to the rubbery state.

**Table 5-4.** Glass transition temperature ( $T_g$ ) of P( $\omega$ -Me-OHFA)s with different  $\bar{M}_n$ .

Entry	$\bar{M}_n$ (g/mol)	$T_g$ (°C)
P( $\omega$ -Me-OHC9)	13831 $\pm$ 988	-23.6 $\pm$ 1.4
	19438 $\pm$ 1015	-25.5 $\pm$ 1.5
	25633 $\pm$ 946	-26.1 $\pm$ 0.8
	28470 $\pm$ 761	-27.8 $\pm$ 1.1
P( $\omega$ -Me-OHC13)	10889 $\pm$ 1022	-19.5 $\pm$ 1.1
	14109 $\pm$ 866	-21.4 $\pm$ 1.3
	20675 $\pm$ 930	-24.3 $\pm$ 1.0
	30377 $\pm$ 975	-26.8 $\pm$ 0.8
P( $\omega$ -Me-OHC18)	17506 $\pm$ 1044	-15.3 $\pm$ 1.3
	24616 $\pm$ 836	-19 $\pm$ 0.9
	30294 $\pm$ 860	-22.4 $\pm$ 1.6
	34779 $\pm$ 528	-23.8 $\pm$ 1.4

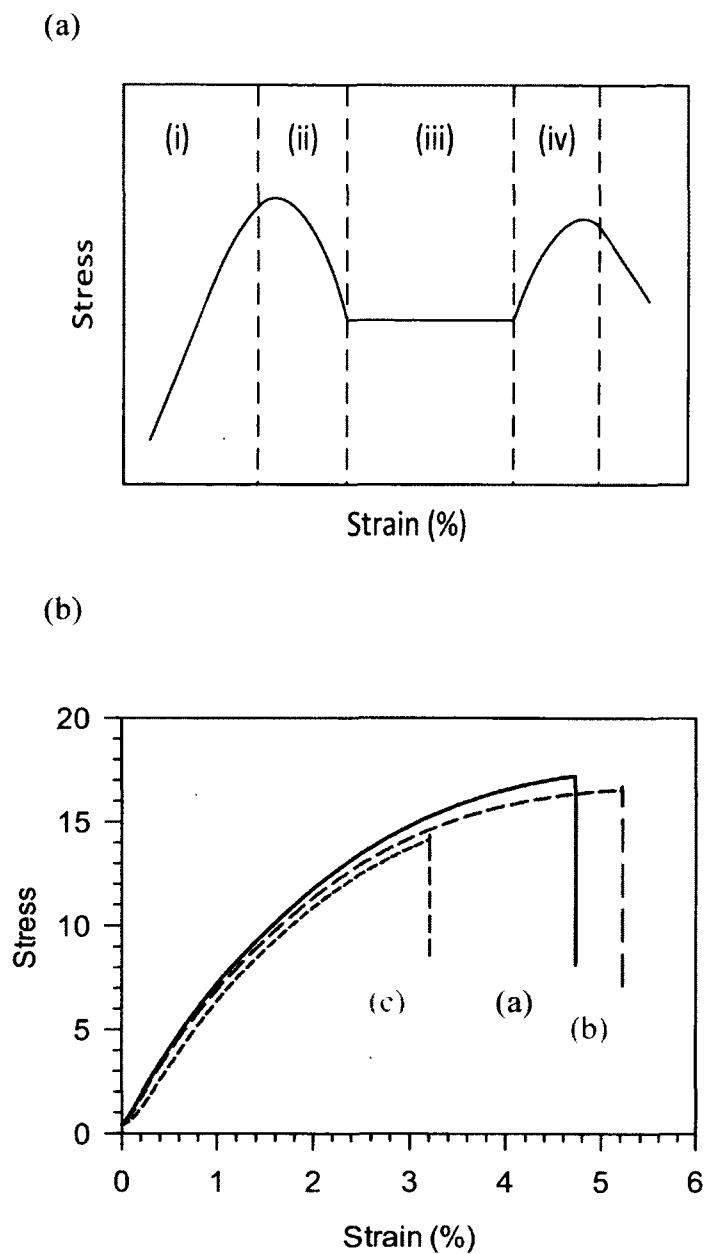


**Figure 5–14.** (a) Glass transition temperature ( $T_g$ ) as a function of  $\bar{M}_n$  for P( $\omega$ -Me-OHC9), (●), P( $\omega$ -Me-OHC13), (▲), and P( $\omega$ -Me-OHC18), (■), (b) Glass transition temperature versus monomeric unit length for the P( $\omega$ -Me-OHFA) with the lowest  $\bar{M}_n$  (●) and highest  $\bar{M}_n$  (▼).

#### 5.4.6 Mechanical properties of P( $\omega$ -Me-OHFA)s by tensile analysis

Mechanical properties were also examined using tensile analysis. The tensile testing of the polymers is based on the stress-strain curve. According to the literature, there are four regions in a polymer stress-strain curve based on the slope change in each region: (i) linear and non-linear (ii) neck region (iii) plastic flow and (iv) strain hardening (Cai, Liu et al. 2010). Figure 5-15 (a) shows a typical stress-strain curve including the four regions. The stress-strain curve of P( $\omega$ -Me-OHFA) samples of this study are displayed in Figure 5-15 (b). As can be seen in Figure 5-15 (b), the stress-strain behaviour of the P( $\omega$ -Me-OHFA) samples did not present a neck point and whole stress-strain curve correspond to the first region of the typical curve. Figure 5-15(b) also illustrates that for each sample, stress first increased rapidly with strain and then the slope of the curve began to decrease slightly until rupture. This behaviour is typical of brittle samples. It is also worthy to note that the P( $\omega$ -Me-OHC18) sample was much more brittle than P( $\omega$ -Me-OHC9) and P( $\omega$ -Me-OHC13) (elongation at the break of 3% compared to 5% and 6%, respectively) probably due to its higher degree of crystallinity. This is not surprising because crystallinity and molecular weight are the primary factors that affect stress-strain behaviour of semi-crystalline polymers (Nunes, Martin et al. 1982; Mandelkern 1990; Capaccio, Crompton et al. 2003).

The ultimate strength (stress at break), the maximum strain (elongation at break) and Young's modulus are important parameters obtained from stress-strain curve that can describe the tensile properties of materials. Crystallinity plays a major role in defining the stiffness of semi-crystalline polymers and therefore specifying the Young's modulus values (Kennedy, Peacock et al. 1994).



**Figure 5–15.** (a) Typical stress-strain curve of polymers<sup>3</sup>. The four regions are (i) linear and non-linear (ii) neck region (iii) plastic flow and (iv) strain hardening. (b). Stress-strain curves obtained for (a)P( $\omega$ -Me-OHC9), (b) P( $\omega$ -Me-OHC13)and (c) P( $\omega$ -Me-OHC18).

<sup>3</sup>Cai, J., C. Liu, et al. (2010). "Effects of molecular weight on poly( $\omega$ -pentadecalactone) mechanical and thermal properties." *Polymer* 51(5): 1088-1099.

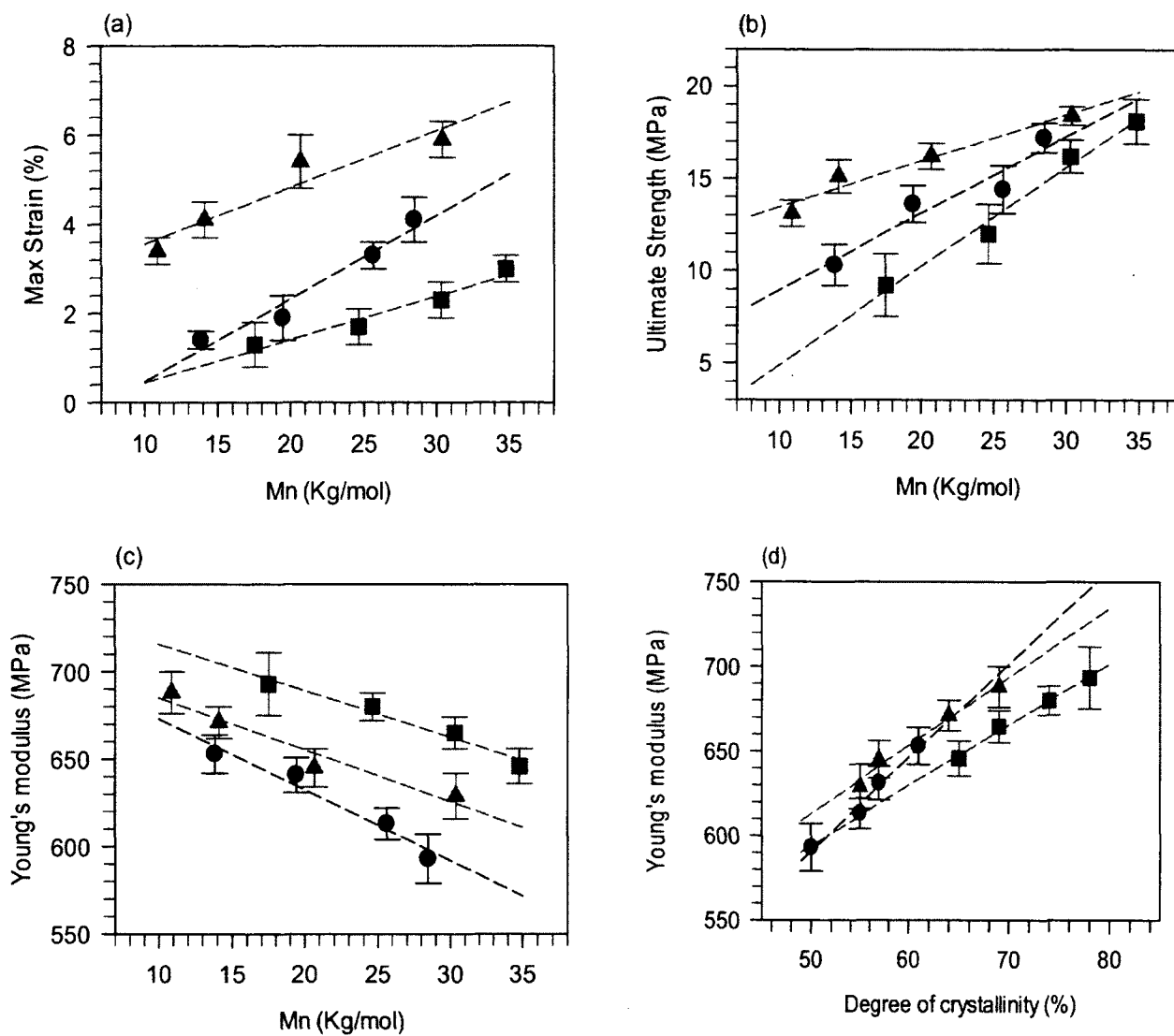
#### 5.4.6.1 Effect of molecular weight on tensile Properties

Table 5-5 summarizes the values of maximum strain (elongation), ultimate strength and Young's modulus for the P( $\omega$ -Me-OHFA) samples. Figure 5-16 (a), (b) and (c) show maximum strain, ultimate strength and Young's modulus of the P( $\omega$ -Me-OHFA)s, respectively, as a function of  $\bar{M}_n$ . As can be seen in the table, the values of stress at break obtained for P( $\omega$ -Me-OHC18) is generally lower than that of P( $\omega$ -Me-OHC9) and P( $\omega$ -Me-OHC13). This can be related to the extreme brittleness of P( $\omega$ -Me-OHC18) samples (higher degree of crystallinity). A linear increase was observed as a function of  $\bar{M}_n$  ( $R^2 > 0.9069$ ), in maximum strain and ultimate strength displayed in Figure 5-16 (a) and (b), respectively. These results are in good agreement with those reported for PLLA and linear polyethylene (Kennedy, Peacock et al. 1994; Renouf-Glauser, Rose et al. 2005). However, the values of max strain and ultimate strength are comparatively low due to the brittleness (elongation at the break less than 10%) of the samples in this study.

Figure 5-16 (c) shows clearly a decrease in the values of Young's modulus when  $\bar{M}_n$  is increased. The data obtained for each P( $\omega$ -Me-OHFA) sample are particularly very well fit with a line ( $R^2 > 0.9803$ ). Crystallinity is the main factor affecting Young's modulus in semi-crystalline polymers as pointed out in several reports (Flory, Yoon et al. 1984; Van der Wal, Mulder et al. 1998). The correlation between crystallinity and Young's modulus in our samples is clearly highlighted in the Young's modulus versus  $X_c$  (%) plot (Figure 5-16 (d)). This result is comparable to what was obtained in polyethylene (Kennedy, Peacock et al. 1994; Renouf-Glauser, Rose et al. 2005; Cai, Liu et al. 2010), probably due to the PE-like crystalline structure of our polyesters.

**Table 5-5.** Tensile properties of P( $\omega$ -Me-OHFA) samples as a function of  $\bar{M}_n$ 

Entry	$\bar{M}_n$ (g/mol)	Max strain (%)	Ultimate strength (MPa)	Young's modulus (MPa)
P( $\omega$ -Me-OHC9)	13831 $\pm$ 988	1.4 $\pm$ 0.2	10.3 $\pm$ 1.1	653 $\pm$ 11
	19438 $\pm$ 1015	1.9 $\pm$ 0.5	13.6 $\pm$ 1.0	641 $\pm$ 10
	25633 $\pm$ 946	3.3 $\pm$ 0.3	14.4 $\pm$ 1.3	613 $\pm$ 9
	28470 $\pm$ 761	4.1 $\pm$ 0.5	17.2 $\pm$ 0.8	593 $\pm$ 14
P( $\omega$ -Me-OHC13)	10889 $\pm$ 1022	3.4 $\pm$ 0.3	13.1 $\pm$ 0.7	668 $\pm$ 12
	14109 $\pm$ 866	4.1 $\pm$ 0.4	15.1 $\pm$ 0.9	671 $\pm$ 9
	20675 $\pm$ 930	5.4 $\pm$ 0.3	16.2 $\pm$ 0.7	645 $\pm$ 11
	30377 $\pm$ 975	5.9 $\pm$ 0.2	18.4 $\pm$ 0.5	629 $\pm$ 13
P( $\omega$ -Me-OHC18)	17506 $\pm$ 1044	1.3 $\pm$ 0.1	9.2 $\pm$ 1.7	693 $\pm$ 18
	24616 $\pm$ 836	1.7 $\pm$ 0.2	12.0 $\pm$ 1.6	680 $\pm$ 8
	30294 $\pm$ 860	2.3 $\pm$ 0.4	16.2 $\pm$ 0.9	665 $\pm$ 9
	34779 $\pm$ 528	3.0 $\pm$ 0.3	18.1 $\pm$ 1.2	646 $\pm$ 10

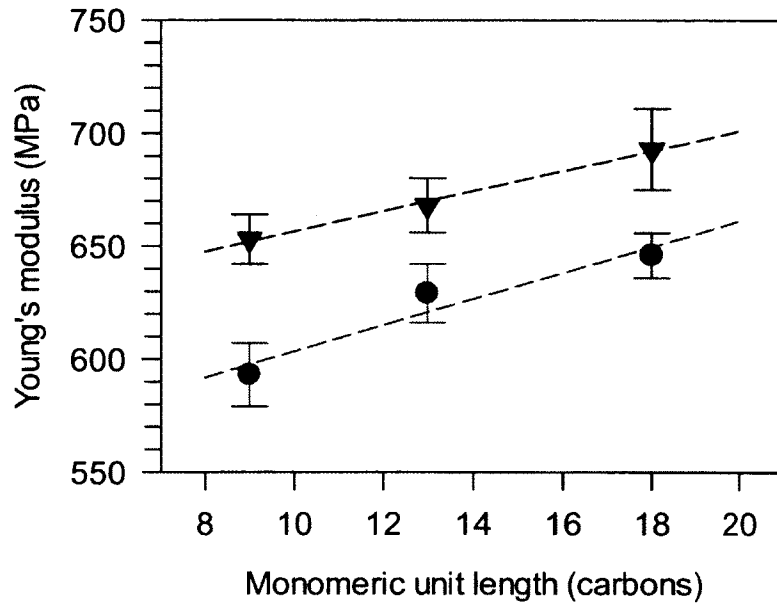


**Figure 5-16.**(a), (b) and (c) Tensile properties as a function of  $\bar{M}_n$  for P( $\omega$ -Me-OHC9), (●), P( $\omega$ -Me-OHC13), (▲), and P( $\omega$ -Me-OHC18), (■). (d) Young's modulus versus degree of crystallinity



#### 5.4.6.2 Effect of monomeric unit length on tensile properties

Both maximum strain and ultimate strength of the P( $\omega$ -Me-OHFA)s were not affected by the length of the monomer (Table 5-5). On the other hand, Young's modulus which is sensitive to the degree of crystallinity was affected by the length of the monomeric unit as illustrated in Figure 5-17 showing Young's modulus as a function of monomeric unit length for the P( $\omega$ -Me-OHFA)s with the lowest and highest  $\bar{M}_n$ . The linear trend ( $R^2 > 0.9937$ ) demonstrated by Young's modulus versus  $\bar{M}_n$  can be unambiguously related to the percent crystallinity of the materials. This is again explained by the fact that crystallinity is the major factor influencing Young's modulus in semi-crystalline polymers.



**Figure 5–17.** Young's modulus as a function of monomeric unit length of the P( $\omega$ -Me-OHFA)s with the lowest (▼) and highest (●)  $\bar{M}_n$ .

## 5.5 Comparison of physical properties of aliphatic polyesters

To better understand the achievements of this study, the physical properties of the P( $\omega$ -Me-OHFA)s of this study are compared to those reported in the literature for other aliphatic polyesters. Table 5-6 summarizes the thermal, crystalline and mechanical properties of the polyesters of this study and those mined from the literature.

The thermal stability of the three polyesters of the present study follow the general trend observed for similar polyesters. Their temperature of maximum decomposition versus monomeric unit length lay within the trend of overall increase observed from PGA ( $n=1$ ) to C18 (the values of TGA analysis of C20 is not reported in the literature) which plateaus closer to  $T_{d(max)}$  of HDPE (see Figure 5-3(b) in Section 5.3.2). However, an exception is observed in C14 ( $T_d$  is very higher than other polyesters listed in table 5-6) which is reported by Liu *et al.* (Liu, Liu et al. 2011).

The values of  $T_m$  of our polyesters are within the overall trend demonstrated by similar polyesters (Table 5-6 and Figure 5-10 (c)). A trend in the table, with the exception of short chain aliphatic polyester (PLA and PGA), shows that with an increase in the number of methylene groups the melting temperature of polymers increases from PCL ( $T_m = 60$  °C) to C20 ( $T_m = 108$  °C). Furthermore, the melting temperature of polymers obtained from this study (C9, C13 and C18) also follows the trend perfectly.

The trend observed for the glass transition temperature as a function of monomeric unit length for the polyesters is similar to that of melting temperature. Note that  $T_g$  of the very short length PGA and PLA ( $n=1$ ) are off the trend. Note also that PE has an extremely low glass transition (-120 °C) and cannot be compared to the others due to an amorphous transition in polyethylene

which occurs at around  $-120\text{ }^{\circ}\text{C}$  (Stehling and Mandelkern 1970). The  $T_g$  data summarized in Table 5-6 shows that C18 demonstrates the highest value of  $T_g$  which mirrors its highly crystalline structure.

The C9, C13 and C18 polyesters of the study are strong polymers with tensile strength values well in the range and superior to other aliphatic polyesters except for PGA and PLA reported in the literature (see Table 5-6). Young's modulus values of the polyesters of this study are similar and superior (except for PGA and PLA) to those published for other polyesters. However, their elongation at break is much lower than that of similar polyesters such as C14 and C15 and much lower than that of HDPE due to their extreme brittleness. The brittleness of our samples is related to their high crystallinity.

PGA for example is the strongest polymer with a tensile strength of 70 MPa but demonstrated an elongation of only few percents. Table 5-6 also indicates that the polyesters with short monomeric length displayed the highest values of Young's modulus due to their high stiffness. The crystalline structure of aliphatic polyesters is similar to that of HDPE except for PLA having hexagonal structure.

The overall comparison exposes that aliphatic polyesters with long linear segments have improved physical properties which tend to that of HDPE. This result is interesting in terms of finding a renewable, biodegradable alternative for polyethylene to address the negative environmental impacts of using HDPE for a long time.

**Table 5-6.** Comparison of thermal, crystalline and mechanical properties of synthetic aliphatic polyesters with HDPE

Polymer	T <sub>d</sub> (°C)	T <sub>m</sub> (°C)	T <sub>g</sub> (°C)	Tensile Strength (MPa)	Elongation (%)	Young's Modulus (MPa)	Crystal structure
PGA	250	220	40	70	below 10	6900	Orthorhombic
PLA	270	160	35	40	below 10	1300	Hexagonal
PCL	350	60	-60	15	80	400	Orthorhombic
P(nonanolactone) (C9)	380	70	-30	--	--	--	--
P(9-hydroxynonanoate) (C9)	410	70	-31	16.1	10	200	--
P( $\omega$ -Me-OHC9) (C9) (Current study)	416	69	-28	17.2	4.1	678	Orthorhombic
P( $\omega$ -Me-OHC13) (C13) (Current study)	425	80	-19	18.1	5.7	682	Orthorhombic
P(hydroxytetradecanoic acid) (C14)	458	92	-29	16.1	5-700	486	Orthorhombic
P(pentadecalactone) (C15)	--	92	-27	17.7	4-700	690	Orthorhombic
P( $\omega$ -Me-OHC18) C18 (Current study)	430	93	-15	18.4	3.0	693	Orthorhombic
P(1,20-eicosadiyl-1,20- eicosanedioate) (C20)	--	108	--	--	--	--	--
HDPE	470	125	-120	35	10-1000	800-1100	Orthorhombic

## 5.6 Summary

The thermal behaviour (stability and transition), mechanical properties and crystallinity were fully characterized and compared by analysing the results of TGA, DSC, DMA, tensile analysis and XRD. The effect of two parameters: number average molecular weight ( $\bar{M}_n$ ) and the length of monomeric unit ( $n$ ) was investigated on physical properties of P( $\omega$ -Me-OHFA)s.

TGA results showed a very good thermal stability for P( $\omega$ -Me-OHFA) which was also increased by increasing the length of monomeric unit. The crystalline structure of P( $\omega$ -Me-OHFA)s obtained from WAXD analysis, was packed in an orthorhombic subcell similar to that of HDPE. A linear increase was also seen in degree of crystallinity as a function of monomeric unit length. The melting and crystallization temperature were also obtained from DSC analysis. The enthalpy of melting and crystallization were affected by  $\bar{M}_n$  very slightly. While a linear increase was observed in melting and crystallization temperatures as the length of monomers increased. Mechanical properties were also significantly influenced by  $\bar{M}_n$  and length of monomeric unit. Storage modulus and glass transition temperature were totally affected by degree of crystallinity. Tensile properties of P( $\omega$ -Me-OHFA)s were also considered such as max strain, ultimate strength and Young's modulus. The overall tensile results revealed the polymers obtained in this study are strong (relatively high ultimate strength) but brittle (very low elongation (%)). A comparison of physical properties of P( $\omega$ -Me-OHFA)s with other aliphatic polyesters demonstrates that P( $\omega$ -Me-OHFA)s in this study perfectly followed the increasing trend in improvement of physical properties of aliphatic polyesters as function of monomeric unit length approachable to that of HDPE.

## 6 Conclusions

$\omega$ -hydroxyfatty acids ( $\omega$ -OHFA)s and their respective methyl ester derivatives ( $\omega$ -Me-OHFA)s were synthesized from vegetable oil-based compounds via a series of reproducible chemical reactions such as ozonolysis, reduction, saponification, and esterification, and cross metathesis. Each  $\omega$ -hydroxyfatty acid and methyl ester derivative monomers were prepared with three different fatty acid chain lengths, i.e., FA= C9, C13 and C18 were obtained in high purity (purity  $\geq$  95%) and yields  $\geq$  80%. The structure of the monomers was fully characterized by  $^1\text{H}$  NMR and Mass Spectroscopy. The hypothesis no. 1 which was about the synthesis of  $\omega$ -OHC18 and  $\omega$ -Me-OHC18 through a cross metathesis was supported by  $^1\text{H}$  NMR and Mass Spectroscopy results.

High molecular weight polyesters were successfully synthesized from the ( $\omega$ -OHFA)s and ( $\omega$ -Me-OHFA)s through melt polycondensation reactions catalyzed by  $[\text{Ti}(\text{OiPr})_4]$ . The chemical structure of the poly( $\omega$ -hydroxyfatty acids) (P( $\omega$ -OHFA)s) and poly( $\omega$ -hydroxymethyl esters) (P( $\omega$ -Me-OHFA)s) was also confirmed by  $^1\text{H}$  NMR.

The effect of the reaction conditions, such as catalyst concentration, reaction time and temperature, on the average number of molecular weight ( $\bar{M}_n$ ) and poly-dispersity index (PDI) of the polymers were investigated in great detail. The optimum polymerization conditions are those which permit to obtain high molecular weight polymers with relatively low PDI. The highest  $\bar{M}_n$  was achieved at catalyst concentration of 200 ppm for the C9 polymers and 300 ppm for the C13 and C18 polymers. The optimal reaction time in the second stage of polymerization was four hours and the optimum temperature needed to achieve the highest molecular weight

was 220 °C for each polymer. From the hypothesis no. 2 it was expected to optimize the molecular weight and polydispersity by optimization the polymerization conditions. The result was obtained from optimization of polymerization is totally supporting hypothesis no.2.

The kinetics of the reaction at optimum catalyst concentration for each polymer was then studied in terms of the variation of  $\bar{M}_n$  as a function of time. Interestingly, the extent of the reaction ( $p$ ) achieved was  $\sim 99\%$  indicating that conversion was almost completed after the time period set for the polymerization. Also, the number average degree of polymerization ( $\bar{X}_n$ ) achieved for most of the polymer samples was  $\geq 100$ , a value required to obtain polymers with sufficient physical properties suitable for practical applications. Equilibrium constant ( $K_c$ ) values obtained were all higher than  $10^4$ , also signalling the practical potential of the polymers of this study. A comprehensive comparison of reaction rate constant between acid and ester-terminated polymers was also considered. The result showed that the polymerization reaction of ester-terminated monomers proceeded more rapidly than that of acid-terminated monomers. Due to the fact that, the formation and removal of the condensation by-product (methanol) in ester-terminated polymerization was easier than water (by-product of acid terminated polymerization) in each different reaction.

The detailed analysis of the molecular weight and molecular weight distribution of the polyesters of this study indicated a relatively high number average of molecular weights for P( $\omega$ -Me-OHFA)s compared to P( $\omega$ -OHFA) samples. The acid terminated P( $\omega$ -OHFA)s also demonstrated very high PDI values ( $\sim 4-6$ ) whereas the P( $\omega$ -Me-OHFA)s showed a narrow range of relatively smaller PDI ( $\sim 2-2.5$ ). Furthermore, the P( $\omega$ -OHFA) samples were not capable to process into useable films suggesting that acid terminated P( $\omega$ -OHFA)s may not be optimal for practical applications and are therefore not presented.



The thermal stability, crystal structure, thermal behaviour and mechanical properties of the P( $\omega$ -Me-OHFA)s were investigated by TGA, XRD, DSC, and DMA and tensile analysis, respectively. The results obtained from these diverse of techniques were discussed in terms of number average molecular weight ( $\bar{M}_n$ ) and length of the constituting monomeric unit ( $n$ ). The physical properties of the P( $\omega$ -Me-OHFA)s were compared with those of aliphatic polyesters reported in the literature, and particularly contrasted with HDPE.

The TGA results indicated that the polyesters of the present study have very good thermal stability which compare favourably with other aliphatic polyesters. Understandably, the temperature of maximum rate of degradation ( $T_{d(\max)}$ ) did not vary with  $\bar{M}_n$  for any given P( $\omega$ -Me-OHFA) but increased with monomeric unit length. This was explained by increasing the hydrophobic nature of polyesters by adding the number of carbons in the monomeric unit length. It has been shown also that the onset temperature of degradation of any given P( $\omega$ -Me-OHFA) scale linearly with  $\bar{M}_n$  but is independent of  $n$ . This was explained by increasing the density of ester bond as a result of increasing  $\bar{M}_n$ . As it was emphasized in hypothesis no. 3, long chain methylene groups in  $\omega$ -hydroxyl fatty acids are factors to improve thermal stability of the polymer by increasing the Van der Waals attractive forces. The result of increasing thermal stability of the polymers as a function of length of monomeric unit length supports hypothesis no.3.

All the P( $\omega$ -Me-OHFA)s packed in an orthorhombic subcell structure similar to that of polyethylene (PE). They are quiet high crystalline materials as revealed by the degree of crystallinity values ( $X_c(\%) \sim 50$  to  $78\%$ ) obtained from WAXD. The degree of crystallinity was directly correlated to the length of the repeating units in all the P( $\omega$ -Me-OHFA) samples. The

increase of  $X_c$  (%) with monomeric unit length has been directly linked to the increase of the van der Waals attractions as a consequence of the added  $\text{CH}_2$  groups. Conversely, a linear decrease was observed in  $X_c$  (%) as  $\bar{M}_n$  was increased due to the fact that lower molecular weight polymers crystallize relatively more easily because of higher chain mobility.

The DSC melting and crystallization temperature which can be related to the nature of the crystal form of the P( $\omega$ -Me-OHFA)s were not affected by  $\bar{M}_n$  unlike, the respective enthalpy of melting and crystallization. The effect of the length of the monomeric unit on the thermal transitions was noticeable. The increase observed in melting and crystallization temperatures as the length of the monomeric units increased from 9 to 18 was particularly correlated to the variation of the degree of crystallinity. Hypothesis no.4 is supported by observing the an increase in degree of crystallinity as well as melting temperature due to the fact that hydrophobic methylene segments are responsible in crystalline properties in aliphatic polyesters.

Mechanical properties were also significantly influenced by  $\bar{M}_n$  and length of the monomeric unit. The DMA results were strongly correlated to crystallinity confirming that mechanical properties of semi-crystalline thermoplastics depend strongly on their crystalline structure. For example, storage modulus decreased linearly as  $\bar{M}_n$  was increased and increased with increasing monomeric unit length similarly to  $X_c$  (%). Unlike DSC, a glass transition was recorded by DMA. The glass transition temperature ( $T_g$ ) varied as a function of  $\bar{M}_n$  and monomeric unit length similarly to the degree of crystallinity revealing also the strong correlation between the glass transition of the P( $\omega$ -Me-OHFA)s and their crystallinity. It was expected from hypothesis no. 5 that increasing in the length of repeating units of the poly( $\omega$ -hydroxyl fatty acids/esters) can affect the glass transition temperature ( $T_g$ ) of the polymers. The linear increasing trend of

$T_g$  as a function of length of monomeric units obtained of the study totally supports the hypothesis no. 5.

Tensile properties of the P( $\omega$ -Me-OHFA)s, such as max strain, ultimate strength and Young's modulus, were also considered. The P( $\omega$ -Me-OHFA)s demonstrated relatively high ultimate strength and very low values of elongation at break indicating that these materials are strong but brittle. The ultimate strength were strongly affected by  $\bar{M}_n$ , showing linearly increase. Young's modulus on the other hand, was completely affected by degree of. The variation observed in Young's modulus as a function of  $\bar{M}_n$  (linear decrease) and monomeric unit length (linear increase) mirrored and correlated very well the respective variation of  $X_c$  (%), illustrating the strong effect of crystallinity on tensile properties. According to hypothesis no. 6, tensile properties such as ultimate strength and max strain are affected by molecular weight of the polymer. The obtained results of increasing tensile properties as a function of  $\bar{M}_n$  support hypothesis no.6.

The P( $\omega$ -Me-OHFA)s presented in this study were comprehensively investigated and analyzed from a structural perspective. The improvement observed in their physical properties as the length of the monomeric unit was increased and which tend to approach those of HDPE, followed perfectly the trends observed in other aliphatic polyesters.

## Appendix A. NMR Spectra

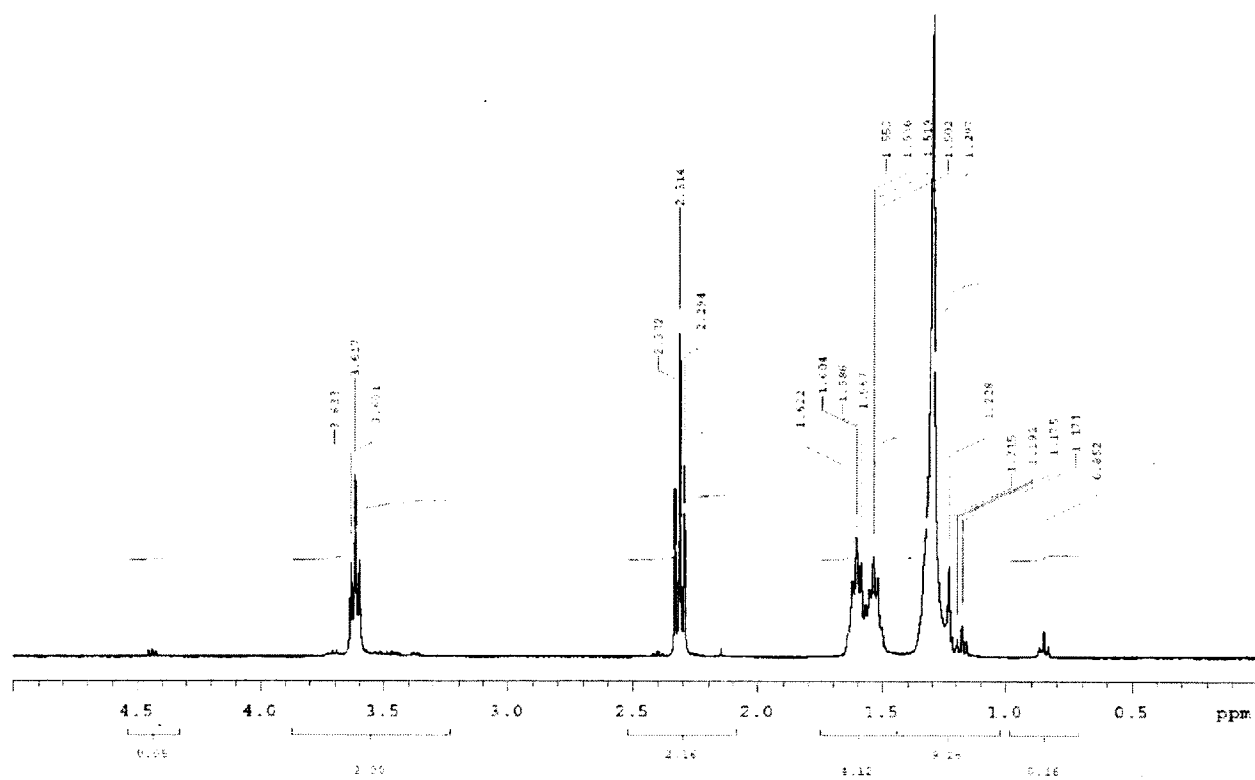
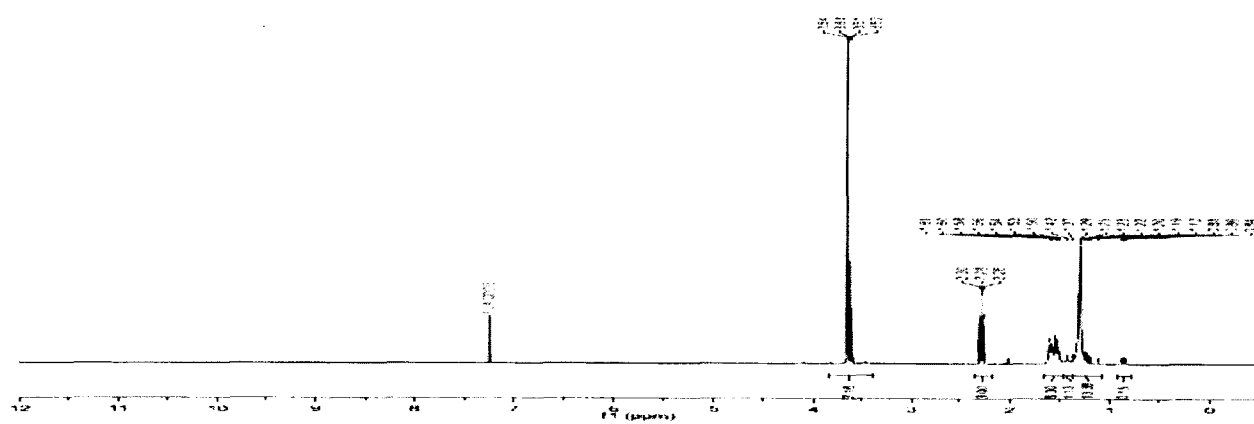


Figure A- 1.NMR Spectrum of (ω-OHC9)



**Figure A- 2.**NMR Spectrum of ( $\omega\text{-Me-OHC}_9$ )

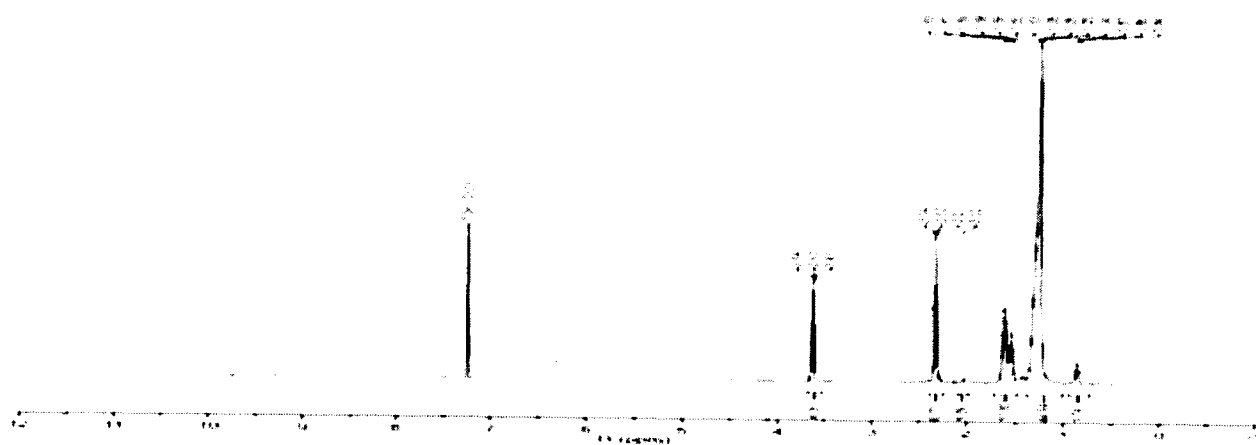


Figure A- 3.NMR Spectrum of (ω-OHC13)

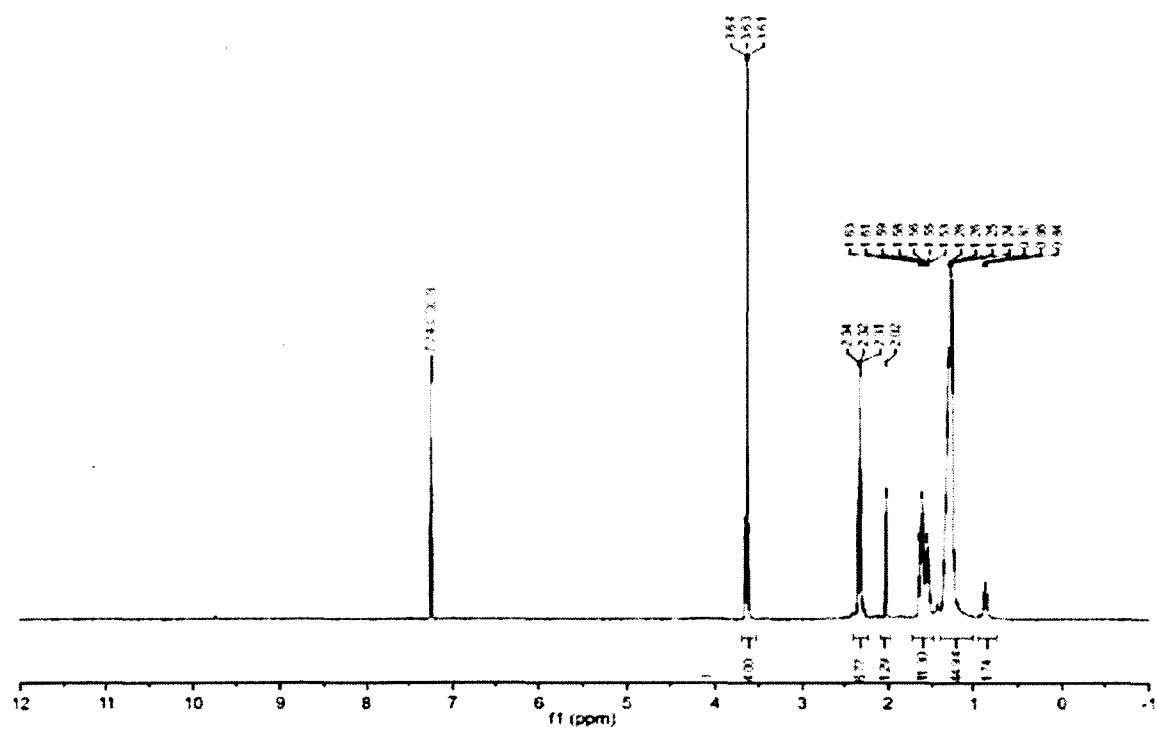


Figure A- 4.NMR spectrum of (ω-Me-OHC13)

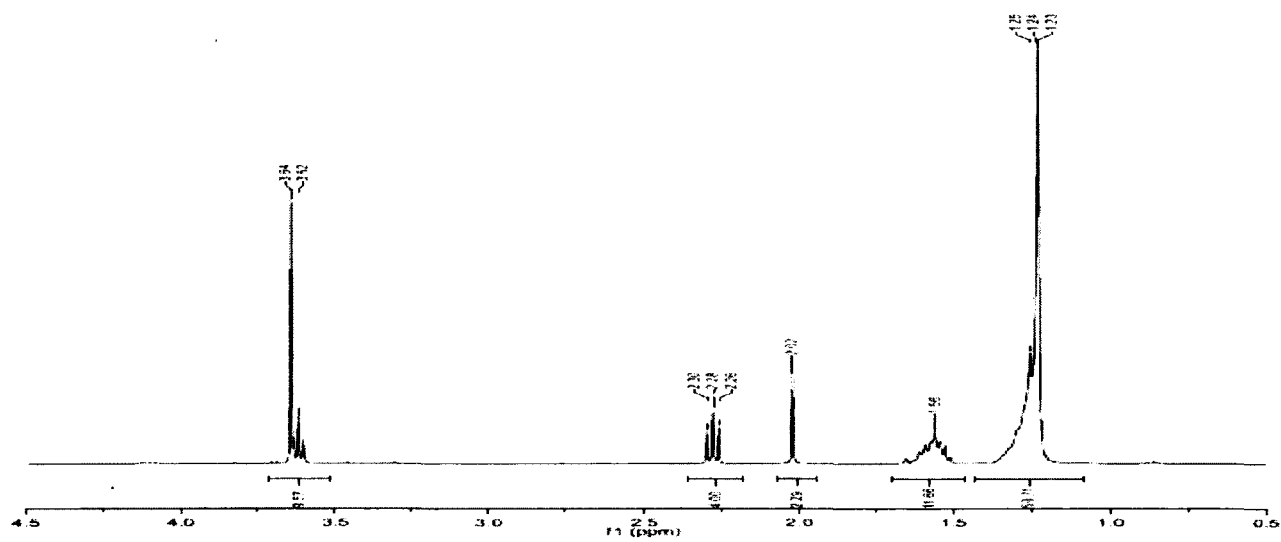


Figure A- 5.NMR spectrum of (ω-Me-OHC18)



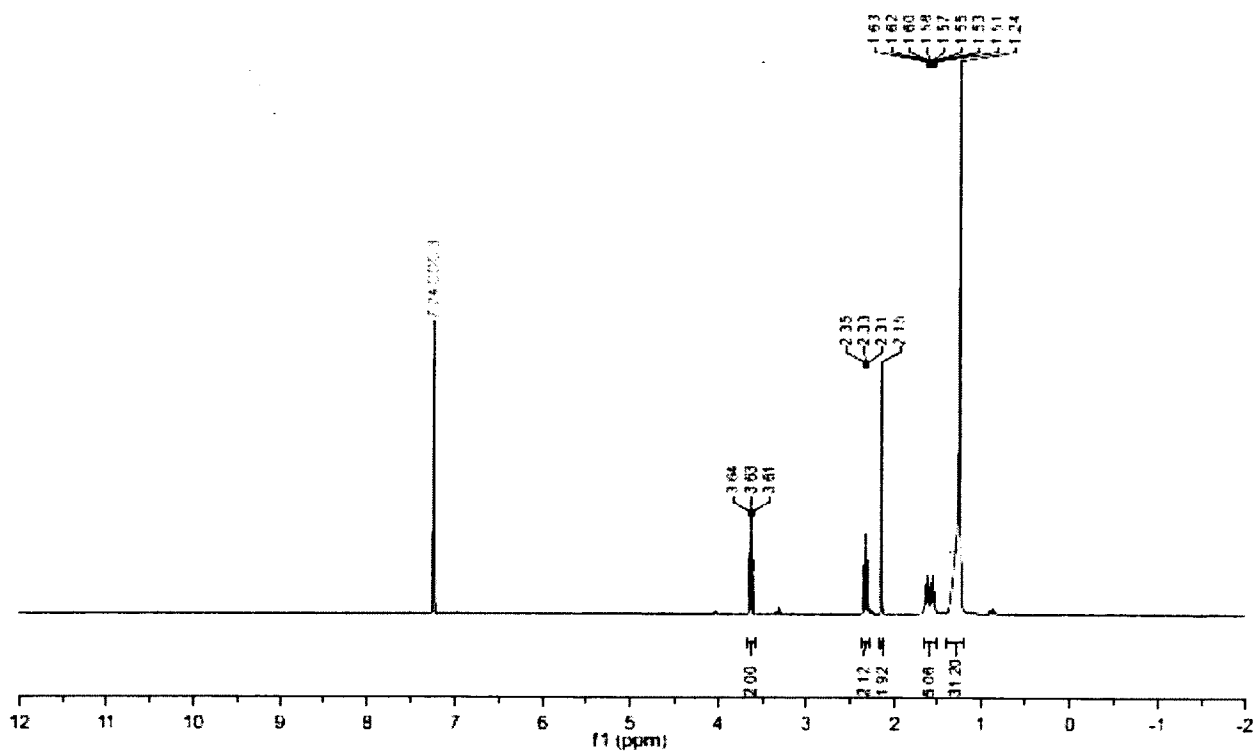
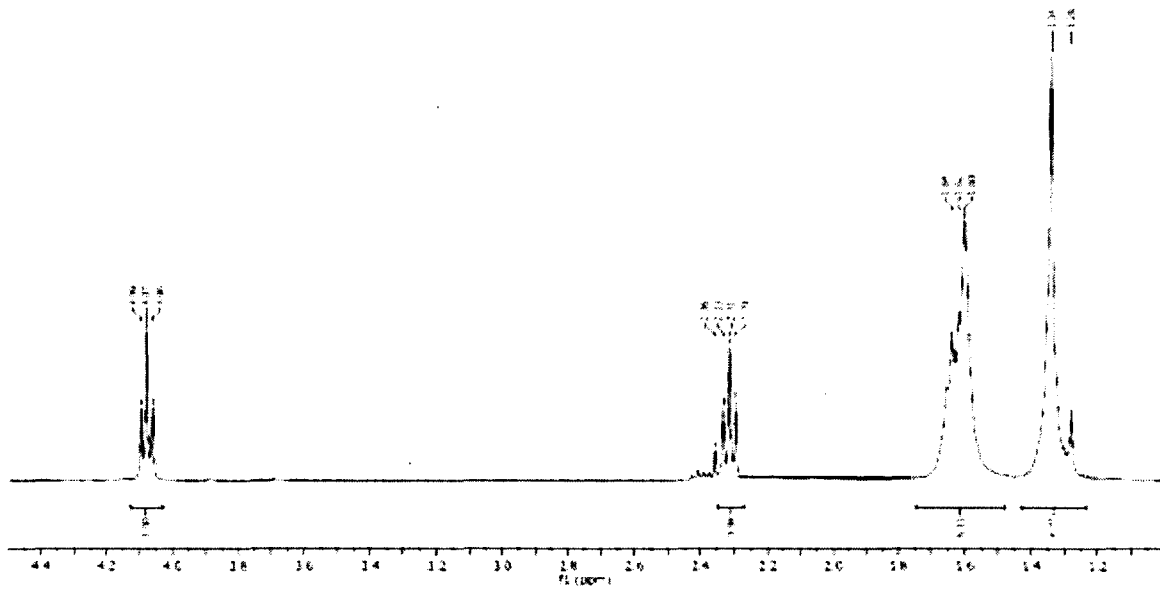
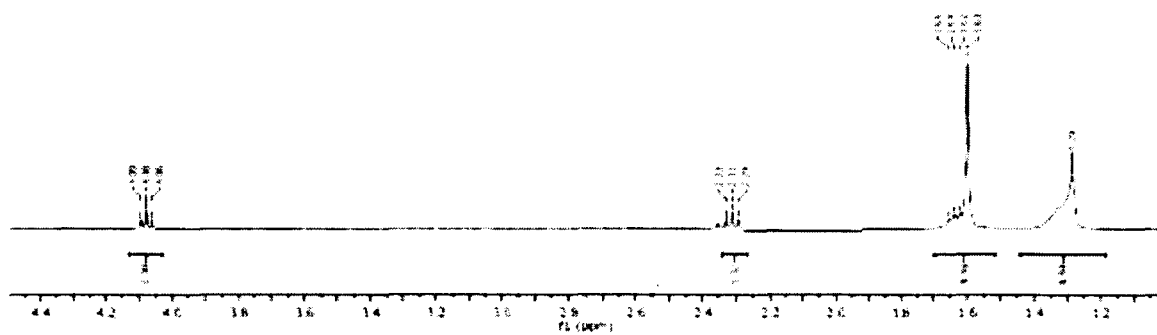


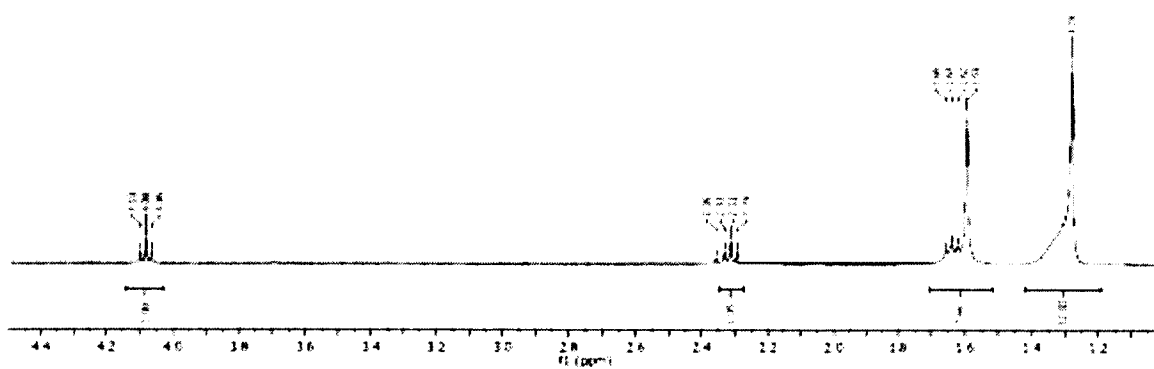
Figure A- 6.NMR Spectrum of (ω-OHC18)



**Figure A- 7.** NMR Spectrum of P( $\omega$ -OHC9) and P( $\omega$ -Me-OHC9)

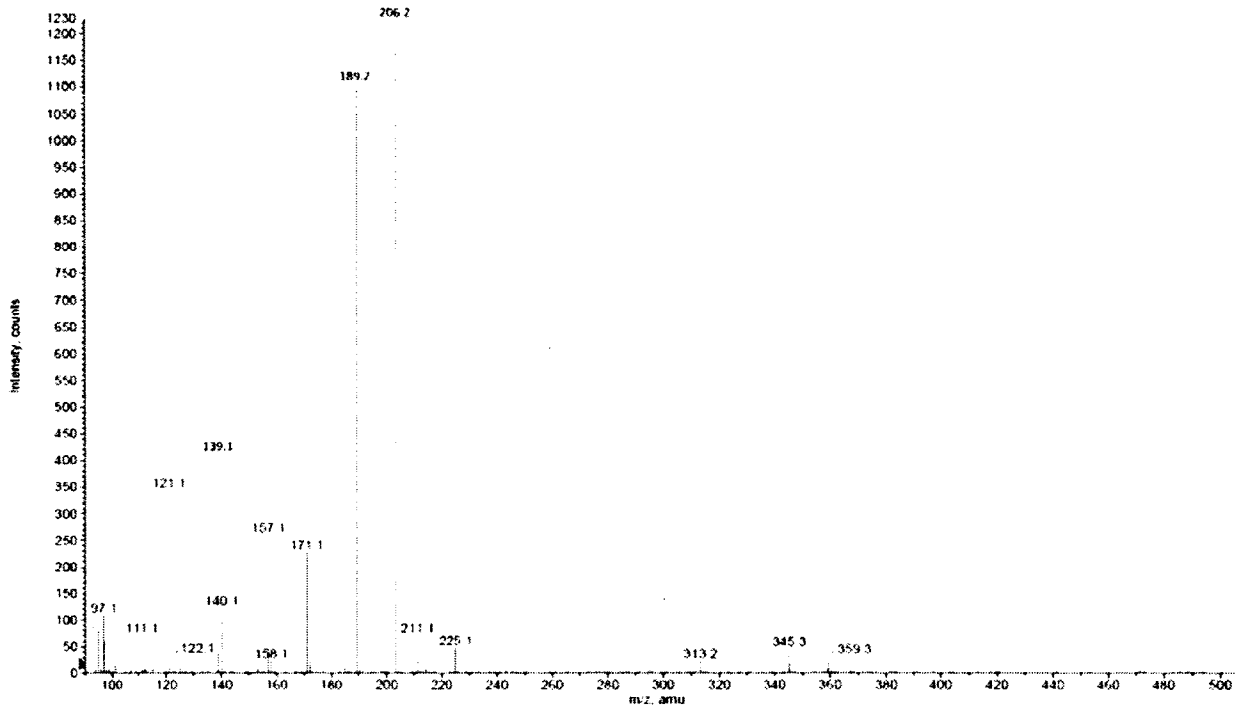


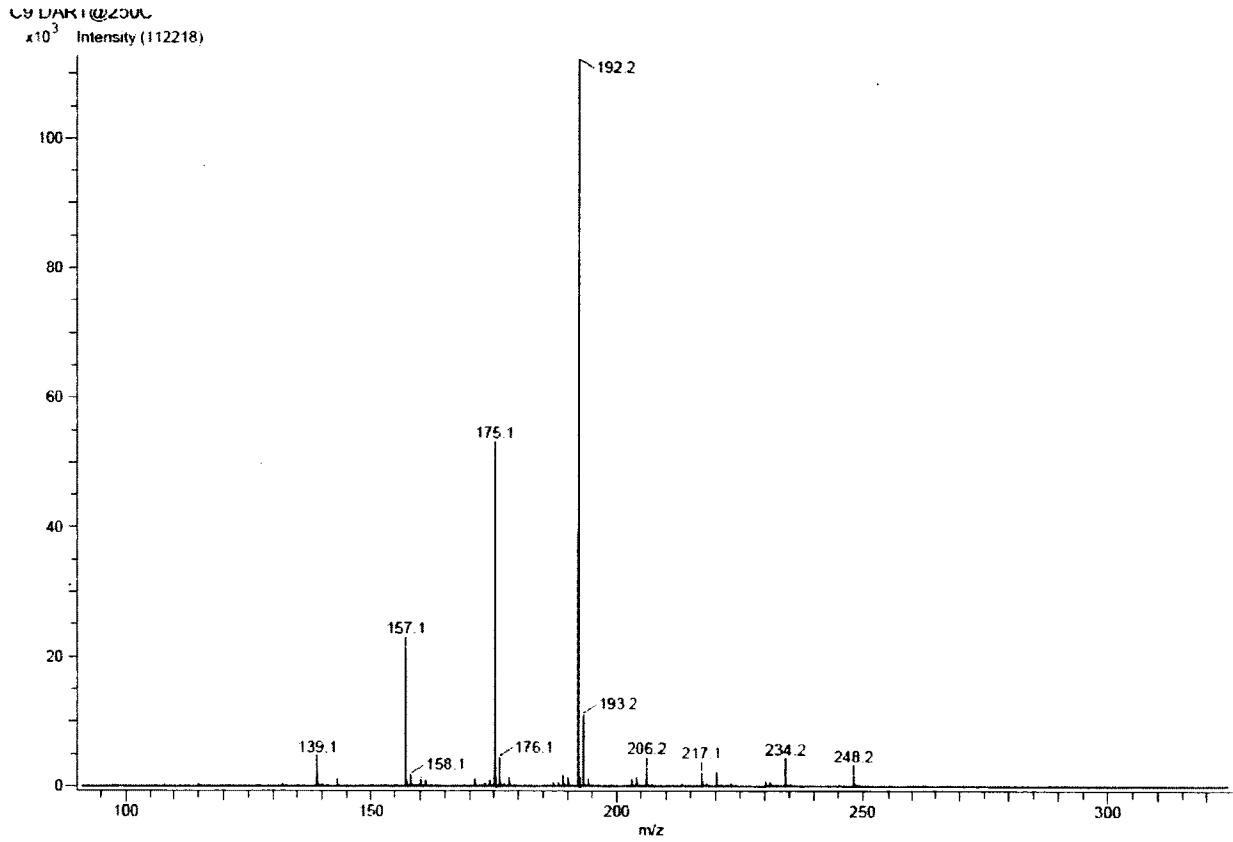
**Figure A- 8.** NMR Spectrum of P( $\omega$ -OHC13) and P( $\omega$ -Me-OHC13)



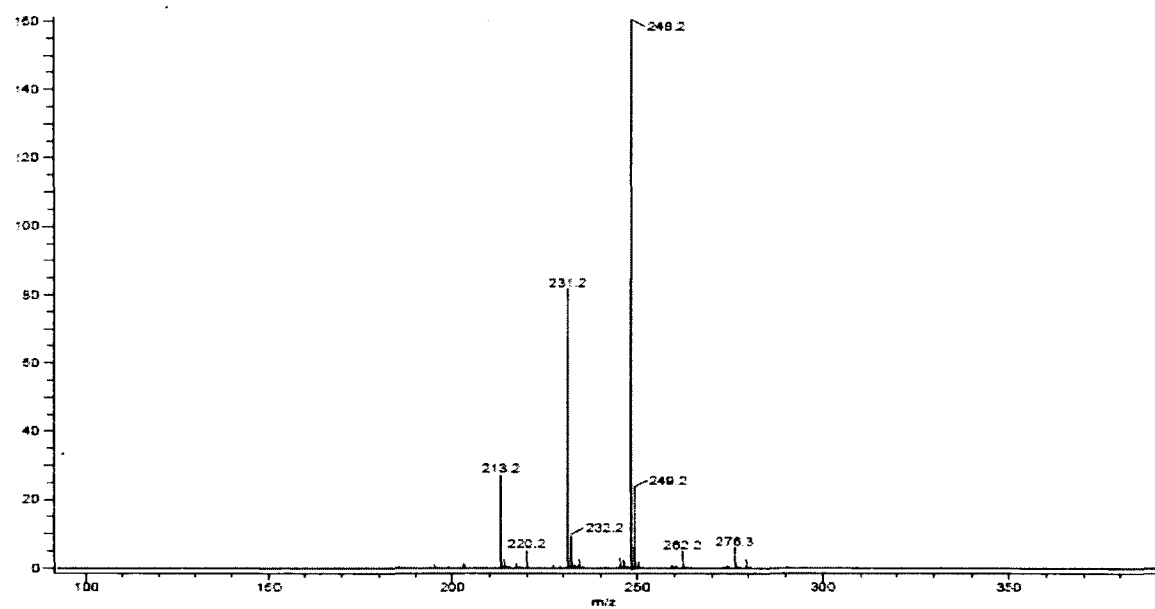
**Figure A- 9.**NMR Spectrum of P( $\omega$ -OHC18) and P( $\omega$ -Me-OHC18)

## Appendix B. Mass spectra

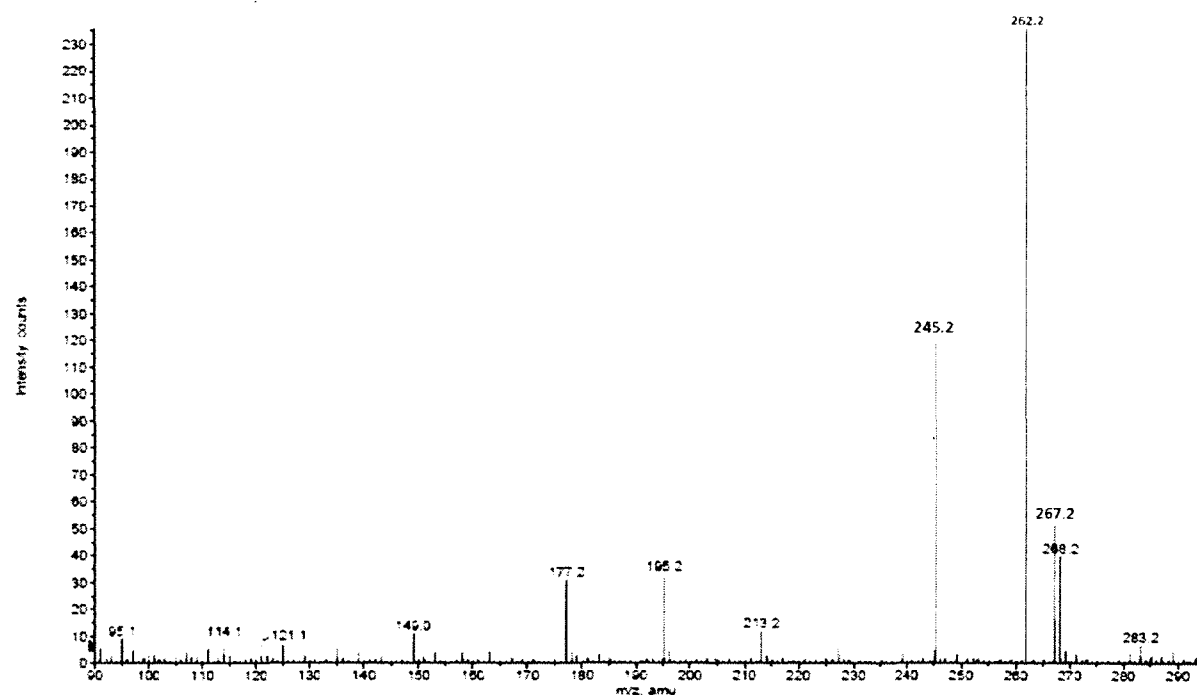
Figure B- 1. Mass Spectrum of ( $\omega$ -Me-OHC9)



**Figure B- 2.**Mass spectrum of ( $\omega$ -OHC9)

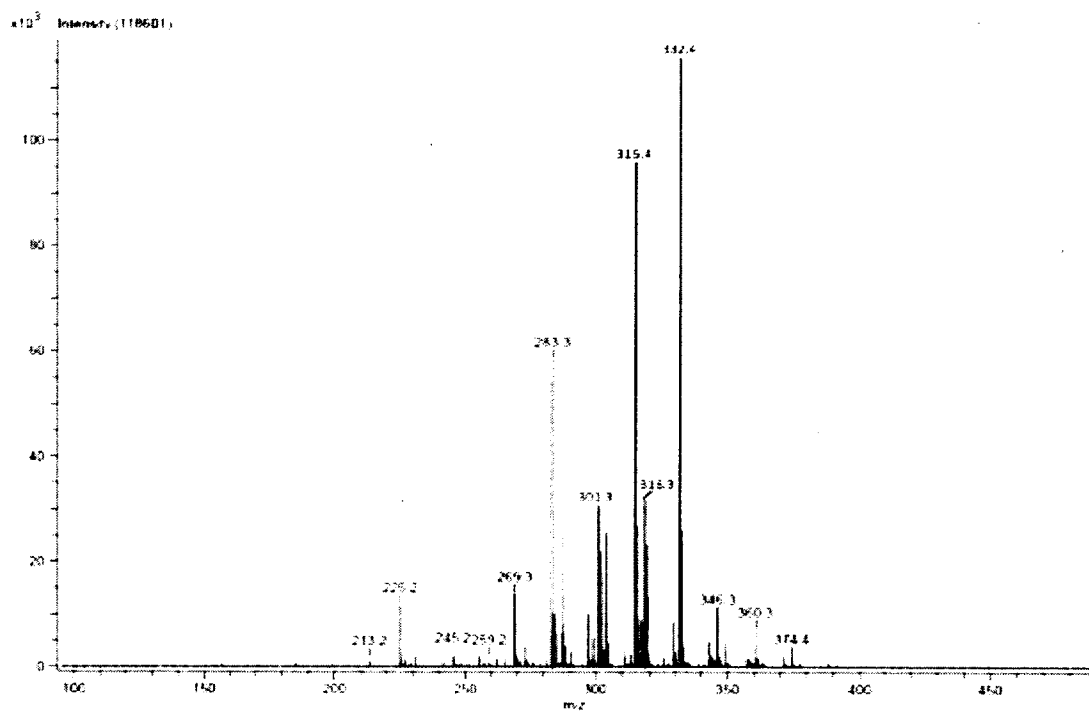


**Figure B- 3.**Mass Spectrum of ( $\omega$ -OHC13)

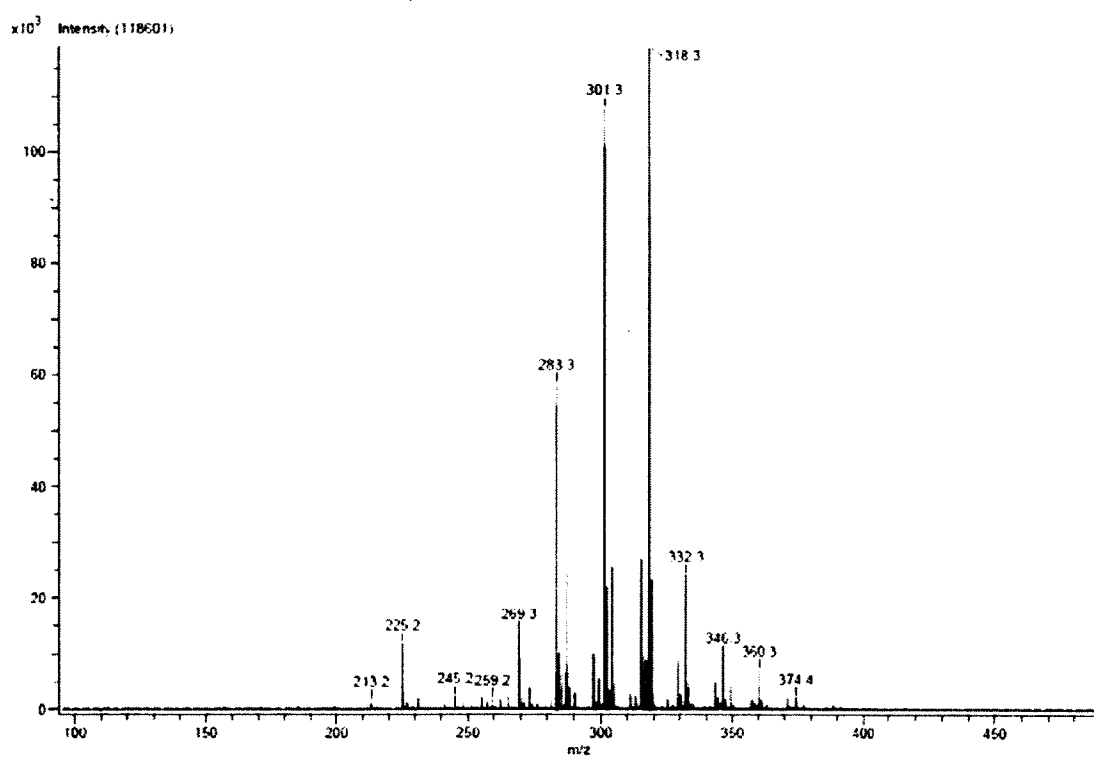


**Figure B- 4.**Mass Spectrum of ( $\omega$ -Me-OHC13)

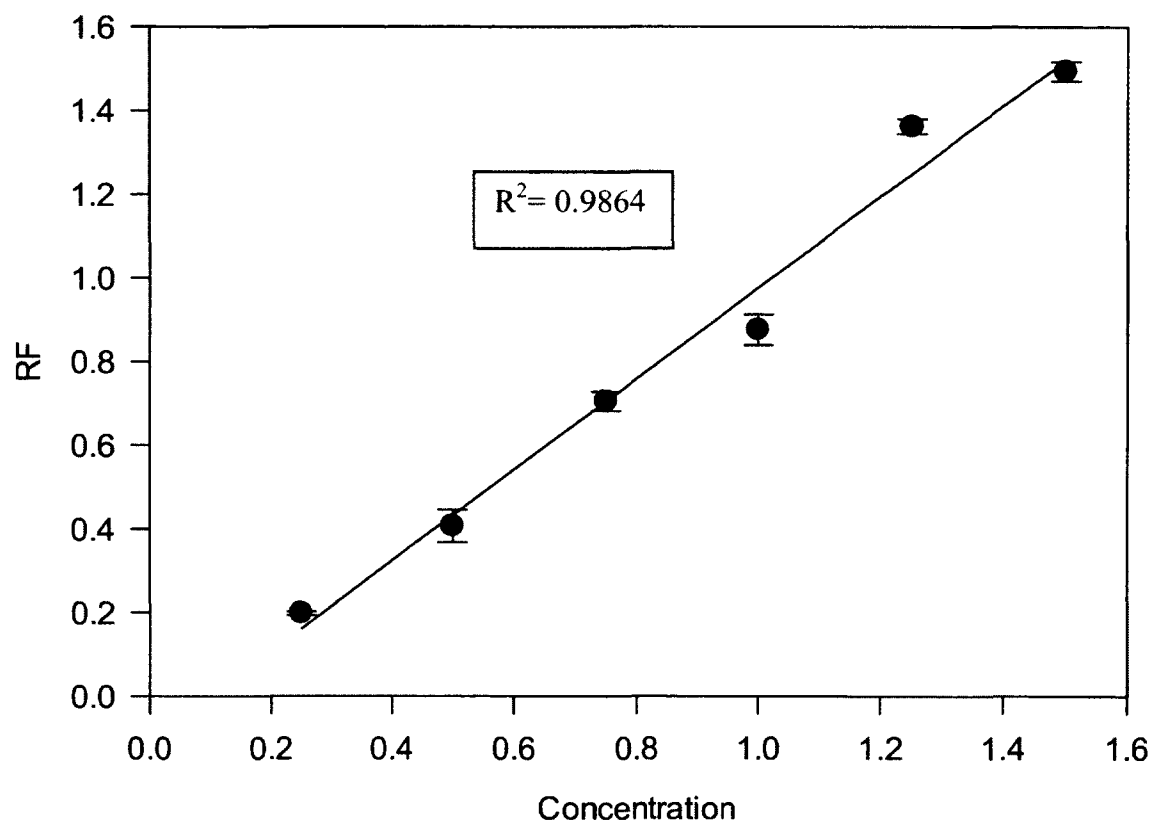


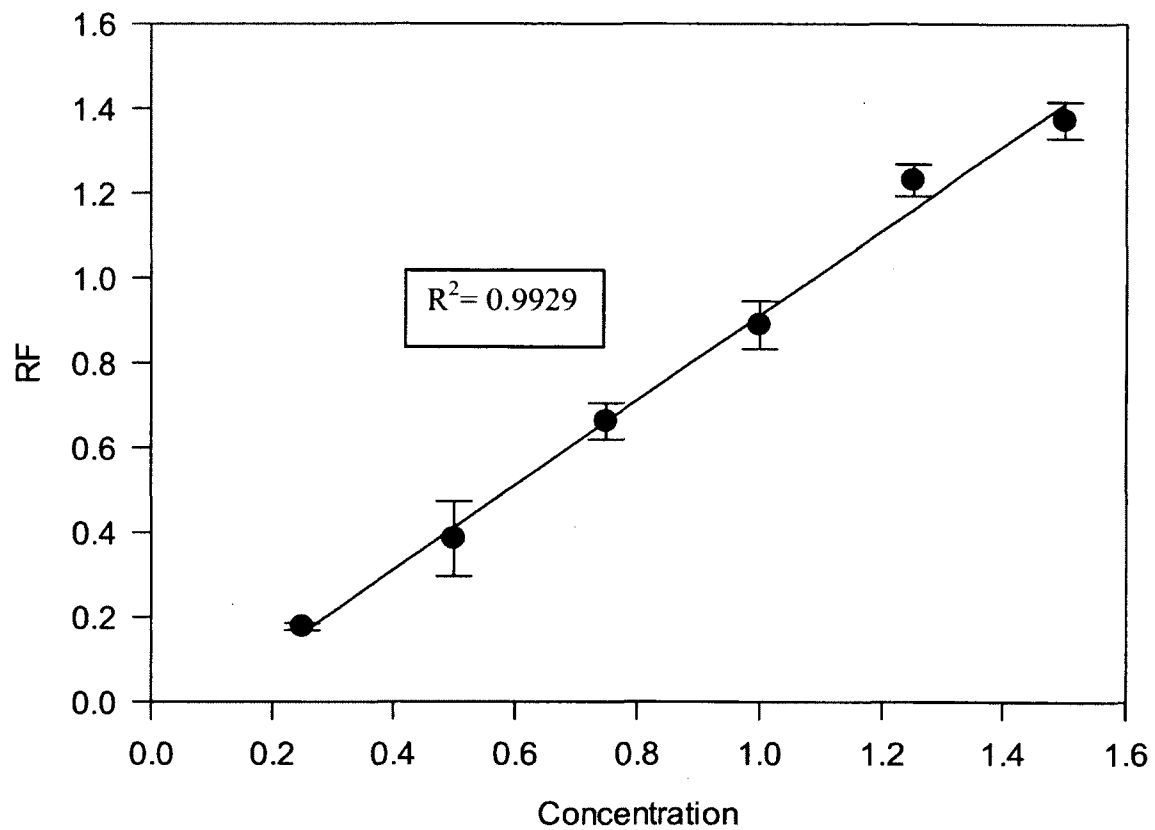


**Figure B- 5.**Mass spectrum of ( $\omega$ -Me-OHC18)

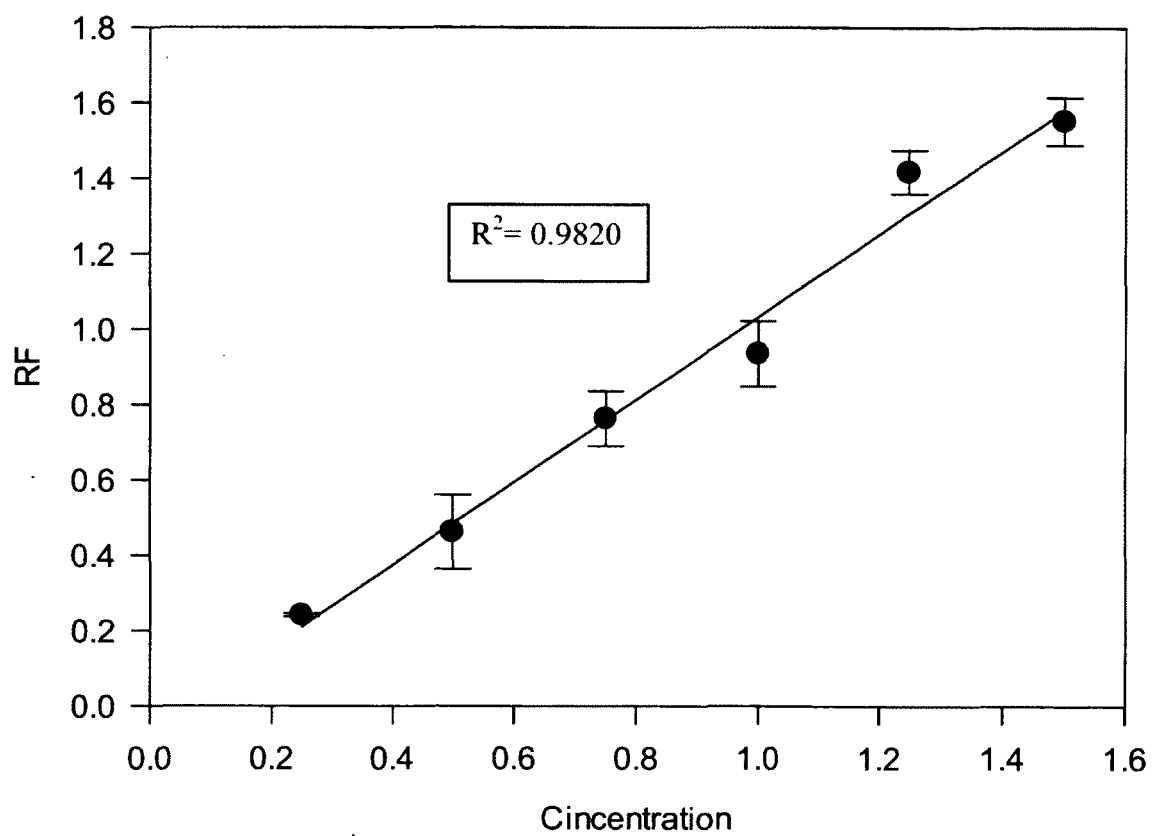


**Figure B- 6.** Mass Spectrum of ( $\omega$ -OHC18)

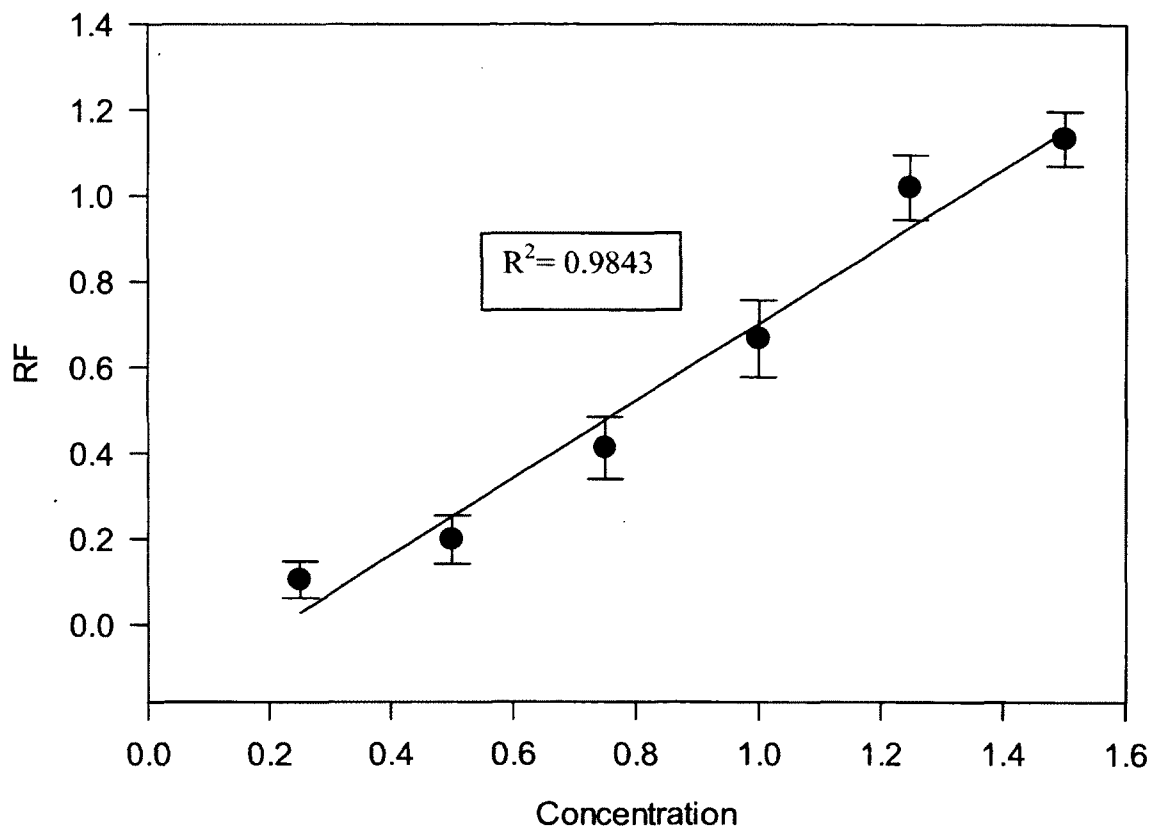
**Appendix C. HPLC Calibration Curves****Figure C- 1. HPLC Calibration Curve of ( $\omega$ -OHC9)**



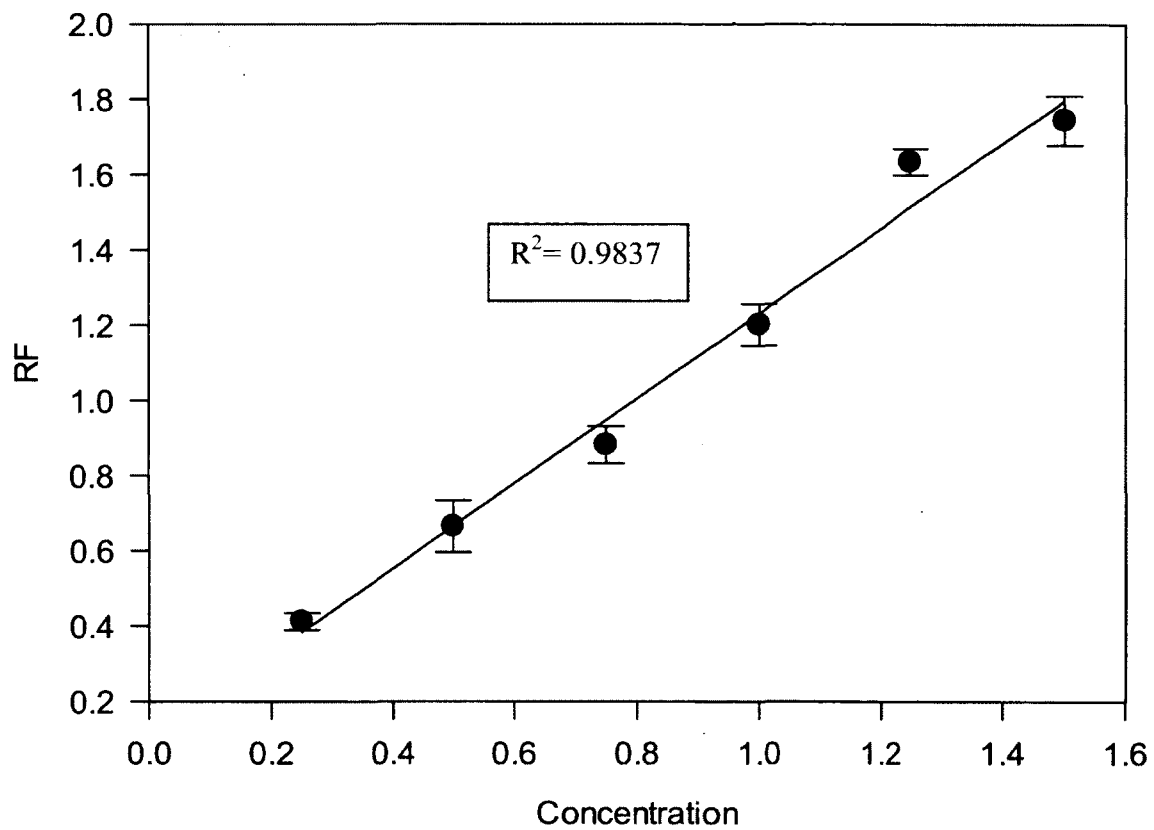
**Figure C- 2.** HPLC Calibration Curve of ( $\omega$ -Me-OHC9)



**Figure C- 3. HPLC Calibration Curve of ( $\omega$ -OHC13)**



**Figure C- 4.** HPLC Calibration Curve of ( $\omega$ -Me-OHC13)



**Figure C- 5.** HPLC Calibration Curve of ( $\omega$ -OHC18)

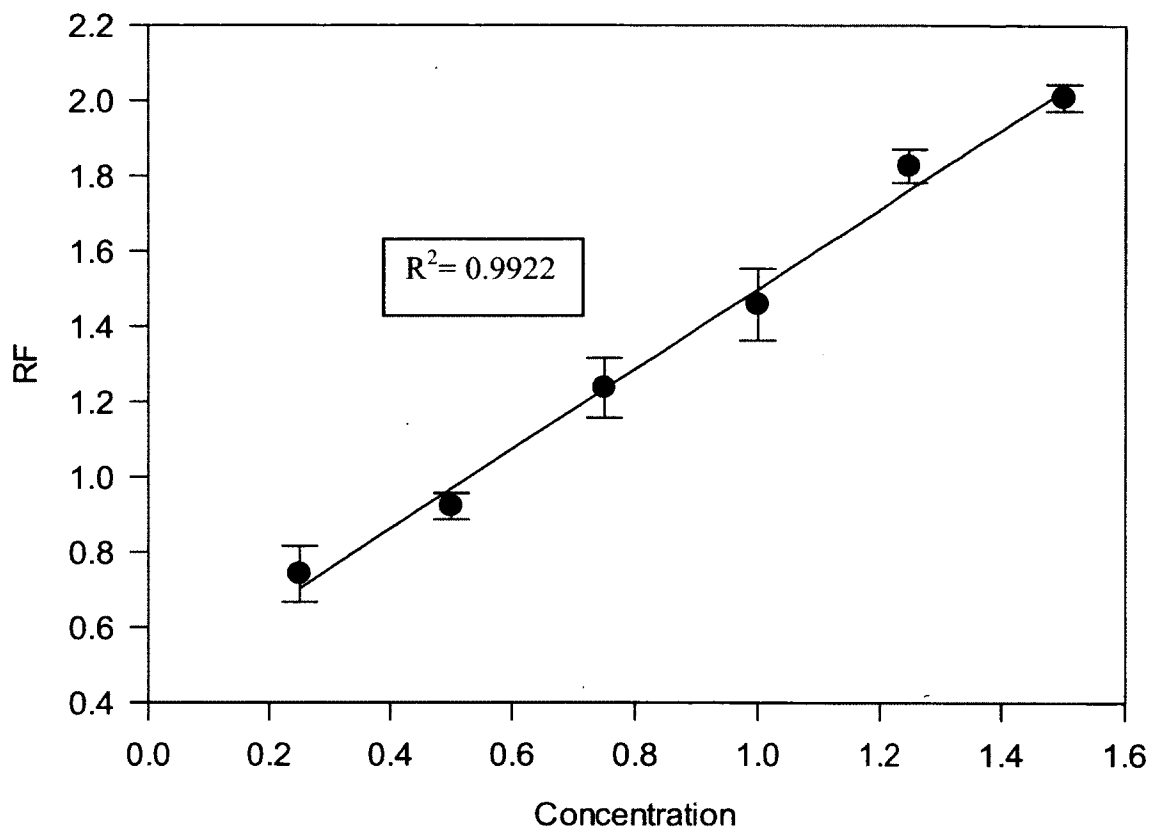


Figure C- 6. HPLC Calibration Curve of ( $\omega$ -Me-OHC18)



## References

- Abraham, S. and S. S. Narine (2009). "Polynonanolactone synthesized from vegetable oil: Evaluation of physical properties, biodegradation, and drug release behavior." Journal of Polymer Science Part A: Polymer Chemistry **47**(23): 6373-6387.
- Albertsson, A. C. and I. Varma (2002). "Aliphatic polyesters: synthesis, properties and applications." Degradable Aliphatic Polyesters: 1-40.
- Aranda, D. A. G., R. T. P. Santos, et al. (2008). "Acid-catalyzed homogeneous esterification reaction for biodiesel production from palm fatty acids." Catalysis letters **122**(1): 20-25.
- Athanasiou, K. A., G. G. Niederauer, et al. (1996). "Sterilization, toxicity, biocompatibility and clinical applications of polylactic acid/polyglycolic acid copolymers." Biomaterials **17**(2): 93-102.
- Auras, R., B. Harte, et al. (2004). "An overview of polylactides as packaging materials." Macromolecular bioscience **4**(9): 835-864.
- Bailey, P. S. and T. M. Ferrell (1978). "Mechanism of Ozonolysis. A more flexible stereochemical concept." Journal of the American Chemical Society **100**(3): 899-905.
- Barbiroli, G., C. Lorenzetti, et al. (2003). "Polyethylene like polymers. Aliphatic polyesters of dodecanedioic acid: I. Synthesis and properties." European polymer journal **39**(4): 655-661.
- Bittiger, H., R. Marchessault, et al. (1970). "Crystal structure of poly--caprolactone." Acta Crystallographica Section B: Structural Crystallography and Crystal Chemistry **26**(12): 1923-1927.
- Bouzidi, L., M. Boodhoo, et al. (2005). "Use of first and second derivatives to accurately determine key parameters of DSC thermographs in lipid crystallization studies." Thermochimica acta **439**(1): 94-102.
- Bunn, C. W. (1939). "The crystal structure of long-chain normal paraffin hydrocarbons. The "shape" of the <CH<sub>2</sub> group." Transactions of the Faraday Society **35**: 482-491.
- Bunn, C. W. (1939). "The crystal structure of long-chain normal paraffin hydrocarbons. The "shape" of the < CH<sub>2</sub> group." Transactions of the Faraday Society **35**: 482-491.
- Cai, J., C. Liu, et al. (2010). "Effects of molecular weight on poly(omega-pentadecalactone) mechanical and thermal properties." Polymer **51**(5): 1088-1099.
- Cai, K., K. Yao, et al. (2002). "Poly (-,l-lactic acid) surfaces modified by silk fibroin: effects on the culture of osteoblast in vitro." Biomaterials **23**(4): 1153-1160.
- Capaccio, G., T. Crompton, et al. (2003). "The drawing behavior of linear polyethylene. I. Rate of drawing as a function of polymer molecular weight and initial thermal treatment." Journal of Polymer Science: Polymer Physics Edition **14**(9): 1641-1658.
- Carothers, W. H. (1929). J. Am. Chem. Soc. **31**: 2548.
- Chandra, R. and R. Rustgi (1998). "Biodegradable polymers." PROG POLYM SCI(OXFORD) **23**(7): 1273-1335.
- Chartoff, R. P., J. D. Menczel, et al. (2009). "Dynamic mechanical analysis (DMA)." Thermal analysis of polymers: fundamentals and applications **387**.
- Chauvin, Y., R. H. Grubbs, et al. (2006). "2005 Nobel Prize in Chemistry." Platinum Metals Rev **50**(1): 35-37.
- Cho, K., H. K. Jeon, et al. (1993). "Thermal and mechanical properties of HDPE/ionomer blends." Journal of materials science **28**(24): 6650-6656.

- Chrissafis, K., K. Paraskevopoulos, et al. (2006). "Effect of molecular weight on thermal degradation mechanism of the biodegradable polyester poly (ethylene succinate)." Thermochemica acta **440**(2): 166-175.
- Chrissafis, K., K. Paraskevopoulos, et al. (2006). "Thermal degradation kinetics of the biodegradable aliphatic polyester, poly (propylene succinate)." Polymer degradation and stability **91**(1): 60-68.
- Connon, S. J. and S. Blechert (2002). "ChemInform Abstract: A Solid-Supported Phosphine-Free Ruthenium Alkylidene for Olefin Metathesis in Methanol and Water." ChemInform **33**(49): no-no.
- de Geus, M., I. van der Meulen, et al. (2010). "Performance polymers from renewable monomers: high molecular weight poly (pentadecalactone) for fiber applications." Polym. Chem. **1**(4): 525-533.
- Dolman, S. J., K. C. Hultsch, et al. (2004). "Supported chiral Mo-based complexes as efficient catalysts for enantioselective olefin metathesis." Journal of the American Chemical Society **126**(35): 10945-10953.
- Duda, A. and S. Penczek (2002). "Mechanisms of aliphatic polyester formation." Biopolymers **3**: 371-430.
- Duh, B. (2002). "Effect of antimony catalyst on solid-state polycondensation of poly (ethylene terephthalate)." Polymer **43**(11): 3147-3154.
- Edlund, U. and A. C. Albertsson (2003). "Polyesters based on diacid monomers." Advanced drug delivery reviews **55**(4): 585-609.
- Ehwald, H., A. A. Shestov, et al. (1994). "Ethylene hydrogenation mechanism on Ag/SiO<sub>2</sub> catalysts elucidated by isotope kinetics." Catalysis letters **25**(1): 149-155.
- Flippin, L. A., D. W. Gallagher, et al. (1989). "A convenient method for the reduction of ozonides to alcohols with borane-dimethyl sulfide complex." The Journal of Organic Chemistry **54**(6): 1430-1432.
- Flory, P. J. (1946). Chem. Soc. Rev. **39**(137).
- Flory, P. J. (1953). "Principles of Polymer Chemistry." Cornell University Press, Chapter VIII and IX.
- Flory, P. J., D. Y. Yoon, et al. (1984). "The interphase in lamellar semicrystalline polymers." Macromolecules **17**(4): 862-868.
- Ganeshpure, P. A. and J. Das (2007). "Application of high-melting pyridinium salts as ionic liquid catalysts and media for Fischer esterification." Reaction Kinetics and Catalysis Letters **92**(1): 69-74.
- Gaur, U. and B. Wunderlich (1980). "The glass transition temperature of polyethylene." Macromolecules **13**(2): 445-446.
- Ghotra, B. S., S. D. Dyal, et al. (2002). "Lipid shortenings: a review." Food Research International **35**(10): 1015-1048.
- Griffith, W. P. (2001). "Ozonolysis in coordination chemistry and catalysis: recent advances." Coordination Chemistry Reviews **219**(221): 259-281.
- Gross, R. A. and B. Kalra (2002). "Biodegradable polymers for the environment." Science **297**(5582): 803-807.
- Gupta, A. and V. Kumar (2007). "New emerging trends in synthetic biodegradable polymers—Polylactide: A critique." European polymer journal **43**(10): 4053-4074.
- Harding, L. B. and W. A. Goddard III (1978). "Mechanisms of gas-phase and liquid-phase ozonolysis." Journal of the American Chemical Society **100**(23): 7180-7188.

- Henton, D. E., P. Gruber, et al. (2005). "Polylactic acid technology." Natural Fibers, Biopolymers, and Biocomposites. Taylor & Francis, Boca Raton, FL, pp. 527-577.
- Hojabri, L., X. Kong, et al. (2009). "Fatty acid-derived diisocyanate and biobased polyurethane produced from vegetable oil: synthesis, polymerization, and characterization." Biomacromolecules **10**(4): 884-891.
- Hojabri, L., X. Kong, et al. (2010). "Functional thermoplastics from linear diols and diisocyanates produced entirely from renewable lipid sources." Biomacromolecules **11**(4): 911-918.
- Horiuti, I. and M. Polanyi (1934). "Exchange reactions of hydrogen on metallic catalysts." Transactions of the Faraday Society **30**: 1164-1172.
- Hu, H. and D. L. Dorset (1990). "Crystal structure of poly ( $\epsilon$ -caprolactone)." Macromolecules **23**(21): 4604-4607.
- Hutmacher, D. W., T. Schantz, et al. (2001). "Mechanical properties and cell cultural response of polycaprolactone scaffolds designed and fabricated via fused deposition modeling." Journal of biomedical materials research **55**(2): 203-216.
- Jain, J. P., M. Sokolsky, et al. (2008). "Fatty acid based biodegradable polymer." Polymer Reviews **48**(1): 156-191.
- Kennedy, M., A. Peacock, et al. (1994). "Tensile properties of crystalline polymers: linear polyethylene." Macromolecules **27**(19): 5297-5310.
- Kirkland, T. A., D. M. Lynn, et al. (1998). "Ring-closing metathesis in methanol and water." Journal of Organic Chemistry **63**(26): 9904-9909.
- Kong, X., J. Yue, et al. (2007). "Physical properties of canola oil based polyurethane networks." Biomacromolecules **8**(11): 3584-3589.
- Labet, M. and W. Thielemans (2009). "Synthesis of polycaprolactone: a review." Chem. Soc. Rev. **38**(12): 3484-3504.
- Larsson, K. (1986). Physical Properties - Structural and Physical Characteristics. in: "The Lipid handbook". F. D. Gunstone, J. L. Harwood and F. B. Padley. London, Chapman and Hall: 335-377.
- Larsson, K. (1994). Lipids : Molecular Organization, Physical Functions and Technical Applications. Dundee, Oily Press.
- Letizia Focarete, M., M. Scandola, et al. (2001). "Physical characterization of poly ( $\omega$ -pentadecalactone) synthesized by lipase-catalyzed ring-opening polymerization." Journal of Polymer Science Part B: Polymer Physics **39**(15): 1721-1729.
- Leverd, F., A. Fradet, et al. (1987). "Study of model esterifications and of polyesterifications catalyzed by various organometallic derivatives—I. Study of esterifications catalyzed by titanium derivatives." European polymer journal **23**(9): 695-698.
- Li, S., L. Hojabri, et al. (2012). "Controlling Product Composition of Metathesized Triolein by Reaction Concentrations." Journal of the American Oil Chemists' Society: 1-13.
- Liu, C., F. Liu, et al. (2011). "Polymers from Fatty Acids: Poly ( -hydroxyl tetradecanoic acid) Synthesis and Physico-Mechanical Studies." Biomacromolecules.
- Liu, C. B., Z. Y. Qian, et al. (2006). "Synthesis, characterization, and thermal properties of biodegradable aliphatic copolyester based on epsilon-caprolactone, adipic acid, and 1,6-hexanediol." Materials Letters **60**(1): 31-38.
- Liu, G., X. Kong, et al. (2008). "Production of 9-hydroxynonanoic acid from methyl oleate and conversion into lactone monomers for the synthesis of biodegradable polylactones." Biomacromolecules **9**(3): 949-953.

- Lu, W., J. E. Ness, et al. (2010). "Biosynthesis of monomers for plastics from renewable oils." Journal of the American Chemical Society.
- Lu, W., J. E. Ness, et al. (2010). "Biosynthesis of monomers for plastics from renewable oils." Journal of the American Chemical Society **132**(43): 15451.
- MacDermott, C. P. and A. V. Shenoy (1997). "Selecting thermoplastics for engineering applications."
- MacDonald, W. A. (2002). "New advances in poly (ethylene terephthalate) polymerization and degradation." Polymer international **51**(10): 923-930.
- Madhavan Nampoothiri, K., N. R. Nair, et al. (2010). "An overview of the recent developments in polylactide (PLA) research." Bioresource technology **101**(22): 8493-8501.
- Mahapatro, A., A. Kumar, et al. (2004). "Solvent-Free Adipic Acid/1, 8-Octanediol Condensation Polymerizations Catalyzed by *Candida antarctica* Lipase B." Macromolecules **37**(1): 35-40.
- Malpass, D. (2010). Introduction to Industrial Polyethylene: Properties, Catalysts, and Processes, Wiley-Scrivener.
- Mandelkern, L. (1990). "The structure of crystalline polymers." Accounts of chemical research **23**(11): 380-386.
- Margolis, J. (1985). "Engineering thermoplastics: properties and applications." Plast. Eng. **41**(11): 63.
- Matsuo, M. and C. Sawatari (1986). "Elastic modulus of polyethylene in the crystal chain direction as measured by x-ray diffraction." Macromolecules **19**(7): 2036-2040.
- Mecking, S. (2004). "Nature or petrochemistry?—Biologically degradable materials." Angewandte Chemie International Edition **43**(9): 1078-1085.
- Mengeloglu, F. and K. Karakus (2008). "Thermal degradation, mechanical properties and morphology of wheat straw flour filled recycled thermoplastic composites." Sensors **8**(1): 500-519.
- Mochizuki, M. and M. Hirami (1998). "Structural effects on the biodegradation of aliphatic polyesters." Polymers for Advanced Technologies **8**(4): 203-209.
- Mol, J. (2004). "Catalytic metathesis of unsaturated fatty acid esters and oils." Topics in catalysis **27**(1): 97-104.
- Muetterties, E. L. and J. R. Bleeke (1979). "Catalytic hydrogenation of aromatic hydrocarbons." Accounts of Chemical Research **12**(9): 324-331.
- Murthy, N. and H. Minor (1990). "General procedure for evaluating amorphous scattering and crystallinity from X-ray diffraction scans of semicrystalline polymers." Polymer **31**(6): 996-1002.
- Nair, L. S. and C. T. Laurencin (2007). "Biodegradable polymers as biomaterials." Progress in Polymer Science **32**(8): 762-798.
- Narine, S. S., X. Kong, et al. (2007). "Physical properties of polyurethanes produced from polyols from seed oils: I. Elastomers." Journal of the American Oil Chemists' Society **84**(1): 55-63.
- Narine, S. S., X. Kong, et al. (2007). "Physical properties of polyurethanes produced from polyols from seed oils: II. Foams." Journal of the American Oil Chemists' Society **84**(1): 65-72.
- Narine, S. S., J. Yue, et al. (2007). "Production of polyols from canola oil and their chemical identification and physical properties." Journal of the American Oil Chemists' Society **84**(2): 173-179.

- Narladkar, A. S. (2008). Conformation, morphology and glass transition of poly (lactic acid) in supported thin films.
- Nisoli, A., M. F. Doherty, et al. (2004). "Feasible regions for step-growth melt polycondensation systems." Industrial & engineering chemistry research **43**(2): 428-440.
- Nunes, R. W., J. R. Martin, et al. (1982). "Influence of molecular weight and molecular weight distribution on mechanical properties of polymers." Polymer Engineering & Science **22**(4): 205-228.
- Ogawa, J., S. Kishino, et al. (2005). "Production of conjugated fatty acids by lactic acid bacteria." Journal of bioscience and bioengineering **100**(4): 355-364.
- Oledzka, E., D. Kaliszewska, et al. (2012). "Synthesis and Properties of a Star-Shaped Poly ( $\epsilon$ -Caprolactone)-Ibuprofen Conjugate." Journal of Biomaterials Science, Polymer Edition **23**(16): 2039-2054.
- Oledzka, E. and S. S. Narine (2011). "Organic acids catalyzed polymerization of  $\epsilon$ -caprolactone: Synthesis and characterization." Journal of Applied Polymer Science **119**(4): 1873-1882.
- Otera, J. (2004). "Reaction of Alcohols with Carboxylic Acids and Their Derivatives." Esterification: Methods, Reactions, and Applications: 3-144.
- Palmisano, A. C. and C. A. Pettigrew (1992). "Biodegradability of plastics." Bioscience: 680-685.
- Pang, K., R. Kotek, et al. (2006). "Review of conventional and novel polymerization processes for polyesters." Progress in polymer science **31**(11): 1009-1037.
- Peponi, L., I. Navarro-Baena, et al. (2012). "Effect of the molecular weight on the crystallinity of PCL-b-PLLA di-block copolymers." Polymer.
- Perveen, S., A. Yasmeen, et al. (2010). "Structure Activity Relationship of Organic Alcohol and Esters for Antidepressant-Like Activity." Letters in Drug Design & Discovery **7**: 14-17.
- Petrović, Z. S., J. Milić, et al. (2010). "A chemical route to high molecular weight vegetable oil-based polyhydroxyalkanoate." Macromolecules **43**(9): 4120-4125.
- Philip, S., T. Keshavarz, et al. (2007). "Polyhydroxyalkanoates: biodegradable polymers with a range of applications." Journal of Chemical Technology and Biotechnology **82**(3): 233-247.
- Quan, C. (2005). High-temperature free-radical polymerization of n-butyl acrylate, Drexel University.
- Renouf-Glauser, A. C., J. Rose, et al. (2005). "The effect of crystallinity on the deformation mechanism and bulk mechanical properties of PLLA." Biomaterials **26**(29): 5771-5782.
- Rodrigues, C. E. C., C. B. Gonçalves, et al. (2007). "Deacidification of vegetable oils by solvent extraction." Recent Patents on Engineering **1**(1): 95-102.
- Rybak, A., P. A. Fokou, et al. (2008). "Metathesis as a versatile tool in oleochemistry." European Journal of Lipid Science and Technology **110**(9): 797-804.
- Rybak, A. and M. A. R. Meier (2007). "Cross-metathesis of fatty acid derivatives with methyl acrylate: renewable raw materials for the chemical industry." Green Chem. **9**(12): 1356-1361.
- Schrock, R. R. (2006). "Multiple metal-carbon bonds for catalytic metathesis reactions (Nobel lecture)." Angewandte Chemie International Edition **45**(23): 3748-3759.
- Schutter, M. E. and R. P. Dick (2000). "Comparison of fatty acid methyl ester (FAME) methods for characterizing microbial communities." Soil Science Society of America Journal **64**(5): 1659-1668.

- Shah, T., J. Bhatta, et al. (1984). "Aspects of the Chemistry of poly (ethylene terephthalate): 5. Polymerization of bis (hydroxyethyl) terephthalate by various metallic catalysts." Polymer **25**(9): 1333-1336.
- Shibasaki, Y., T. Araki, et al. (2002). "Control of Molecular Weight Distribution in Polycondensation Polymers. Polyamide Synthesis." Polymer journal **34**(4): 261-266.
- Siegel, S. and G. V. Smith (1960). "Stereochemistry and the Mechanism of Hydrogenation of Cycloolefins on a Platinum Catalyst 1, 2." Journal of the American Chemical Society **82**(23): 6082-6087.
- Singh, V. and M. Tiwari (2010). "Structure-Processing-Property Relationship of Poly (Glycolic Acid) for Drug Delivery Systems 1: Synthesis and Catalysis." International Journal of Polymer Science **2010**: 1687-9422.
- Sousa, J. A. and A. L. Bluhm (1960). "The reductive cleavage of ozonides to alcohols." The Journal of Organic Chemistry **25**(1): 108-111.
- Stehling, F. C. and L. Mandelkern (1970). "The glass temperature of linear polyethylene." Macromolecules **3**(2): 242-252.
- Stille, J. (1981). "Step-growth polymerization." Journal of Chemical Education **58**(11): 862.
- Stoffel, W., F. Chu, et al. (1959). "Analysis of long-chain fatty acids by gas-liquid chromatography." Analytical Chemistry **31**(2): 307-308.
- Sung, Y., C. Kum, et al. (2005). "Effects of crystallinity and crosslinking on the thermal and rheological properties of ethylene vinyl acetate copolymer." Polymer **46**(25): 11844-11848.
- Suzuki, K. E., T.; Otsuka, T.; Abe, S.; Yoshikawa, S. (1981). Process for the Preparation of Omega-hydroxy Fatty Acids from Omega-hydroxy (or acyloxy)-alkyl- $\gamma$ -Butyrolactones U.S. Patent, Patent#
- Talbott, M. F., G. S. Springer, et al. (1987). "The effects of crystallinity on the mechanical properties of PEEK polymer and graphite fiber reinforced PEEK." Journal of composite materials **21**(11): 1056-1081.
- Timms, R. E. (2003). The Confectionary Fats Handbook: Properties, Production, and Application. Chapter 2: Physical Chemistry. Bridgewater, England, The Oily Press.
- Tomita, K. and H. Ida (1973). "Studies on the formation of poly (ethylene terephthalate): 2. Rate of transesterification of dimethyl terephthalate with ethylene glycol." Polymer **14**(2): 55-60.
- Trzaskowski, J., D. Quinzler, et al. (2011). "Aliphatic Long-Chain C20 Polyesters from Olefin Metathesis." Macromolecular rapid communications **32**(17): 1352-1356.
- Tung, L. and S. Buckser (1958). "The Effects of Molecular Weight on the Crystallinity of Polyethylene." The Journal of Physical Chemistry **62**(12): 1530-1534.
- Ulery, B. D., L. S. Nair, et al. (2011). "Biomedical applications of biodegradable polymers." Journal of Polymer Science Part B: Polymer Physics **49**(12): 832-864.
- Uyama, H., S. Yaguchi, et al. (2000). "Lipase-catalyzed polycondensation of dicarboxylic acid-divinyl esters and glycols to aliphatic polyesters." Journal of Polymer Science Part A: Polymer Chemistry **37**(15): 2737-2745.
- Van de Velde, K. and P. Kiekens (2002). "Biopolymers: overview of several properties and consequences on their applications." Polymer Testing **21**(4): 433-442.
- van der Meulen, I., E. Gubbels, et al. (2011). "Catalytic Ring-Opening Polymerization of Renewable Macrolactones to High Molecular Weight Polyethylene-like Polymers." Macromolecules.

- Van der Wal, A., J. Mulder, et al. (1998). "Fracture of polypropylene: The effect of crystallinity." Polymer **39**(22): 5477-5481.
- Vert, M., S. Li, et al. (1992). "Bioresorbability and biocompatibility of aliphatic polyesters." Journal of Materials Science: Materials in Medicine **3**(6): 432-446.
- Vesna, O., M. Sax, et al. (2009). "Product study of oleic acid ozonolysis as function of humidity." Atmospheric Environment **43**(24): 3662-3669.
- Wurm, A., M. Merzlyakov, et al. (1999). "Crystallization of polymers studied by temperature-modulated techniques (TMDSC, TMDMA)." Journal of Macromolecular Science—Physics **38**(5-6): 693-708.
- Yamanaka, T. I., T. (1982). Process for Producing Polycondensates of Omega-hydroxypentadecanoic Acid. U.S. Patent, Patent#
- Zen, A., M. Saphiannikova, et al. (2006). "Effect of molecular weight on the structure and crystallinity of poly (3-hexylthiophene)." Macromolecules **39**(6): 2162-2171.
- Zhang, J. and L. Jiang (2008). "Acid-catalyzed esterification of *Zanthoxylum bungeanum* seed oil with high free fatty acids for biodiesel production." Bioresource technology **99**(18): 8995-8998.
- Zuo, J., S. Li, et al. (2011). "Thermoplastic polyester amides derived from oleic acid." Polymer **52**(20): 4503-4516.